(12)

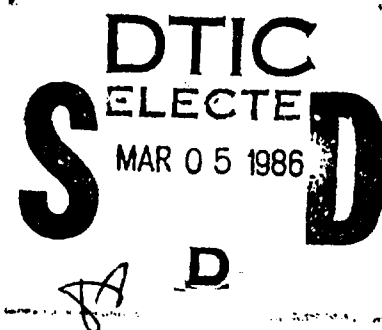**USAAVSCOM TR-85-D-11**

US ARMY
AVIATION
SYSTEMS COMMAND

CRASH-RESISTANT CREWSEAT LIMIT-LOAD OPTIMIZATION THROUGH DYNAMIC TESTING WITH CADAVERS

J. W. Coltman, C. Van Ingen, F. Selker

SIMULA INC.
10016 S. 51st Street
Phoenix, AZ 85044

DTIC
S ELECTE D
MAR 0 5 1986
D

January 1986

Final Report for Period May 1979 - December 1985

Prepared for

AVIATION APPLIED TECHNOLOGY DIRECTORATE POSITION STATEMENT

This report explores aspects of human tolerance to short-duration headward accelerations which are typical of those resulting from Army helicopter crash impacts. Due to their advanced age, the human cadaver specimens tested generally displayed a reduced tolerance to spinal compressive loads as compared with data based on young, physically fit Army aviators. The approach used to compare these two diverse groups is one of the more unique aspects of this program. The results, though not statistically conclusive, are suggestive of real-world human G tolerance to vertical accelerations and should be useful in the design of future military and civilian energy absorbing seats.

The entire test program was a result of joint sponsorship by the U.S. Army, U.S. Navy, U.S. Air Force and Federal Aviation Administration. This technical analysis and report was sponsored by the Aviation Applied Technology Directorate (AATD).

Mr. George T. Singley, III, and Mr. Kent F. Smith of the Aeronautical Systems Division served as project engineers.

ADA 164 828

REPORT DOCUMENTATION PAGE

1a. REPORT SECURITY CLASSIFICATION	1b. RESTRICTIVE MARKINGS
Unclassified	

2a. SECURITY CLASSIFICATION AUTHORITY	3. DISTRIBUTION/AVAILABILITY OF REPORT
2b. DECLASSIFICATION/DOWNGRADING SCHEDULE	Approved for public release; distribution is unlimited.

4. PERFORMING ORGANIZATION REPORT NUMBER(S)	5. MONITORING ORGANIZATION REPORT NUMBER(S)
TR-85422	USAAVSCOM TR 85-D-11

6a. NAME OF PERFORMING ORGANIZATION	6b. OFFICE SYMBOL (If applicable)	7a. NAME OF MONITORING ORGANIZATION
Simula Inc.		Aviation Applied Technology Directorate

6c. ADDRESS (City, State, and ZIP Code)	7b. ADDRESS (City, State, and ZIP Code)
10016 S. 51st Street Phoenix, Arizona 85044	U.S. Army Aviation Research and Technology Activity (AVSCOM) Fort Eustis, Virginia 23604-5577

8a. NAME OF FUNDING/SPONSORING ORGANIZATION	8b. OFFICE SYMBOL (If applicable)	9. PROCUREMENT INSTRUMENT IDENTIFICATION NUMBER
		DAAK51-79-C-0016

8c. ADDRESS (City, State, and ZIP Code)	10. SOURCE OF FUNDING NUMBERS			
	PROGRAM ELEMENT NO.	PROJECT NO. 1L162,	TASK NO.	WORK UNIT ACCESSION NO.
	62209A	209AH7605	00 032	EK WSA

11. TITLE (Include Security Classification)
CRASH-RESISTANT CREWSEAT LIMIT-LOAD OPTIMIZATION THROUGH DYNAMIC TESTING WITH CADAVERS

12. PERSONAL AUTHOR(S)
J. W. Coltman, C. Van Ingen, and F. Selker

13a. TYPE OF REPORT	13b. TIME COVERED	14. DATE OF REPORT (Year, Month, Day)	15. PAGE COUNT
Final Report	FROM 5/79 TO 12/85	January 1986	107

16. SUPPLEMENTARY NOTATION

17. COSATI CODES			18. SUBJECT TERMS (Continue on reverse if necessary and identify by block number)
FIELD	GROUP	SUB-GROUP	

19. ABSTRACT (Continue on reverse if necessary and identify by block number)
The threshold of spinal injury for seated humans subjected to $+G_z$ loading was investigated. The $+G_z$ loading was induced by simulating crash conditions typically found in helicopter crashes, and modified by the use of energy-absorbing mechanisms incorporated in the seat structure. Fifteen tests were conducted with unembalmed cadavers as human surrogates at various limit-load settings to attempt to identify the load threshold causing spinal injury. Bone strength analysis was used to normalize the results of the cadaver test program. Performance data and autopsy results for the 15 crash tests are presented. A correlation was derived relating the frequency of spinal injury to the energy absorber limit-load factor for use in design of crashworthy seating systems. Comparison of the incidence of spinal injury between the experimental test data developed through testing with cadavers and field performance of production energy-absorbing seats is discussed. The report also contains a discussion of the biomechanics of trauma associated with the human spine, including mechanical properties of the spine, typical injury mechanisms for $+G_z$ loading, and theoretical models for predicting injury.

20. DISTRIBUTION/AVAILABILITY OF ABSTRACT	21. ABSTRACT SECURITY CLASSIFICATION
☐ UNCLASSIFIED/UNLIMITED ☐ SAME AS RPT. ☐ DTIC USERS	Unclassified

22a. NAME OF RESPONSIBLE INDIVIDUAL	22b. TELEPHONE (Include Area Code)	22c. OFFICE SYMBOL
Kent Smith	(804) 878-2103/5875	SAVRT-TY-ASV

DD FORM 1473, 84 MAR
83 APR edition may be used until exhausted.
All other editions are obsolete.

PREFACE

Accesion For

NTIS CRA&I	☑
DTIC TAB	☐
Unannounced	☐
Justification	

By

Distribution /

Availability Codes

| Dist | Avail and/or Special |

A-1

TABLE OF CONTENTS

TABLE OF CONTENTS (CONTD)

LIST OF FIGURES

LIST OF TABLES

ix

1.0 INTRODUCTION

Spinal injury in helicopter accidents has been shown to be a very serious problem due to the human body's inability to tolerate excessive $+G_z$ acceleration. Fractures resulting from this type of injury mechanism typically occur in the lower thoracic and lumbar vertebral segments. This type of injury sometimes exhibits spinal cord damage resulting in permanent disability. The U.S. Army Safety Center has studied the incidence of spinal injury in Army helicopter accidents; it was found to be both widespread and directly related to the magnitude of the aircraft vertical velocity change (Reference 1). Figure 1 shows this relationship. The figure is based on older, non-crashworthy, U.S. Army helicopters.

The U.S. Army undertook a series of research efforts in the 1960's to eliminate this serious hazard. The concept of energy-absorbing seating systems was developed at this time (Reference 2). This concept utilized the principal of limiting the maximum load that could be transmitted to the occupant of the seat. It was theorized that by limiting the maximum transmitted load to the seat the severity and incidence of spinal injury could be reduced. A research effort to develop design criteria for this type of seat was conducted (Reference 3). Performance criteria evolved from this effort and were based on vertical acceleration measured on the seat. In an early study, Eiband had compiled results from human tolerance and animal studies showing the effect of acceleration on the body (Reference 4). His interpretation of human tolerance to $+G_z$ acceleration became the yardstick against which seat performance was assessed. The test conditions from the research programs that Eiband included in his summary of human tolerance were widely varied, and it was not known at the time the energy-absorbing seat performance criteria were formulated how well they would relate to the conditions present in a helicopter crash. However, for lack of other substantial experimental data, Eiband's work was incorporated as the performance criteria in the Crash Survival Design Guide and MIL-S-58095(AV) (References 5 and 6, respectively).

The term "limit-load factor" came into use in the above-referenced documents. It represented the ratio between the design vertical limit load of the seat and the moving weight of the seat/occupant system that was to be decelerated by this load. The limit-load factor was expressed in units of G, or multiples of gravitational acceleration. In the Army-sponsored criteria development program (Reference 3) it was found that a limit-load factor of approximately 14.5 G resulted in energy-absorbing seat performance acceptable according to the Eiband criteria.

Subsequent to the development of the design criteria, energy-absorbing seats were developed for the U.S. Army's UH-60A Black Hawk and AH-64A Apache helicopters (Reference 7). Also, the U.S. Army's Aircraft Crash Survival Design Guide was updated and published in an enhanced form to include specific design details for crashworthy, energy-absorbing crewseats based on the development and testing of the UH-60A and AH-64A seating systems (Reference 8). However, no additional human tolerance data regarding $+G_z$ acceleration was accumulated. As late as 1979 energy-absorbing seating systems were being procured and installed in operational aircraft without conclusive experimental data showing how the limit-load concept would actually perform with a human occupant.

Under the leadership of the Aviation Applied Technology Directorate (AATD), Fort Eustis, Virginia, and the U.S. Army Aeromedical Research Laboratory (USAARL), Fort Rucker, Alabama, a multiservice effort was initiated with goals of performing research in many areas of energy-absorbing seat design. The overall program is illustrated in Figure 2. The research effort described in this report, which was one segment of the overall study, had the following objectives:

- To investigate the performance of energy-absorbing seats using cadavers as human surrogates, as opposed to anthropomorphic dummies that had been used in the criteria development testing.

- To establish the effect of energy absorber limit-load on spinal injury, and if possible, determine the limit-load setting that represented a threshold for spinal injury.

Results from this investigation for the first objective were incorporated into a parallel study of 13 parameters that influenced energy-absorbing seat design, and were subsequently reported in Reference 9. The remainder of this report describes the investigation to determine the relationship between energy absorber limit-load settings and spinal injury by testing with cadavers.

A discussion of the biomechanics of the spinal column and the characteristics of spinal trauma is presented in Section 2.0. Sections 3.0 and 4.0, respectively, describe details of the dynamic test program with cadavers and vertebrae compression testing to establish a baseline for evaluating the dynamic test results. An analysis is presented in Section 5.0 which shows the development of a correlation between the energy absorber limit-load setting and the rate of spinal injury. This analysis was based on the results of the dynamic test program. Conclusions and recommendations derived from this study are presented in Sections 6.0 and 7.0.
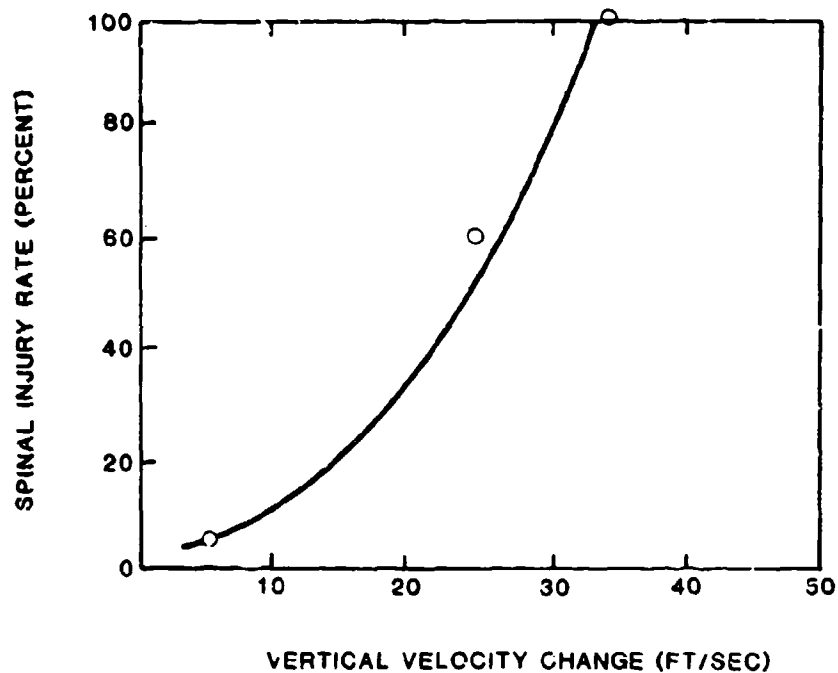
Figure 1. Relative frequency of spinal injuries versus change in vertical
velocity for U.S. Army aviators (Reference 1).
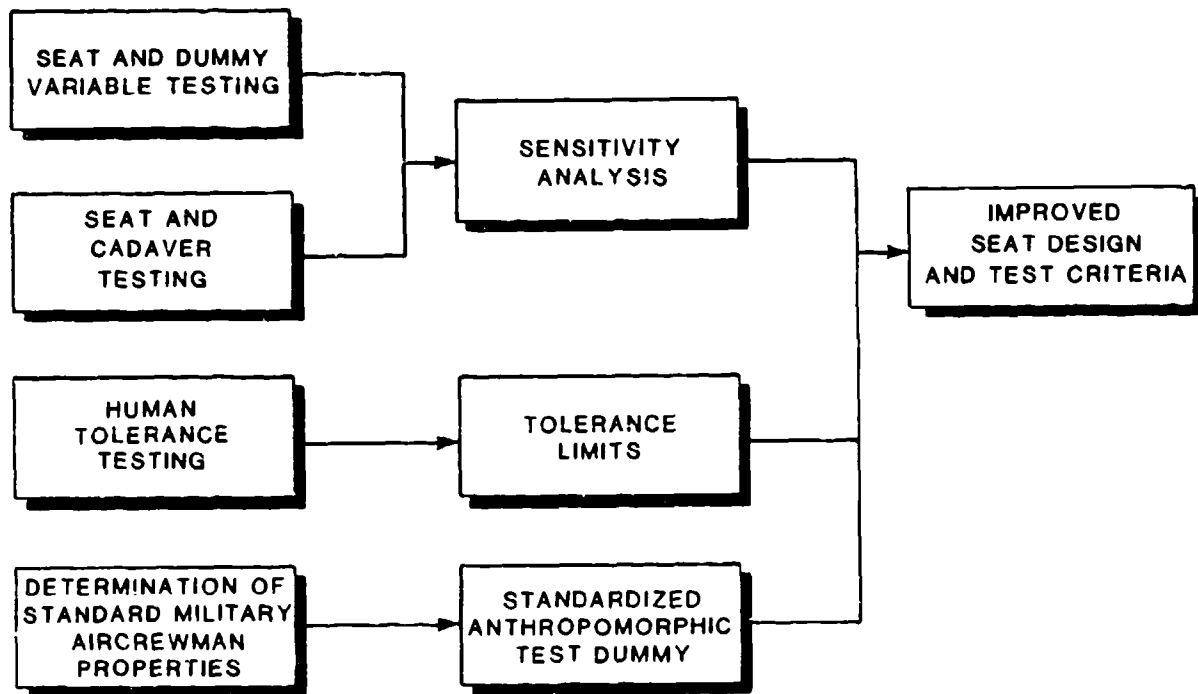
Figure 2. Overall program elements leading to improved
seat design and test criteria.

2.0 BIOMECHANICS OF INJURIES OF THE THORACOLUMBAR SPINE

As the principal supporting structure of the torso, the spine works together
with the structures of the torso to provide great strength and flexibility.
Comprehensive treatments of spinal anatomy (References 10-12) and biomechan-
ics (References 10, 13-15) have been compiled. In this section the anatomy
and biomechanics of the spine are briefly reviewed, types and mechanisms of
injury are discussed, and theoretical and empirical studies relating acceler-
ations to spinal injuries are summarized. The cervical spine is not con-
sidered in this report (for a comprehensive review see Reference 16).

2.1 ANATOMY OF THE THORACOLUMBAR SPINE

The spine consists of a curved column of 33 vertebrae, typically, together
with ligaments and intervertebral discs. At the lower end four vertebrae are
fused to form the coccyx, and immediately above this five vertebrae are fused
to form the sacrum. The sacrum articulates with, and is tightly connected
to, the pelvis. The flexible portion of the spine is customarily divided in-
to three sections: seven vertebrae of the cervical spine (neck), 12 verte-
brae of the thoracic spine (articulated with ribs), and five vertebrae of the
lumbar spine in the lower back (see Figure 3).

The vertebrae of the thorax and lumbar regions consist of a roughly cylindri-
cal vertebral centrum, or body, and posterior structures, including the pedi-
cles, lamina, facet joints, and spinous and transverse processes (Figure 4).
The posterior elements, together with the centrum, form the spinal foramen
through which the spinal cord runs. The vertebrae are composed of trabecular
bone with a thin shell of dense cortical bone. Both the trabecular and corti-
cal bone contribute significantly to the strength of the vertebrae (Refer-
ence 17). The trabecular bone is filled with marrow, which may act to distri-
bute loads hydrostatically. The cortical shell on each surface of the verte-
bral centrum is referred to as the bony end plate. Facing this bony end
plate is a thin layer of hyaline cartilage, which actually forms the outer
surface of the intervertebral disc and is referred to as simply the end
plate.

The compressive strength of the spine, which has been investigated in numer-
ous studies (References 18-28), is measured in either an isolated vertebra,
the vertebral centrum alone, or most realistically, two vertebrae with the
included intervertebral disc and hyaline cartilage. This section is referred
to as the intervertebral joint or "motion segment" (Figure 5A).

When a motion segment is loaded in compression there is a characteristic pat-
tern of failure. Before damage occurs there is a slight decrease in disc vol-
ume, bulging of the disc, and deflection of the bony end plates and vertebral
body (Figure 5B) (References 24, 29-30). As the compressive load increases,
fluid is forced from the disc, through the end plates, into the vertebral cen-
trum, and in turn, out of the vertebral centrum through small vascular fora-
men (openings) on its surface. Disc failure first occurs at the cartila-
ginous end plates. The bony end plates, with the underlying trabecular bone,
also fracture and yield. A typical load deflection curve from such a test is
shown in Figure 6. Some values of compressive strengths that have been re-
ported are shown in Table 1.

4

TABLE 1. VALUES FOR COMPRESSION STRENGTHS OF VERTEBRAE FROM VARIOUS STUDIES

ULTIMATE COMPRESSION STRENGTH (1b)

Study (Reference) Vertebral Level	Messerer 1880 (10)	Ruff 1950 (22)	Perey 1957 (23)	Yamada 1970 (26)	Hutton, et al 1979 (32)	Kazarian and Graves 1977 (18)	Hansson, et al 1980 (28)	Brinckmann, et al 1983 (30)
T1	450							
T2	450							
T3	425							
T4	470							
T5	495			875		830		
T6	495							
T7	560							
T8	560	1188-1412		875		1030		
T9	715	1345-1590						
T10	810	1460-1750						
T11	895	1590-1880		1210		1390		
T12	895	1525-1970						
L1		1590-1970	1145		1255	1525		1460
L2		1750-2175	1320		1410		740	985
L3		1970-2420	1390	1320	1795		850	1525
L4		1970-2420	1435		1500		920	1345
L5		2195-2645	1300		1860		1075	1525

There is considerable variation in strength values both within and between studies. This reflects, in part, the importance of secondary variables, such as strain rate, age, bone mineral content, and the particular kinematics of load application (Reference 31). As is frequently the case with viscoelastic structures, vertebral strength has been found to increase significantly with increasing strain rate (References 18 and 32). Vertebral strength drops significantly beyond the age of about 40. For example, Yamada reports that compared with vertebrae from the 20-39 age group, vertebrae from the 40-59 group are 22 percent weaker, and vertebrae from the 60-79 group are 51 percent weaker (Reference 26). Perey also found lower compressive strengths in older vertebrae: in tests of vertebral centra, specimens over 60 years old averaged 43 percent of the strength of those under 60, with the decrease becoming evident at about the age of 35-45 (Reference 23). Interestingly, Nachemson found no significant change with age in the stiffness of intervertebral joints, or disc pressures under load (Reference 33). Hansson, et al., has shown a positive correlation between bone mineral content and vertebral strength (Reference 28). However, even with all of the obvious variables controlled, significant variation persists. In using strength data, the variation and uncertainty must be taken into account.

The facet joints and other posterior elements are important in providing limits to motion in shear and rotation (References 34-38). Although their role in supporting loads within the normal range of motion is controversial, it appears that the posterior elements are important in sharing axial loads with the centrum when the spine is relatively straight or extended, i.e., bent backwards (References 39-42). The mechanics of the vertebrae have also been investigated using the finite element method (Reference 43).

The intervertebral discs including the cartilaginous end plates, make up about one third of the length of the spinal column. The disc is a remarkable structure composed of a central gelatinous region, the nucleus pulposus, and a tough surrounding ring of fibrous and cartilaginous material, called the annulus (Figure 7). The structure of the disc has been reviewed extensively elsewhere (References 10, 44-46). The mechanical properties will be briefly reviewed, with particular reference to injury mechanisms.

ung person the nucleus pulposus is composed of from 85-90 percent
gether with gelatinous mucoproteins and mucosaccharides (Refer-
Also, the nucleus is readily deformed but is hydrostatically
re sible. With aging, the water content of the nucleus decreases, and
i   omes increasingly fibrous and indistinct from the annulus (References
47-   . The annulus, which makes up most of the disc, is composed of
concentric cartilaginous layers, with sturdy fibers wound obliquely at about
30 degrees from horizontal (Figure 7) (References 44, 49-50).

When a disc from a young person is compressed, the hydrostatic pressure within the nucleus increases (References 51-52), and the annulus is put in circumferential tension (Reference 41). Thus, in a general sense, compressive loads are transmitted by hydrostatic pressure in the central region, and by the strength of the annulus in resisting circumferential tension (Reference 53). However, there is still uncertainty about the mechanical function of the nucleus (References 54-55). As the water content of the disc decreases with increasing age, compressive loads are increasingly carried by the annulus of the disk (References 53, 56-57). Intervertebral discs are

6

about one-third as stiff as the vertebral bodies in compression (Reference 49), but are also stronger, and are rarely the first element to fail in the spine (References 23-24, 53, 57).

A number of models have been constructed to investigate the mechanics of the disc. Material properties of the annulus have been estimated by constructing finite element models of the disc and tuning parameters to give the correct overall responses to loads (References 27, 58). Burns and Kaleps modeled the disc as combinations of springs and dashpots, and chose parametric values to match the response of the disc to deflection and creep data (Reference 59). In this way, a three-parameter solid, consisting of a spring and dashpot in parallel (a Kelvin unit) together in series with a spring, was constructed. Finite element models have also been constructed for purposes of stress analysis and to study the disc's mechanical performance (References 53, 60). Shirazi constructed a detailed three-dimensional finite element model, incorporating geometric and material nonlinearities and the composite construction of the annulus. This model gave good agreement with experimental values of intradiscal pressure and end plate deformations. The model predicted that:

- Removal of the nucleus reduces disc stiffness in compression by up to 50 percent.

- For a normal disc the highest vertebral stresses occur in the trabecular bone adjacent to the nucleus. When the nucleus is removed, the stresses in the central region drop considerably and stresses in the cortical shell increase.

- When the disc has degenerated, the ground substance (matrix) of the annulus and the cortical shell become vulnerable (Reference 53).

Broberg also modeled the mechanical behavior of discs (Reference 61). Spinal movements are governed by a series of ligaments which bind together the vertebral bodies and intervertebral discs. The condition of ligaments after injury is important to the stability of the spine. Ligaments of the spine are shown in Figure 8.

2.2 THE SPINE IN THE BODY

In order to understand the mechanical function of the spine it is necessary to consider the support and loading by associated structures of the torso.

2.2.1 Supporting Structures

The spine depends on the overall structure of the abdomen and thorax to maintain its form. While the spine can resist high axial and shear loads, it is quite flexible in bending. The primary means by which the body generates and resists bending is through the action of muscles acting parallel to the spine, putting the spine in compression. Because some muscles are rather close to the spine (e.g., the muscles of the back), large forces are necessary to generate moments. For example, when a person weighing 154 lb sits with the back flexed 20 degrees forward, holding 22 lb in each hand, the compressive load on the L3 vertebra is about 583 lb (Reference 65). Forces approaching the ultimate strengths of vertebrae have been predicted using more indirect methods.

7

The abdominal pressure may also help support the spine in resisting flexion (References 63-65). Finally, the rib cage contributes significantly to the strength and stiffness of the thoracic spine (References 10, 66-67).

2.2.2 Spinal Loading

The spine supports the weight of the head, arms, thorax, and abdomen. Any external forces on the upper body or arms are also transmitted to the spinal column. Further, since the center of gravity of both the head and torso lies anterior to the spine, their weight creates a bending moment within the spine (Reference 68). As discussed above, the leverage that external loads exert on the spine is often impressive.

Spinal loads can also be generated by rapid accelerations of the body, such as those occurring in automobile or aircraft accidents. The stresses that are generated within the spine are associated with the transmission of momentum between the mass of the body and the areas of contact where the forces of acceleration are applied. The injuries resulting from these stresses will depend on the areas and nature of contact with supports, the position of the body, and the nature of the acceleration. Injuries associated with accelerations are considered in Section 2.4.

2.3 THEORETICAL MODELS OF SPINE BIODYNAMICS

Biomechanical models of the spine are primarily concerned with the stresses on the head and spine when the body is subjected to dynamic loading. There has been particular interest in developing a qualitative and quantitative understanding of injuries associated with accelerations of ejections from aircraft. Early models of the spine were one-dimensional, only permitting axial loads and deflections. There have been two varieties of such models: lumped, or discrete parameter models in which the spine and head are modeled as a column of one or more rigid masses connected by springs and dashpots (References 69-70), and continuous rod models (References 71-72).

More recent models have considered the effects of bending and shear displacements and stresses. Orne and Liu constructed a detailed two-dimensional, discrete parameter model (Reference 69). In this model, the intervertebral discs are modeled as massless three-parameter viscoelastic solids under axial loading and as elastic solids in shear and bending. The vertebrae are modeled as rigid bodies. Orne and Liu found significant bending stresses which contributed to compressive stresses in the anterior portions of the thoracic vertebrae. This model was later extended to include seat backs and shoulder restraints (Reference 73). Prasad and King considered the effects of the posterior elements in another two-dimensional discrete parameter model (Reference 74). This model also included the seat and restraint system. The model predicts reduced stresses when the spine is hyperextended prior to ejection, due to the load sharing of posterior elements in that configuration. No dynamic overshoot is predicted.

Cramer, et al., constructed a curved continuum model which incorporated the effects of bending due to the inertial loads of the torso (Reference 75). The spine was modeled as linearly elastic with the load representing the mass of the torso in the horizontal plane with the section of spine. The model

8

predicted severe flexion with headward acceleration, resulting in compression
of the anterior portions of vertebrae. The model also predicted that:

- The eccentricity of the torso loading had little effect on stresses.

- The small deflection approximations of the spine are inadequate.

- The highest stresses occur in the first 150 milliseconds after
  acceleration begins.

This last finding suggests that restraint systems which often do not come
into play this quickly simply provide initial posture and prevent secondary
injuries in headward accelerations. A modification of this paper, in which
the spine was considered viscoelastic, has been described by Liu, et al.
(Reference 76).

Belytschko developed and tested an extensive three-dimensional, discrete para-
meter model (Reference 77). In this model, which includes the head and rib
cage, the bone is again rigid and the soft tissue is viscoelastic. Seat and
restraint systems are included. Again, significant flexion was predicted for
axial, ejection-like accelerations. Including the viscera and rib cage in
the model stiffened the torso significantly and reduced spinal stresses. The
model predicted that for accelerations of over 10 G the restraint system and
musculature are essential to spine stability. The model's predictions of
impedance were tested, leading to modifications of the damping coefficients
of the spine and viscera (Reference 78). In this more recent report a simpli-
fied version of the model was constructed and validated for use in design
applications, such as the design of ejection seats. Postprocessing was added
to give predictions of the risk of spinal injuries under various configur-
ations and accelerations.

Soechting and Pasley investigated the effect of musculature on stresses in
the spine during spineward acceleration (Reference 79). They found that
muscle action is too slow to be significant in an unanticipated accident
(muscles have also been found to be too weak to have a significant effect).

2.4 INJURIES OF THE SPINE

Injuries occur when stresses within the spine exceed the material strength of
the spinal structures. The nature of the injury reflects the forces acting
on the spine, the position of the spine, and the condition of the spinal
structures (e.g, age or mineral content). Spinal injuries can be classified
as dislocations, fractures, or fracture-dislocations. A dislocation refers
to a change in the normal anatomy of the spine, through damage to ligaments
or the disc. Fractures involve damage to the vertebrae, and fracture-
dislocations involve both bony damage and displacements of structures from
their normal positions. Spinal injuries are also commonly classified as
"stable" or "unstable" (References 10, 80-81). While the definitions of
these classifications have varied, the intention has consistently been to
evaluate the degree of medical intervention and treatment that is
appropriate. Other classifications of spinal injuries have been based on

9

the general structural nature of the damage (References 82-83). Injuries of the thoracolumbar spine can generally be characterized as one of several types:

- Anterior or lateral wedge fractures

- Noncomminuted and comminuted compression fractures

- Injuries involving hyperflexion with distraction

- Rotational injuries

- Hyperextension injuries.

Such a classification is, of course, arbitrary to some degree. In reality, injuries generally consist of a combination of injury-types. However, this classification, or variations of it, permits convenient discussion of major types of injuries. (For more exhaustive treatments see References 15-16, 85-86).

2.4.1 Wedge Fracture

When the spine is either hyperflexed or severely bent laterally the centrum may be crushed in the anterior or lateral regions, giving the vertebra a wedge-like shape (Figure 9). This fracture is particularly common when flexion is combined with compression (Reference 25, 87).

However, compression is not necessary for this type of injury to occur (Reference 29). In its mildest form, a wedge fracture does not result in any comminution (pieces of bone breaking loose), damage to the disc, or damage to ligaments. Such an injury is commonly asymptomatic, aside from initial pain. A piece of bone can break loose, particularly due to an obliqu fracture of the superior lip of a vertebra. Fortunately, such pieces are generally displaced anteriorly or laterally, so little danger is posed to the cord or nerve roots. In severe cases, however, the wedge fracturing is associated with dislocation of the superior portion of the spine anteriorly (References 15, 80) and/or fractures of the posterior elements (Reference 88). This can result in a highly unstable fracture, which poses a serious threat to the spinal cord.

2.4.2 Compression Fractures

When compressed uniformly, the end plate of the vertebra may fracture, allowing herniation of the disc into the vertebra or uniform crushing of the vertebra. These two fractures are quite stable and may be virtually asymptomatic. When forces and energies are higher the nucleus of the disc can be forced into the centrum, bursting the vertebra. This "burst fracture" may be either stable or unstable, depending on the condition of the posterior elements and ligaments (References 29, 82, 89). Regardless, the burst fracture poses a serious threat to the spinal cord from fragments of bone and gross distortion of the spine.

10

2.4.3 Hyperflexion with Distraction

As discussed above, in hyperflexion the anterior portion of the vertebra generally crushes before other damage occurs, leading to a wedge fracture (Reference 29). However, if distraction accompanies flexion the posterior ligaments, the joints, and the disc may be disrupted (Reference 81). Another possibility is that a vertebra fractures horizontally, starting at the back of the spinous process (Figure 10). This horizontal splitting of a vertebra was first described by Dr. Chance and is referred to as the Chance fracture. Hyperflexion/distraction injuries are commonly associated with the use of lap restraining belts in automobile accidents (Reference 90).

2.4.4. Rotational Injuries

As well as dislocations of the facet joints, rotational injuries can result in fractures of the vertebral centrum (Reference 81, 89). Kazarian reports that the highest frequency of rotational injuries occur in the T2-T6 and T7-T10 regions (Reference 15). He groups them into two categories: those in which the vertebral fracture is fairly uniform, and those in which there is an asymmetrical wedge-like fracture (Figure 11). Rotational fracture-dislocations are frequently unstable and pose serious threats to the spinal cord and nerve roots.

2.4.5 Hyperextension Injuries

When the spine is hyperextended the anterior structures will be subjected to tension, and the posterior elements will be in compression. The particular pattern of fracture-dislocation will depend on the forces, e.g., the amount of compression or extension. Hyperextension injuries can be classified as those with compression injuries to the posterior region of the vertebral centrum and those without compression of this area. The latter are often associated with tearing of the anterior longitudinal ligament, and damage to the disc and facet joints. While fairly common in the cervical spine due to whiplash loading (sternumward acceleration), it is very rare in the thoracolumbar spine (References 82, 91).

2.5 ACCELERATIONS AND SPINAL INJURY

Rapid acceleration is frequently the source of spinal injury (deceleration, an acceleration that tends to bring a body to a stop, has the same effect as an acceleration in the appropriate direction, thus no distinction is made). In considering injuries associated with accelerations, it is helpful to keep clearly in mind the mechanism by which these injuries are caused. Of course the acceleration itself does not cause spinal injuries. It is the stress within the spine, resulting from acceleration, that causes injury. As an example, we can consider the acceleration of ejection. When the ejection rocket is ignited a high load is applied over a limited area of the body; the entire accelerating impulse will be transmitted through this area. Stresses arise as the impulse, or change in momentum, is transmitted from the areas of contact to the entire mass of the body. If we knew the exact distribution of forces at the body's surface, we would still be one step removed from the stresses that cause injury: the stresses will depend on the mechanical properties and distribution of mass within the body. If we know only the acceleration of the seat, which is usually the case, we are another step

11

removed from the stresses. In this case, the character of the contact between the seat and occupant (e.g., seat cushion or air bag) will also become significant.

There are a number of variables that are important in determining the threat of accelerations to the spine:

- The onset time (seconds) or onset rate (G's of acceleration per second). This reflects the time it takes for an acceleration to go from 0 to its peak value.

- The magnitude of the acceleration at its peak or plateau (G).

- The duration of the acceleration (milliseconds).

- The direction of the acceleration and the position and support of the body.

A short onset time, high peak magnitude, and long duration can all increase the severity of accelerations. A number of structures of the torso are vulnerable to injury under high accelerations. Experiments with Rhesus monkeys have shown (in order of decreasing sensitivity) vulnerability of the lungs, vertebrae, liver, heart and large vessels, and gastrointestinal track (Reference 93). This sensitivity order may or may not hold for humans. Because of the severity of spinal injuries, and because they are among the first to be produced with increasing accelerations, the relationship between high accelerations and spinal injury has been studied for some time.

2.5.1 Clinical Findings

Most information on injuries associated with accelerations is from either aircraft ejections or automobile accidents. As well as being socially and economically important, these injuries often occur in a relatively controlled and known acceleration environment. The extensive literature on automobile accidents is not reviewed here.

There have been numerous accounts of injuries associated with ejections from aircraft (References 86-87, 96-99). Most injuries are wedge or uniform compression fractures. In addition to the seat acceleration, the occurrence and nature of injuries depend strongly on initial posture, direction of acceleration relative to the spine, and adjustment of the restraint system (References 68, 74, 100-101). In particular, when flexion is avoided it appears that higher accelerations can be tolerated without injury. Injuries occur most frequently at either the mid-thoracic spine or the T12-L1 region (Figure 12). The most common level of injury seems to vary with the ejection system.

Shanahan has reviewed vertebral fractures in helicopter crashes involving U.S. Army Aviators from January 1972 to August 1980 (Reference 102). Figure 13 shows the distribution of fractures according to the vertebral level in which fracture occurred (based on preliminary data). The distribution of fractures was primarily in the T11 to L4 region, with the highest incidence of fracture occurring in L1. In comparison to the ejection-related fracture distribution, helicopter-related spinal injuries appear to have a similar distribution pattern.

2.5.2 Tolerance to Accelerations

The literature up to 1959 was reviewed and summarized by Eiband (Reference 4). For a seated, restrained person, accelerations were considered in each of four directions: spineward ($-G_x$, e.g., rapid stop for forward-facing passenger), sternumward ($+G_x$, e.g., rapid stop for rearward-facing passenger), tailward ($-G_z$, e.g., downward ejection from an aircraft), and headward ($+G_z$, e.g., upward ejection from an aircraft). Eiband's goal was to compile specific tolerances, using the results of available studies. In order to compare and combine data, all accelerations were fit to a trapezoidal pulse, in which accelerations increased linearly to a plateau and remained uniform for their duration (see Figure 14). This is clearly an approximation to the true timecourse of accelerations. The tolerances found by Eiband are shown in Figures 14-17. Highest accelerations could be tolerated in the sternumward direction, followed respectively by spineward, headward, and tailward directions.

Eiband's data on the effect of rate of onset is sparse but suggests that slower rates of onset are preferable. For example, in headward accelerations a 500-G/sec rate of onset was very uncomfortable, while a 180-G/sec rate of onset was not. The rate of onset is important in determining whether there will be significant "dynamic overshoot" of accelerations and stresses within the body; while a slow rate of onset will allow the body to come to the equilibrium-deformed configuration gradually, a rapid rate of onset will effectively result in an impact between the seat and the body, creating high transient stresses. Eiband reports that given spineward sinusoidal pulses for periods of less than .075 sec, the occupant experiences less acceleration than the seat. For periods of from .075 to .28 sec, the occupant experiences significantly greater accelerations than the seat, with the maximum dynamic overshoot occurring at .11 sec (Figure 18).

Since 1959 there has been no such comprehensive attempt to quantify tolerable accelerations. However, several studies have provided additional information. Headward accelerations of less than 10 G are certainly well tolerated (References 68, 74 and 103). Studies of ejection injuries indicated that fractures occur in about 10 to 40 percent of ejections, depending in large part on the ejection system (References 87, 94-95, 97-98, 104-105). Ejection seats impose between 15 and 20 G. It appears that at this acceleration, injuries will depend on factors such as posture, restraint, and condition of the spine.

Stech developed curves relating headward accelerations to the risk of vertebral fracture (Reference 92). These curves were based on vertebral strength and estimates of the mass supported at each vertebral level. The calculations do not account for dynamic overshoot or flexion that generally accompanies headward acceleration but are conservative in the absence of these factors. Risk curves for L1-L5 are shown in Figure 19. End plate damage is predicted to occur at 9 to 12 G, and compression fractures are predicted at 17 to 20 G.

13

CERVICAL VERTEBRAE

ATLAS
AXIS

1
2
3
4
5
6
7

THORACIC VERTEBRAE

1
2
3
4
5
6
7
8
9
10
11
12

LUMBAR VERTEBRAE

1
2
3
4
5

SACRUM — SACRO-VERTEBRAL ANGLE

COCCYX — ARTICULAR PORTION OF SACRUM

VERTEBRAL COLUMN IN RELATION TO BODY OUTLINE
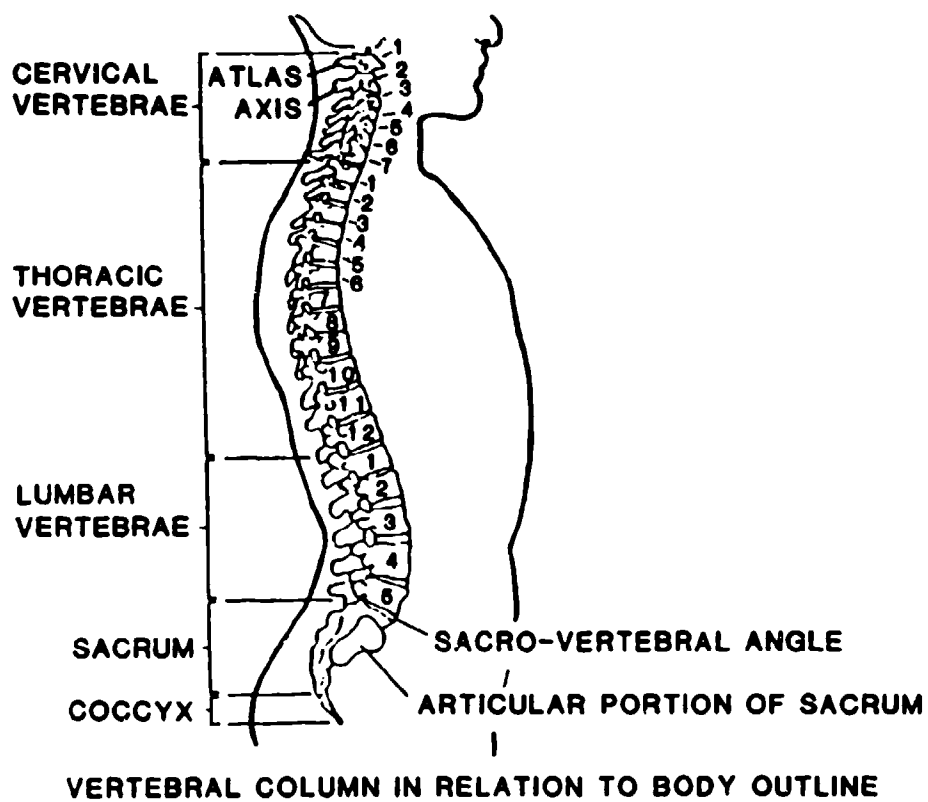
Figure 3. View of the vertebral column.

SUPERIOR ARTICULAR
PROCESS

SUPERIOR DEMIFACET FOR
HEAD OF RIB

ARTICULAR FACET
ON TRANSVERSE
PROCESS

BODY

INFERIOR DEMIFACET FOR HEAD OF RIB

INFERIOR ARTICULAR PROCESS

SPINOUS PROCESS

TRANSVERSE PROCESS

SPINAL FORAMEN

LAMINA

SPINOUS PROCESS

BODY

PEDICLE
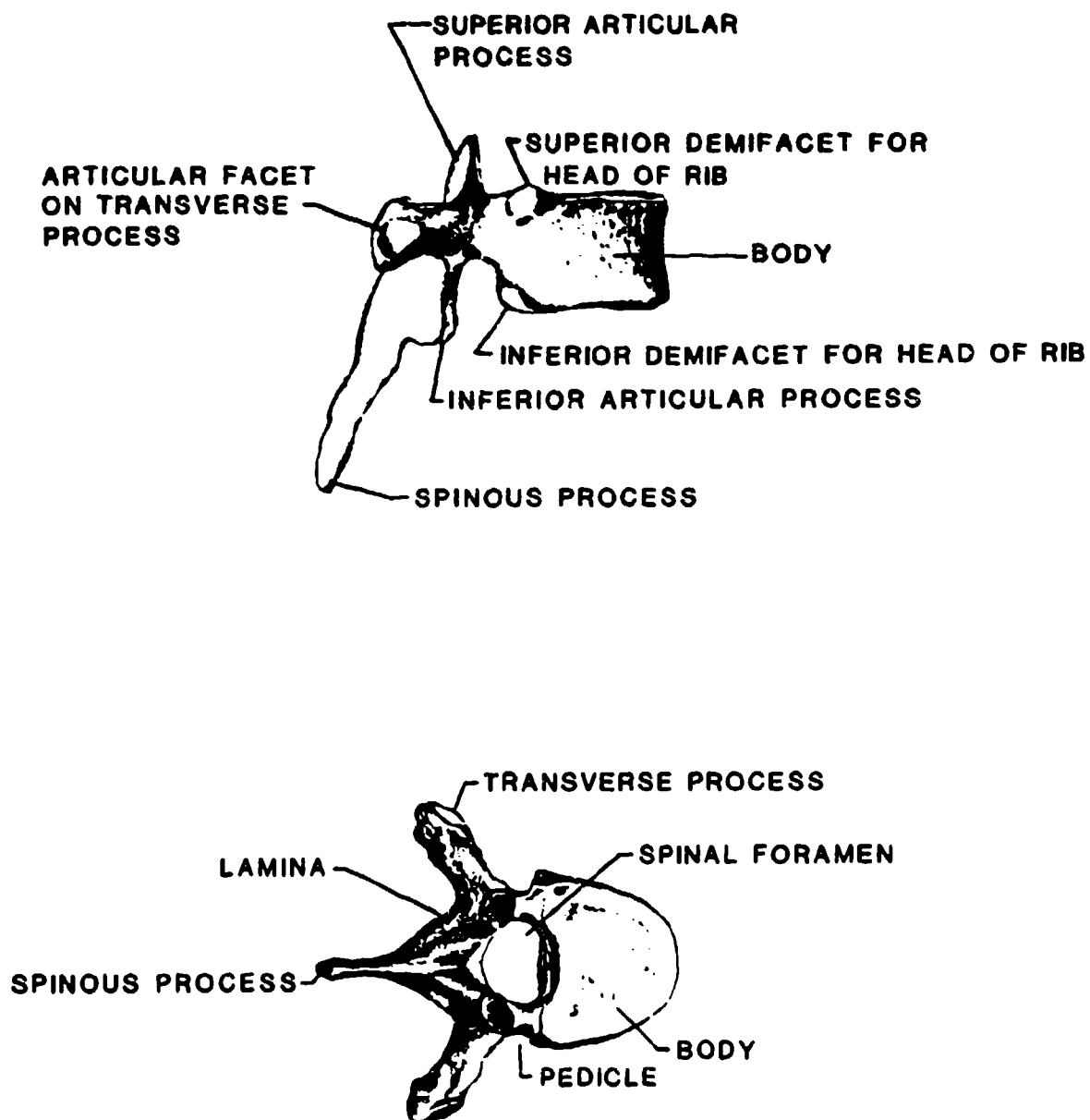
Figure 4.   A typical thoracic vertebra; a lateral view (top figure)
and superior view (bottom figure).

15

VERTEBRAL BODY

CARTILAGE
END PLATES

INTERVERTEBRAL
DISC
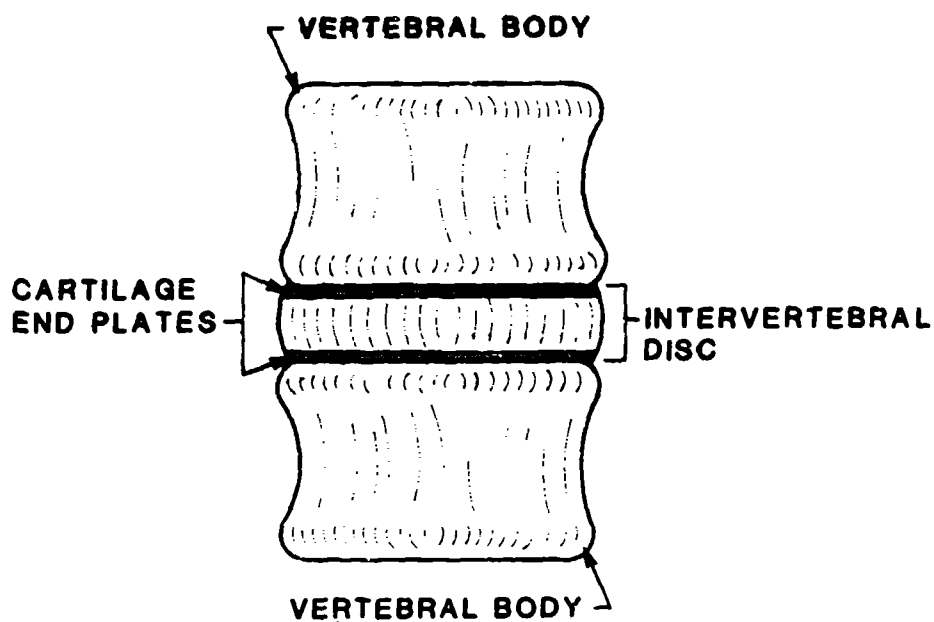
VERTEBRAL BODY

A. SCHEMATIC OF INTERVERTEBRAL JOINT SPECIMEN OR "MOTION SEGMENT"

DEFLECTION OF
BONY END PLATE AND
VERTEBRAL BODY

BULGING
DISC

P
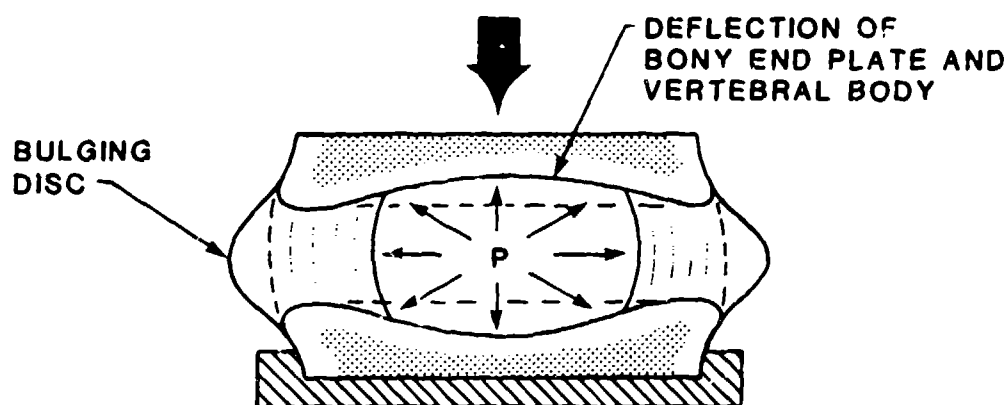
B. COMPRESSION LOAD IN A NORMAL NONDEGENERATED DISC OF A "MOTION SEGMENT"

Figure 5.   A "Motion Segment."
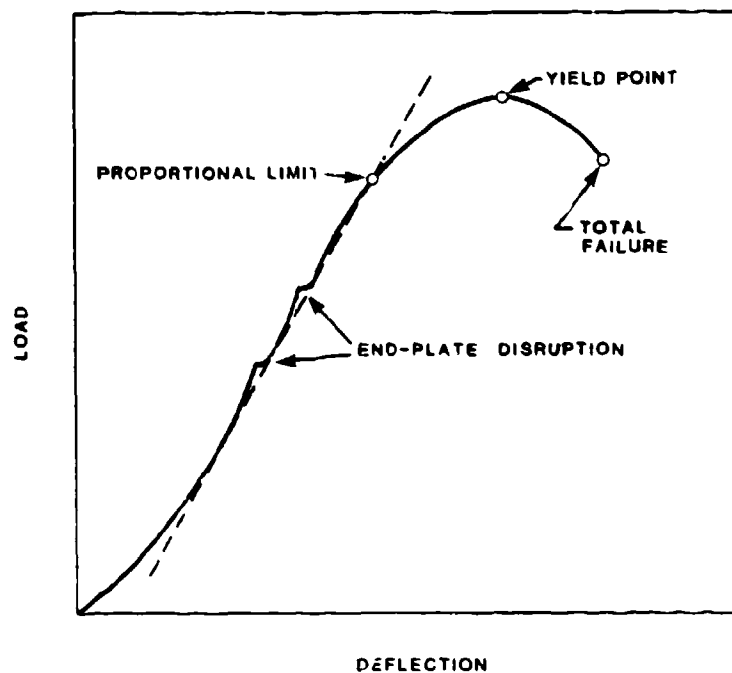
Figure 6. Schematic load-deflection curve illustrating alterations in vertebral body structure during compressive stress.
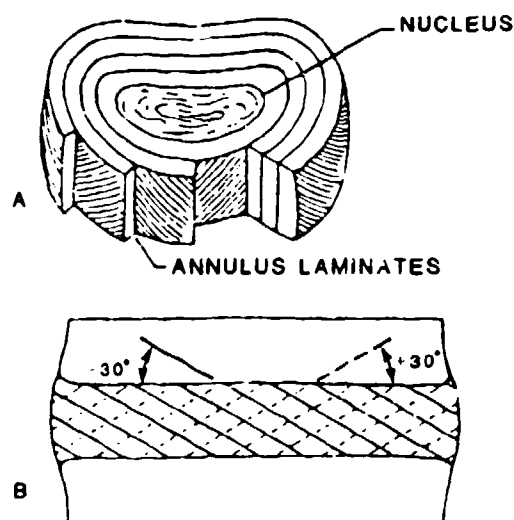
Figure 7. Inter ertebral disc. (A) Concentric laminated bands of annular fibers. (B) Orientation of annular fibers to the disk plane.

17
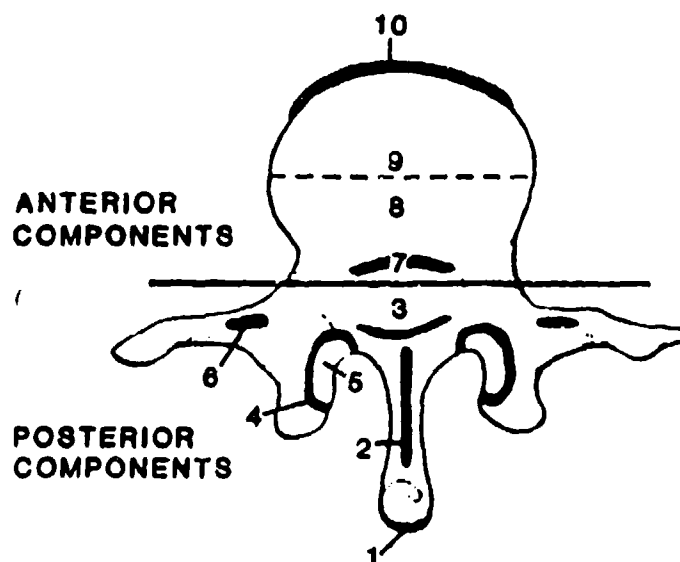
A. VIEW OF THE SUPERIOR SURFACE OF A VERTEBRA

(1) supraspinous ligament, (2) interspinous ligament,
(3) ligamentum flavum, (4) facet capsular ligament,
(5) facet joints, (6) intertransverse ligament,
(7) posterior longitudinal ligament,
(8) posterior one-half of disc,
(9) anterior one-half of disc,
(10) anterior longitudinal ligament.
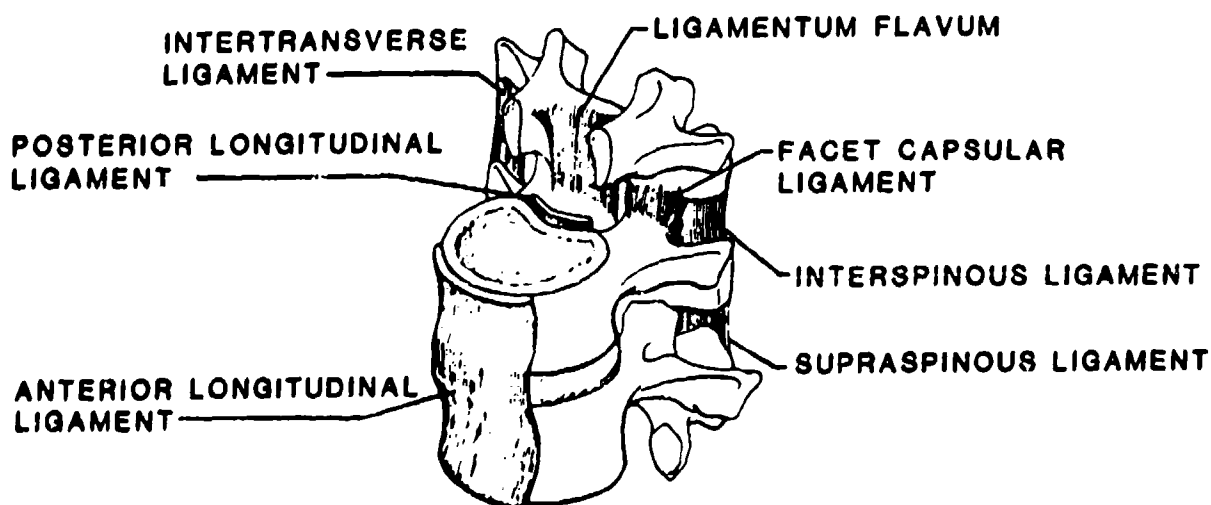
B. VIEW OF A "MOTION SEGMENT"

Figure 8. Ligaments of the spine.

18

**ECCENTRIC
COMPRESSIVE
FORCE**

INDUCED BENDING MOMENT
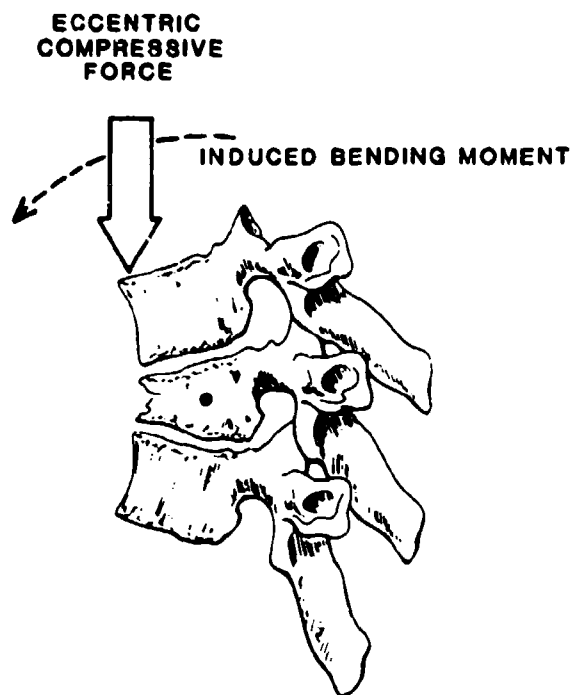
Figure 9.   Wedge fracture: an eccentrically located force
away from the neutral axis results in a greater
bending moment and produces a compressive fracture
of the body, with characteristic wedging.
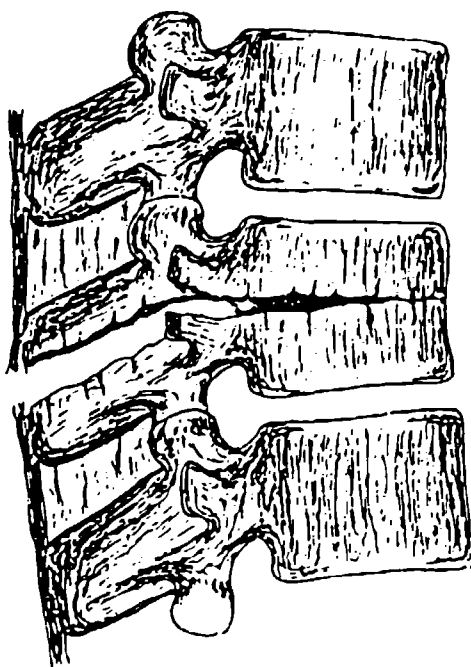
Figure 10.   The Chance fracture: a flexion-distraction injury.

a) DIRECTION OF APPLIED LOAD
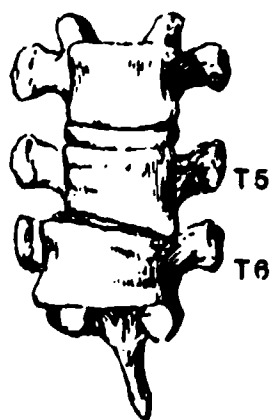
b) SCHEMATIC REPRESENTATION OF
   ROTATIONAL INJURY MODE
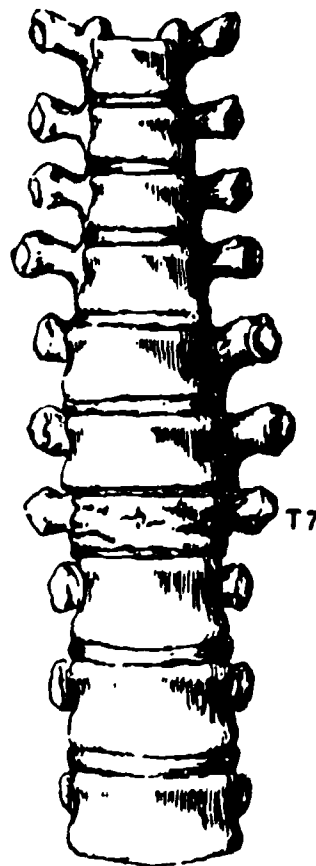
Figure 11. Rotational lateral wedge compression fracture (Reference 15).
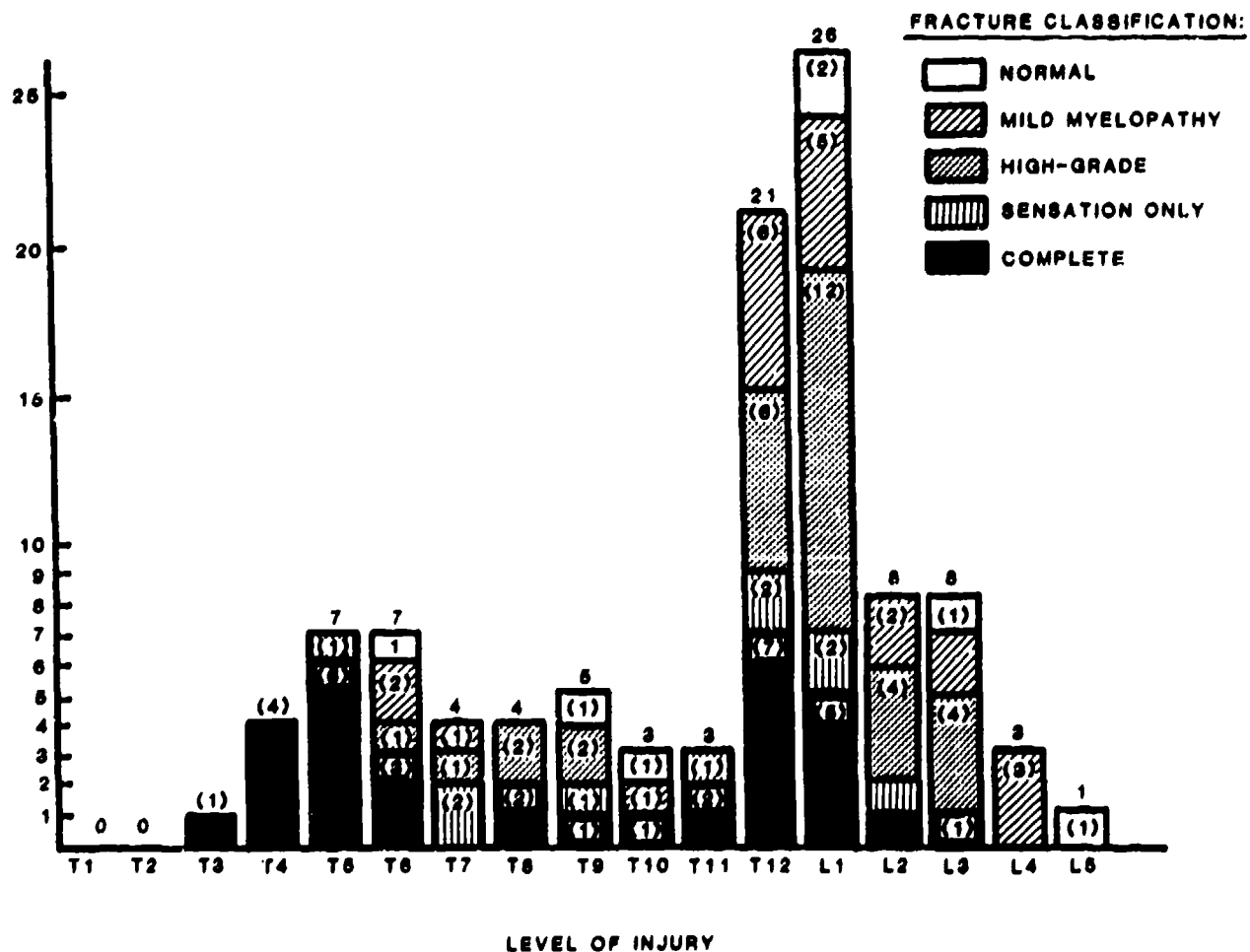
Figure 12. Distribution of vertebral fractures associated with ejections from aircraft.
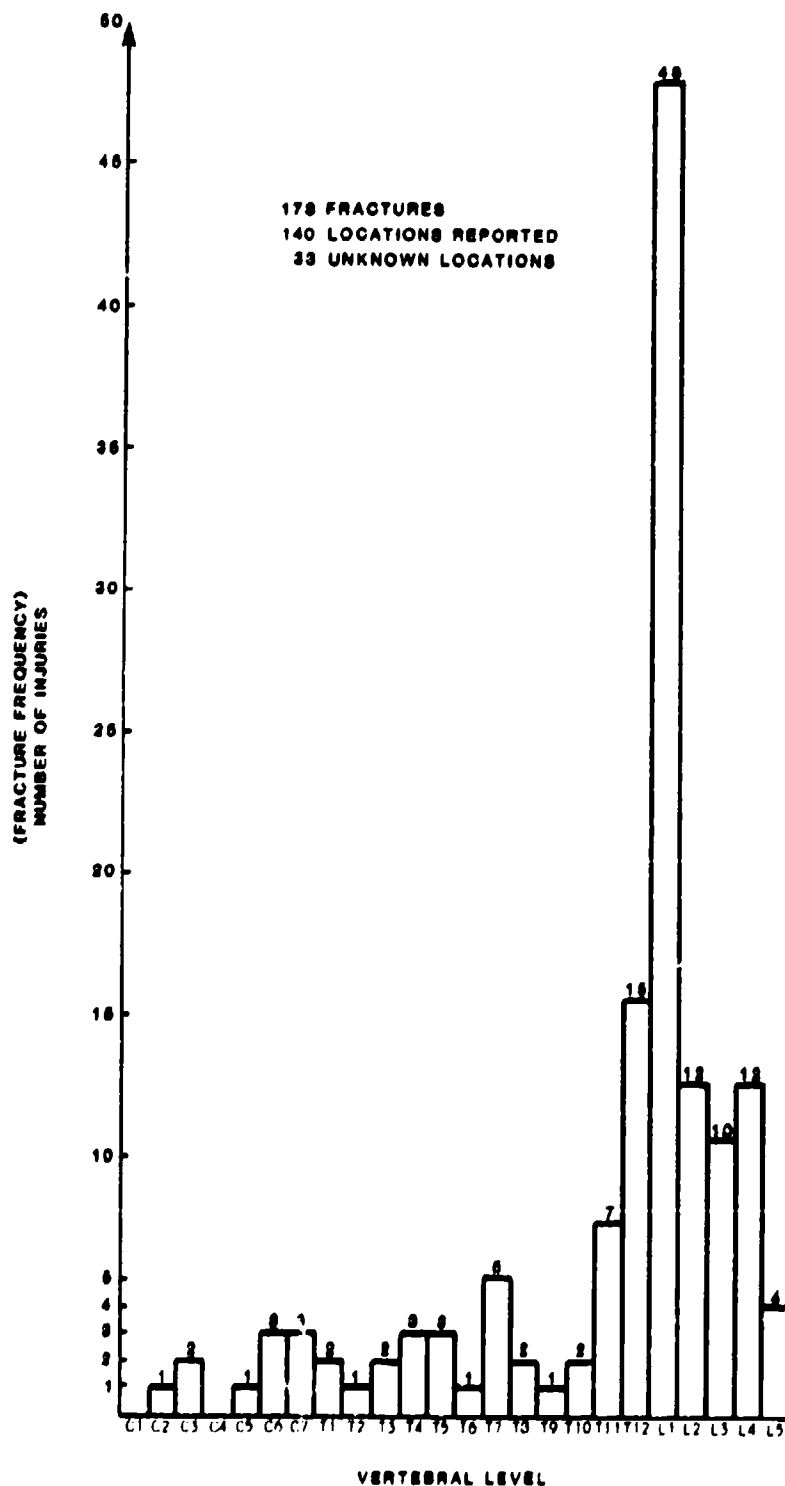
Figure 13. Distribution of vertebral fractures of U.S. Army aviators in helicopter crashes.
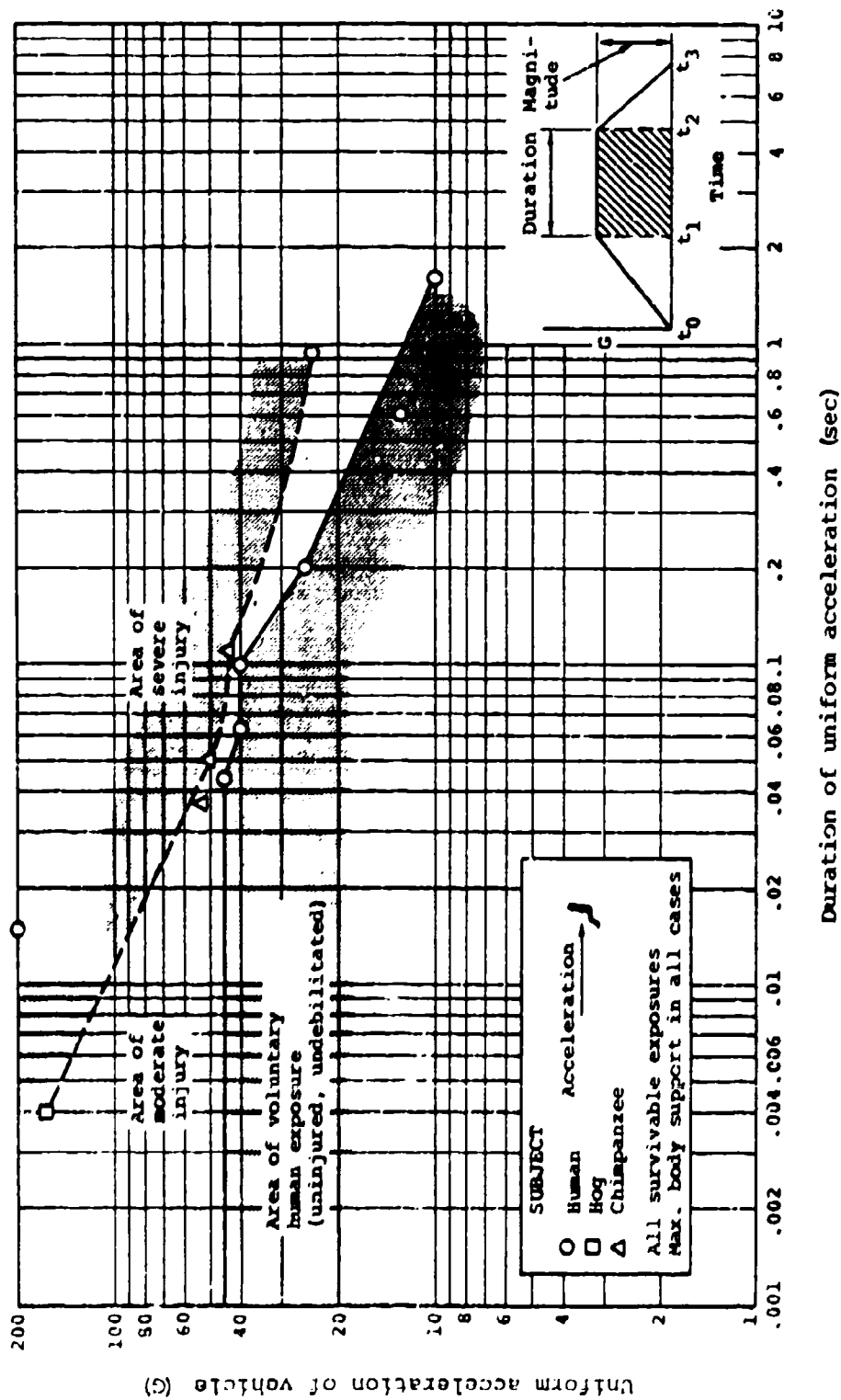
Figure 14. Duration and magnitude of spineward acceleration endured by various subjects.

23
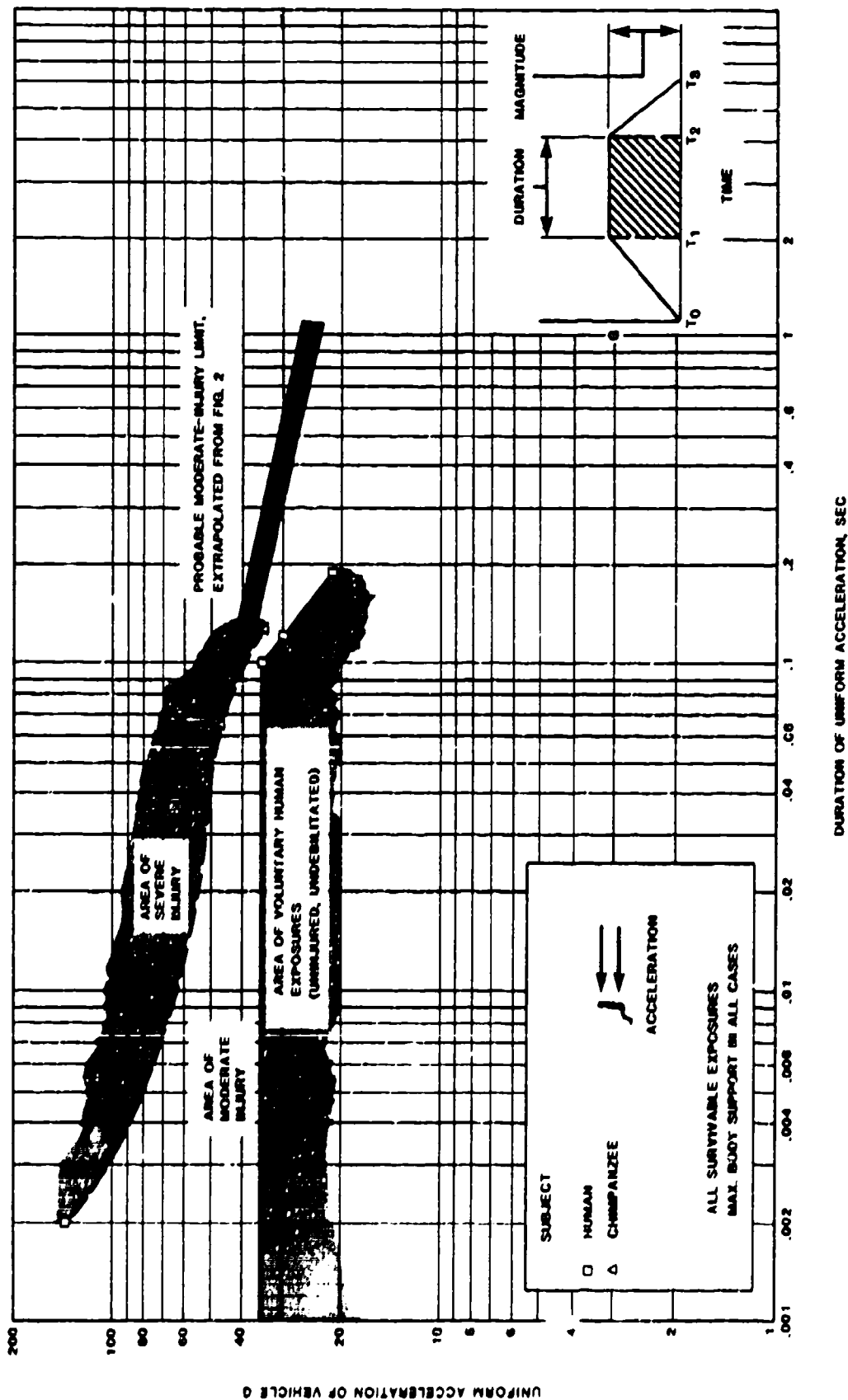
Figure 15. Duration and magnitude of sternumward acceleration endured by various subjects.
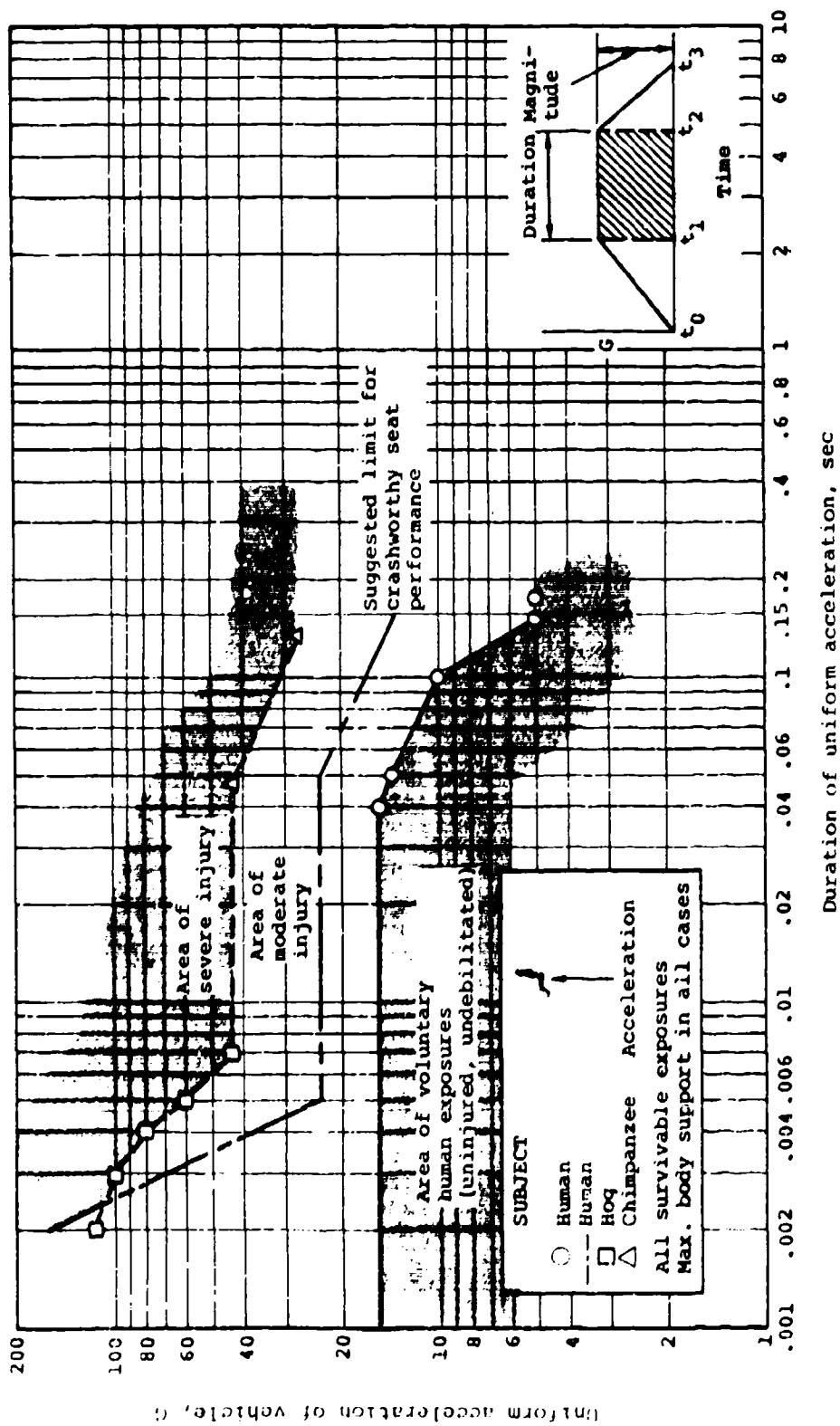
Figure 16. Duration and magnitude of headward acceleration endured by various subjects.

25
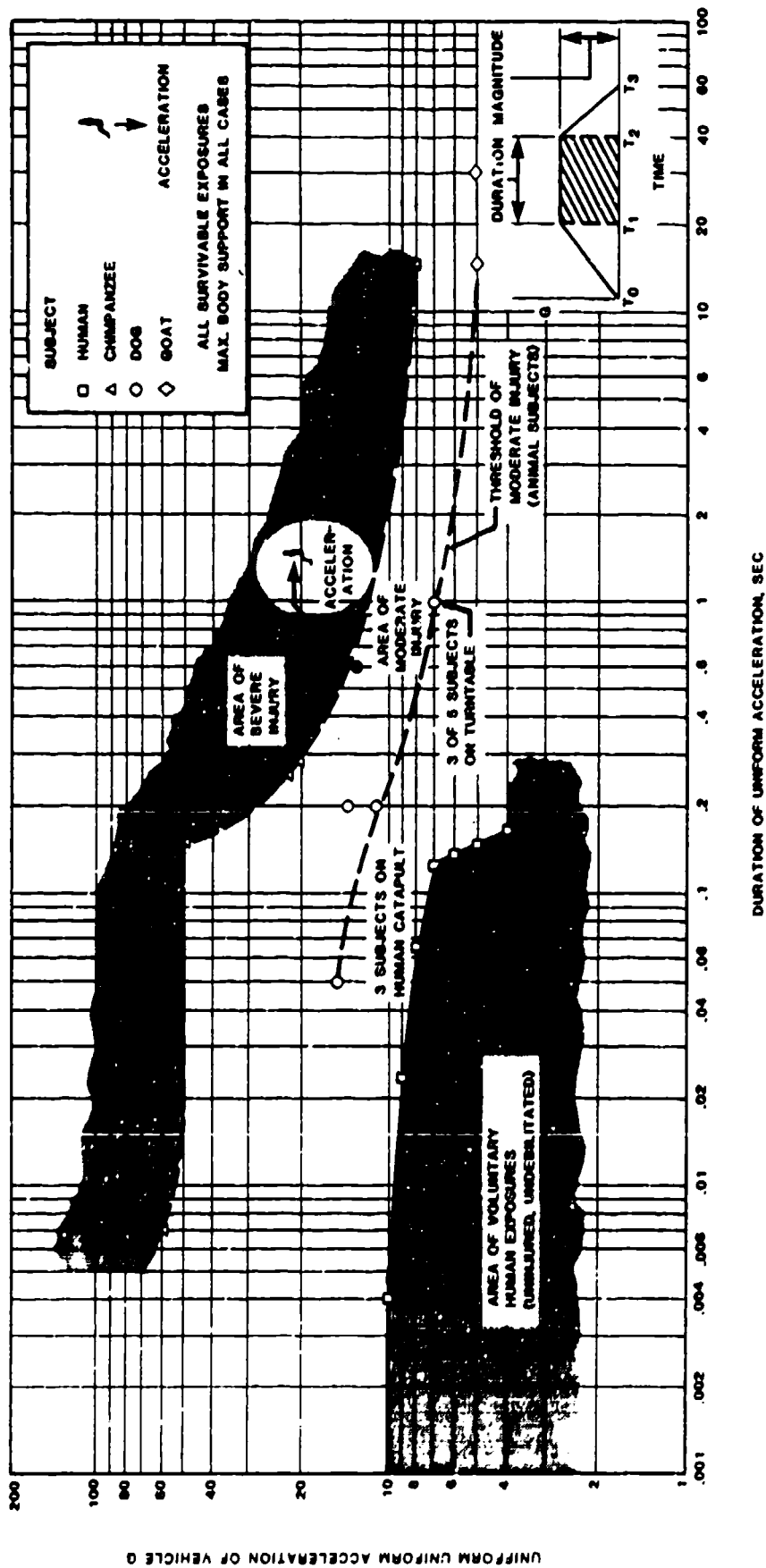
Figure 17. Duration and magnitude of tailward acceleration endured by various subjects.

26
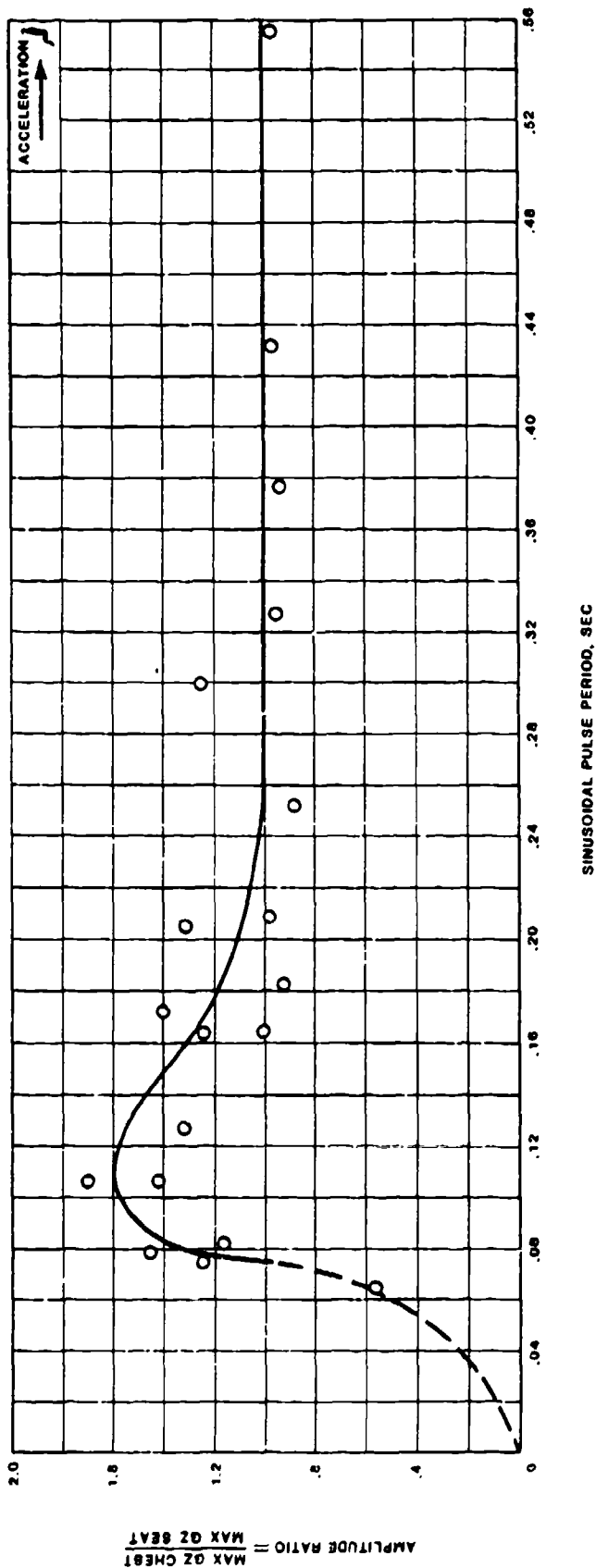
Figure 18. Spineward acceleration of human subjects: frequency response as function of amplitude ratio. Period corrected to standard subject weight of 172 lb (Seat and subject = 232 lb). (Reference 4).
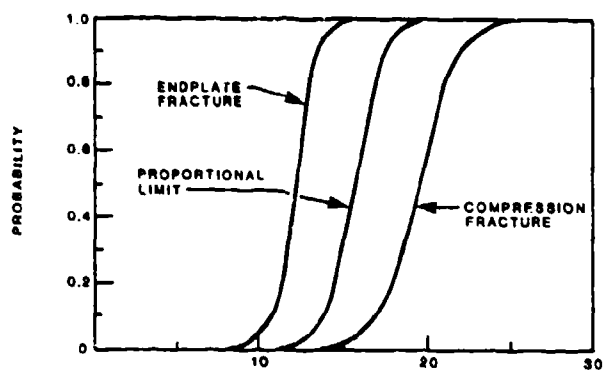
Figure 19. Probability of injury curves for L1-L5
vertebrae during steady state acceleration
(Reference 92).

3.0 DYNAMIC TEST PROGRAM

The dynamic test program was conceived to determine the threshold of spinal injury to $+G_z$ accelerative loading of the type experienced in a helicopter crash. It was theorized that the energy absorber limit-load setting would directly influence the magnitude of loads in the spine, hence the incidence of spinal injury could be greatly reduced by the use and proper selection of the appropriate limit-load factor.

The test matrix was originally comprised of rigid seat tests with three cadavers (tested until spinal fracture occurred) and nine tests with a Norton/Simula production UH-60A Black Hawk energy-absorbing crewseat. The test protocol with the energy-absorbing crewseat called for starting with a 14.5-G energy-absorber limit-load factor, conducting tests with three cadavers at this level, and then reducing the energy-absorber limit-load factor until a threshold for spinal injury was achieved.

However, as testing progressed it became apparent that the threshold for spinal injury in the cadavers used for this study was significantly below that for young, healthy U.S. Army aviators. A technical review meeting was held in Atlanta, Georgia on December 21, 1981 with representatives from all participating organizations. In this meeting it was suggested that there could be a ratio of as much as 2 to 1 between the bone strength of the cadaver population being used and the U.S. Army aviator population (which was the only population in the study at that time).

As a result of this meeting additional tests were added to the test matrix, with funding from the Federal Aviation Administration Technical Center. Eventually, a total of 15 tests were conducted with energy absorber limit-load settings of 14.5, 11.5, and 8.5 G. Also, posttest analysis of the vertebral bone strength for each cadaver was added to the test protocol. It was thought that the bone compression strength data could provide a baseline for interpreting the test-to-test variation in fracture pattern, and to relate the population of cadavers used to the U.S. Army aviator population.

The following pages in this section describe the preparation and testing procedure for the dynamic test program. The dynamic test matrix is included for ease of reference.

3.1 DESCRIPTION OF THE DYNAMIC TEST CONDITIONS

3.1.1 Simulation of Crash Impact Conditions

The impact conditions to which the cockpit area of an aircraft is subjected are controlled by the velocity and attitude at impact, as well as the design characteristics of the fuselage section impacting the ground. Seat orientation to the impact vector is a function of the aircraft orientation at impact and the design angle of the seat, which is usually pitched backward in the aircraft to enhance seated comfort. The velocity change is controlled mainly by the input velocity; however, the restitution characteristics of the fuselage sections crushed during impact can allow the aircraft to attain a significant rebound velocity. The velocity change is a function of the magnitudes of the initial velocity and the velocity achieved during rebound.

The load-deformation characteristics of the landing gear and fuselage sections crushed during impact will also determine the rate of onset, which is a measure of the rate at which loads can build up in the structure, and the maximum impact load in the structure, which is characterized by the peak input deceleration.

In a dynamic impact test of an occupant/seat system, crash forces are simulated by inertial loading that is induced either by acceleration from rest or deceleration from an initial velocity. Although it was originally thought that these conditions were equivalent, Hearon, et al., has recently shown that there is an inherent difference in the two methods due to dynamic preload (Reference 106). Dynamic preload results from the elastic segments of the body and seat (cushions, etc.) having an initial compression due to gravitational or other forces acting prior to the major input deceleration pulse. The effect of dynamic preload is to reduce the amount of dynamic overshoot during impact. In this study, the Wayne State University test facility used the deceleration technique to simulate inertial loading. There was no significant difference between the amount of dynamic preload in the test conditions as compared to an actual crash situation.

A programmable hydraulic ram was used at Wayne State to simulate the load-deformation characteristics of a typical aircraft structure. The nominal input deceleration pulse for this test program was a triangular pulse as shown in Figure 20. It has a peak deceleration of 42 G and a velocity change of 42 ft/sec. The pulse has similar characteristics to the vertical component of the input pulse from Dynamic Test No. 1, MIL-S-58095(AV) (Reference 6).

3.1.2 Occupant Characteristics

This research program was conceived to evaluate the relationship between energy absorber limit-load factor and the potential for spinal injury. Unembalmed human cadavers were selected as human surrogates for the test program. It was believed that in the unembalmed state the tissue properties of the cadavers would most closely represent that of a live subject. Of course, muscle tone and resistance were not present with the cadavers. Evaluation of the energy-absorbing seat performance was based on posttest autopsies of each cadaver to determine the extent, if any, of skeletal injuries.

Additional testing was also conducted with an instrumented Part 572 anthropomorphic dummy. This model dummy was selected because it had the most realistic performance characteristics of any dummy available at the initiation of this study. Government specifications regulate these performance characteristics, and it is commonly used for dynamic testing of energy-absorbing seats. However it should be noted that this dummy and all other currently available anthropomorphic dummies used for crash testing were optimized for the automotive crash environment which has predominately $-G_x$ accelerations. The particular Part 572 dummy used in this study was modified to incorporate a six-axis spinal load cell which played an important role in evaluating the magnitude of spinal injuries.

3.1.3 Energy Absorber Limit-Load Factor

The energy absorber limit-load setting is of particular interest because it directly affects the magnitude of inertial loading in the body. For a

30

constant-load energy-absorbing system, the limit-load factor is normally expressed as a multiple of the effective weight of the occupant plus movable seat weight.* This limit-load factor is set to prevent the accelerative loading in the spine from exceeding tolerable levels. Ideally, the limit load should be set at the highest tolerable level to maximize the use of the available stroke distance in severe crashes. Data gathered from this cadaver test program and from field experience with production energy-absorbing seats should allow the limit-load factor to be optimized. In this study, the relationship between the energy absorber limit load and incidence of spinal injury was examined.

3.2 TEST FACILITIES

The test facility used for this study was provided by the Wayne State University (WSU) Bioengineering Center. This facility had the capability to conduct laboratory-type tests in a controlled, indoor, horizontal decelerator facility and to obtain the necessary cadaver specimens.

The WSU WHAM (Wayne Horizontal Accelerator Mechanism) IV test facility uses a horizontal sled accelerated by pneumatic pressure to within 5 ft of the impact point. During the ensuing constant-velocity phase and prior to impact, a magnetic proximity sensor was used to estimate average velocity over a 1-ft distance. The decelerating mechanism was a hydraulic cylinder in which the pressure was controlled by regulating the flow of hydraulic fluid through a series of orifices. Although the deceleration pulse has a smooth shape, it is characterized by a high rate of onset. A minimal amount of the velocity change is due to rebound. A typical example of the WSU input pulse is shown in Figure 21.

3.3 DYNAMIC TEST PROGRAMS CONDUC   'YNE STATE UNIVERSITY

Two types of test programs were   t WSU. These consisted of:

1) Tests with human cadavers ... both rigid seats and the production UH-60A Black Hawk energy-absorbing crewseat.

2) Duplicate tests conducted with a modified Part 572 anthropomorphic dummy designed to measure spinal loads and moments.

These programs are described in the following sections.

3.3.1 Cadaver Test Series

The cadaver test program was conceived to provide a design base of human body tolerance data for optimization of energy-absorbing seating systems. The main objective was to determine the highest energy absorber limit-load setting that could be tolerated by the human body without acquiring an injury.

---

*The effective body weight is a measure that excludes the weight of the lower extremities from the total body weight, and is typically calculated as approximately 80 percent of the total body weight.

The limit-load threshold was evaluated by conducting dynamic tests with cadavers and assessing the spinal condition following each test.

The dynamic test program conducted at WSU with cadavers utilized two types of seats: a rigid seat and a UH-60A Black Hawk energy-absorbing crewseat. The rigid seat tests were conducted with an input pulse shape that was designed to simulate the response of a constant-load energy absorber. Multiple tests with each cadaver were conducted at increasingly higher acceleration levels until a spinal fracture occurred. However, due to the difficulty encountered in assessing spinal injuries with X-rays, the rigid seat test series was inconclusive. For this reason, detailed results of the rigid seat series are not presented in this report.

The test program with the UH-60A Black Hawk energy-absorbing crewseat was designed to initiate testing at the operational limit-load setting of 14.5 G and gradually reduce the limit load until a threshold was achieved. Originally, it was planned to conduct a purely vertical dynamic test and, if no spinal fracture occurred, a combined-mode test would also be conducted (Section 3.6.1 describes the seat orientation for these sled tests). However, it became apparent after the first test series of 14.5 G that the spinal condition could not be reliably assessed with posttest X-rays. The remainder of the test program followed the protocol of one test per cadaver in the combined mode, which was believed to be more severe, followed by a spinal dissection to determine if an injury had occurred.

As mentioned above, the test series began with a 14.5-G energy absorber limit-load setting. Subsequent series were conducted at 11.5 and 8.5 G. The typical fracture encountered in this test program was an anterior wedge fracture of the vertebral body due to a combination of compressive loading and bending.

Table 2 summarizes the test matrix comprised of the three rigid seat series and the fifteen tests conducted with the energy-absorbing crewseat.

3.3.2 Modified Anthropomorphic Dummy Program

Concurrent with this research effort, the U.S. Army Aeromedical Research Laboratory initiated a program to modify a set of dummies for dynamic testing to assess the feasibility of using this device to evaluate seat performance and the potential for spinal injury (Reference 107). Two anthropomorphic dummies, a 50th-percentile Hybrid II (conforming to the Part 572 specification) and a 95th-percentile Alderson VIP-95 dummy with elastomeric spine, were modified. The modifications consisted of inserting a six-axis load cell at the base of the lumbar spine projecting into the pelvic accelerometer cavity. A schematic drawing of the Hybrid II lower torso is shown in Figure 22 with the installed load cell.

The goal of the modified dummy test program conducted at WSU using the modified Hybrid II was to provide a measurement of spinal load under test conditions identical to those used in the cadaver test series, and to develop a correlation between the energy absorber limit-load factor and spinal load.

32

TABLE 2. SUMMARY OF THE TEST MATRIX FOR THE CADAVER TEST PROGRAM

Test No.	Cadaver No.	Sex	Condition*	Age	Height	Weight (lb)	Seat Type	Peak G_z or E/A Limit Load (G)	Seat Stroke (in.)	Fracture Condition
Rigid Seat Series #1 (3 Runs)	4612	M	E	52	5'10"	161	Rigid	4,6,8	N/A	T9 @ 8 G
Rigid Seat Series #2 (11 Runs)	4654	M	E	49	5'7"	202	Rigid	4 to 30	N/A	T10 & T11 @ 30 G, Compression Failure
Rigid Seat Series #3 (8 Runs)	4660	M	E	51	5'7"	216	Rigid	4 to 30	N/A	T8 @ 13 G, Anterior Wedge Fracture
AFQ20	4784	F	U	44	5'3"	166	Black Hawk	Vertical 14.5 Combined	7.6	None
AF021									5.5	T12, End Plate, C1-C2 Articulation Failure
AF025	4840	M	U	55	5'7"	160	Black Hawk	Vertical 14.5	7.4	L3, Anterior Wedge Fracture
AF028	4850	F	U	61	5'4"	140	Black Hawk	Vertical 14.5 Combined	7.1	None
AF029									4.5	T12, Anterior Wedge Fracture
AFC31	4875	F	U	63	5'5-1/2"	148	Black Hawk	Vertical 14.5	7.1	T9, Compression Fracture

*E = embalmed; U = unembalmed.

33

TABLE 2. SUMMARY OF THE TEST MATRIX FOR THE CADAVER TEST PROGRAM (CONTD)

Test No.	Cadaver No.	Sex	Condition	Age	Height	Weight (lb)	Seat Type	Peak G_z or E/A Limit Load (G)	Seat Stroke (in.)	Fracture Condition
AF033	4921	M	U	52	5'9"	218	Black Hawk	Combined 11.5	9.4	L1, Anterior Wedge Fracture
AF035	4975	M	U	63	5'8"	141	Black Hawk	Combined 11.5	7.0	L3, Anterior Wedge Fracture
AF037	4983	F	U	58	5'3"	160	Black Hawk	Combined 11.5	8.3	L1, Anterior Wedge Fracture
AF039	5229	M	U	52	5'10"	201	Black Hawk	Combined 8.5	12.3	None
AF040	5257	M	U	63	5'6"	142	Black Hawk	Combined 8.5	9.7	L2, End Plate Fracture
AF041	5343	M	U	54	5'10"	165	Black Hawk	Combined 8.5	8.9	None
AF042	99	M	U	47	5'10"	155	Black Hawk	Combined 8.5	9.0	T9, L4, Compression Fracture; C1-C2 Separation
AF043	135	M	U	61	5'10"	147	Black Hawk	Combined 8.5	11.2	T5, T9, Fracture Type Unknown; Multiple Anterior Rib Fractures
AF044	140	M	U	54	5'11"	174	Black Hawk	Combined 8.5	12.2	T12, Fracture Type Unknown; Multiple Anterior Rib Fractures

34

An attempt was made to duplicate test conditions for four cadaver tests conducted at Wayne State University. A summary of this test series is presented in Table 3.

TABLE 3. TEST MATRIX FOR MODIFIED PART 572 ANTHROPOMORPHIC DUMMY SERIES

Test Description	Test No.	Comparable Test No.	Rate of Onset (G/sec)	ΔV (ft/sec)	G	p	Modified Dummy Type	Percen- tile	E/A LL (G)	Test Orienta- tion	Right E/A Load (lb)	Left E/A Load (lb)	Spine-X Load (lb)	Spine-Z Load (lb)
WSU Energy-	WSU-156	AF021	1990	40.5	36.7		Hybrid II	50	14.5	Combined	1101	1087	376	1136
Absorbing	WSU-157	AF037	1890	42.1	38.0		Hybrid II	50	11.6	Combined	923	870	323	866
Seat Series	WSU-158	AF020	1818	-	37.9		Hybrid II	50	14.9	Vertical	1243	1181	396	795
	WSU-159	AF020	1710	41.1	36.7		Hybrid II	50	14.6	Vertical	1304	1204	192	660
	WSU-160	AF035	1610	40.9	36.4		Hybrid II	50	11.5	Vertical	985	908	1660	1923

3.4 EQUIPMENT

Two types of seats were used in the test program: a rigid seat and a UH-60A Black Hawk energy-absorbing crewseat. The rigid seat was used to isolate the effects of the seat, whereas the energy-absorbing seat was used to show the influence of the energy absorber limit-load factor on spinal injury.

The majority of testing was conducted with a production UH-60A Black Hawk crewseat, which has energy absorption capability in the vertical direction and is described in Reference 108. As shown in Figure 23, the seat frame includes two vertical guide tubes which serve as races for the linear bearing, bucket-carrier assemblies. Each bearing assembly contains four contoured rollers located at 90-degree increments to surround the guide tube, thus permitting low-friction translation of the bucket along the axis of the guide tube.

Two energy absorbers that restrain the seat bucket in its vertical position are attached at the upper crossmember of the frame and at the yoke mounted on the vertical adjustment mechanism, which is attached to the seat bucket back. Vertical inertial crash loads force the seat bucket down the guide tubes against the resistance of the energy absorbers, producing an energy-absorbing stroke in that direction. Tensile, inversion-tube type energy-absorbing devices are used on this seat.

The interface between the bucket and the yoke is provided by a T-track mounted on the back of the seat bucket, a sliding fitting with T-slot (through which the T-track passes) attached to the yoke, and a spring-loaded adjustment locking pin. Withdrawal of the pin releases the attachment between the seat bucket and frame so that the seat weight is carried by counterbalance springs, which were removed for all testing on this program. Five inches of vertical position adjustment are provided by this mechanism. Longitudinal adjustment is achieved by releasing spring-loaded adjustment locking pins in each of the front track fittings, permitting 5 in. of fore and aft adjustment.

The bucket of the production seat, in its operational configuration, provides ballistic protection and structural support for the bottom, back, and sides of the thighs of the occupant.

35

3.4.1 Cushions

The standard bottom cushion used in the UH-60A crewseat bucket is a unique design that maximizes comfort and crash safety. The surface of the cushion is contoured to distribute load over the greatest buttocks area, in order to minimize any local concentration of loading that would cause discomfort. The cushion base is made from foamed polyethylene, and the contour is lined with a thin layer of Temperfoam to distribute local loads and maximize comfort. Temperfoam is a loading-rate-sensitive polyurethane foam to help develop a more rigid, yet comfortable, link between the occupant and the seat bucket.

A final layer of reticulated polyurethane foam is provided for both load distribution and thermal comfort. The cushion is enclosed in a protective covering of fire-retardant, open-weave nylon material. Also, provisions are made to allow fore and aft circulation of air that can pass through the open-celled, reticulated foam for cooling purposes.

The back and lumbar support cushions are of typical design, using standard upholstery foam and open-weave nylon covers. The headrest cushion is formed of Temperfoam for cushioning of head impact. A new bottom cushion core was inserted into the nylon cover for each test. Back cushions and headrest cushions were reused throughout the test series.

3.4.2 Energy Absorbers

Each of the energy-absorbing devices on the production seat exerts a constant load during stroking. As illustrated in Figure 24, these devices make use of the inversion of a thin-walled ductile aluminum tube. The total energy absorber load is determined by multiplying a given load factor times the total moving weight of seat and occupant. For the UH-60A Black Hawk, the weight of the stroking part of the seat is 60.6 lb. Adding the effective weight of the 50th-percentile Army aviator, 139.0 lb, the total movable weight is 199.6 lb, which when multiplied by a load factor of 14.5 G gives a total dynamic stroking load of 2894 lb.*

The stroking load of the energy absorber is determined by the diameter and wall thickness of the inverting tube. Two test series were also conducted at WSU using energy absorbers with reduced limit load factors of 11.5 and 8.5 G which gave dynamic stroking loads of approximately 2295 and 1697 lb, respectively. Figure 25 illustrates the dynamic energy-absorbing load as a function of time measured in one of the cadaver tests which used a 14.5-G limit-load factor.

3.4.3 Restraint System

A five-point restraint system with a lap belt tiedown strap was used in the UH-60A Black Hawk crewseat tests. As illustrated in Figure 26, adjusters were provided in both shoulder straps and both lap belt straps, and the buckle was a rotary-release type, backed by a comfort pad. The webbing used in this restraint system was of the low-elongation polyester type.

---

*Total weight of 50th-percentile U.S. Army aviator is 174 lb, therefore, the effective weight is $(0.8) \times (174 \text{ lb}) = 139.0$ lb.

3.5 CADAVER SELECTION

Cadavers were provided by Wayne State University and used as seat occupants for the tests.

3.5.1 Cadaver Specifications

The cadaver selection process was as follows:

- When a cadaver became available, Wayne State University provided cadaver specifications (age, sex, body weight, height, cause of death) to the Air Force Contract Monitor (at AFAMRL).

- The Contract Monitor then polled the parties involved to determine whether the cadaver was suitable for this test program.

- Suitability of each cadaver as a test specimen was, in some cases, determined by radiographic examination of the spinal column to rule out preexisting conditions.

Due to the possibility of exceeding available seat stroke, with the inherent danger of spinal damage, the upper weight limit on cadavers was set at 200 lb. The lower weight limit was left to the discretion of the research team. Due to the difficulty in obtaining cadavers for testing, the cadaver selection process was not as restrictive as desired. The cadavers selected were considered to be a poor representation of the U.S. Army aviator population. This factor complicated the analysis of results from the test program.

In the course of the test program, USAARL expressed concern about selecting postmenopausal female cadavers due to the prevalence of osteoporosis, which could lead to substantially lower bone strength. Some of the older female cadavers did exhibit signs of osteoporosis, so after the ninth test with the energy-absorbing crewseat, the cadaver selection process was altered to accept only male specimens.

3.6 STANDARDIZED TEST PROCEDURES

The following standardized procedures for orienting the seat, maintaining the seat, and handling the cadavers were used.

3.6.1 Seat Orientation for Horizontal Sled Tests

For the tests conducted in the vertical configuration at Wayne State University, the seat was pitched forward 17 degrees with respect to the velocity vector. This configuration is illustrated in Figure 27. The first 13 degrees of pitch were provided to align the back tangent line with the horizontal surface of the sled, or parallel to the velocity vector. This was done to eliminate initial extension of the spine that would be caused by an angle oriented downward to the seat back. The additional 4 degrees of pitch were added to counteract the 1 G of gravity that reduces the overturning moment on the cadaver. Thus, under stroking loads the overturning moment on the cadaver was somewhat corrected for the 1 G of gravity, duplicating the response of a seat in the upright-oriented position in a vertical drop. For the combined orientation tests on the horizontal sled facilities, the seat was pitched forward 34 degrees from the velocity vector.

3.6.2 Seat Preparation

The UH-60A Black Hawk crewseat was locked in the top of the vertical adjustment range for all tests. For each test, the seat was locked in the middle of the fore and aft adjustment range.

The seat was inspected for damage prior to each test, and the four linear bearing assemblies were replaced after every five tests. A new set of energy absorbers and a new seat bottom cushion were installed for each test.

3.6.3 Cadaver Preparation and Handling

Following instrumentation, each cadaver was dressed in a tight-fitting garment to insure a repeatable cadaver/seat interface and to enable tracking the cadaver motion unencumbered by the motions of loose clothing. Prior to the first test with a cadaver, targets were positioned on the head, shoulder, hip, and knee joints for use in film analysis.

A complete pretest series of X-rays were performed for each cadaver. The nine-axis head accelerometer cluster was attached to the maxilla (or to the cranium) with screws.* The initial position and orientation of each accelerometer relative to the coordinate system of the head was established with X-rays. A triaxial accelerometer mount was attached to the posterior process of one of the lumbar vertebra, and its location was also established with X-rays. However the usefulness of this instrumentation was questionable since it was difficult to establish the spatial orientation of the accelerometers in the seat coordinate system.

Upon completion of the specimen preparation, the cadaver was placed in the test seat. The following sequence was followed when placing the cadaver in the seat to insure repeatable positioning:

- The cadaver's upper torso was folded forward around the hip joints until the torso touched, or was as close as possible to, the thighs.

- The cadaver was placed in the seat and its buttocks pushed into the seat back as far as possible.

- The cadaver's upper torso was rotated around the hip joints and forced against the back of the seat. The rotation of the cadaver's torso tended to push it further back in the seat.

- The restraint system was fastened and adjusted as follows:

  - All fittings were inserted into the buckle with the inertia reel locked.

  - The lap belt and shoulder straps were adjusted by pulling the free end of the straps toward the buckle with an approximate 30-lb force.

---

*A nine-axis accelerometer cluster was used in order to determine linear and rotational acceleration of the head.

38

- An 80 in.-lb torque was applied directly to the inertia reel to tighten the inertia reel strap.

● The locations of the targets were measured from a selected reference point on the seat for the first test and for each subsequent test using the same cadaver. (There was a unique target location for each different cadaver.)

● The cadavers were not fitted with a helmet. The head was restrained with a thin band of duct tape used to maintain its initial position during the acceleration portion of the sled run.

● The feet of the cadaver were positioned firmly against a load-bearing footrest set at an angle of 40 degrees. The feet were attached to the footrest with duct tape.

3.7 INSTRUMENTATION

The following instrumentation were used in the tests at WSU:

	Number of Channels
Accelerometers	
● Seat bucket, triaxial (aircraft axes)	3
● Seat bucket, vertical (parallel to the seat back tangent line), (redundant)	1
● Chest, triaxial*	3
● Pelvis, triaxial	3
● Head, triaxial (A nine-axis accelerometer was used in the cadaver tests)	3
● Sled platform (parallel to velocity vector)	1
● Sled (parallel to velocity vector) (redundant)	1
● Fixture, triaxial (aircraft axes)	3
Loads	
● Strain-gaged energy absorber clevises	2
● Restraint system webbing tensiometers (as shown in Figure 28)	5
● Footrest loads (2 channels for each foot)	4
● Spinal loads, triaxial*	3
● Spinal moments, triaxial*	3

*Dummy tests only.

Displacement

- Vertical, parallel to guide tubes, attached   1
  to bucket on centerline, either below seat
  reference point for operation in retraction
  mode or near headrest for operation in ex-
  tension mode
- Vertical, parallel to guide tubes (redundant)   1
- Longitudinal, perpendicular to guide tubes,   1
  attached at center of upper crossmember
  (not used in all tests)

Impact Switch

- 1 channel for each data tape   <u>1</u>

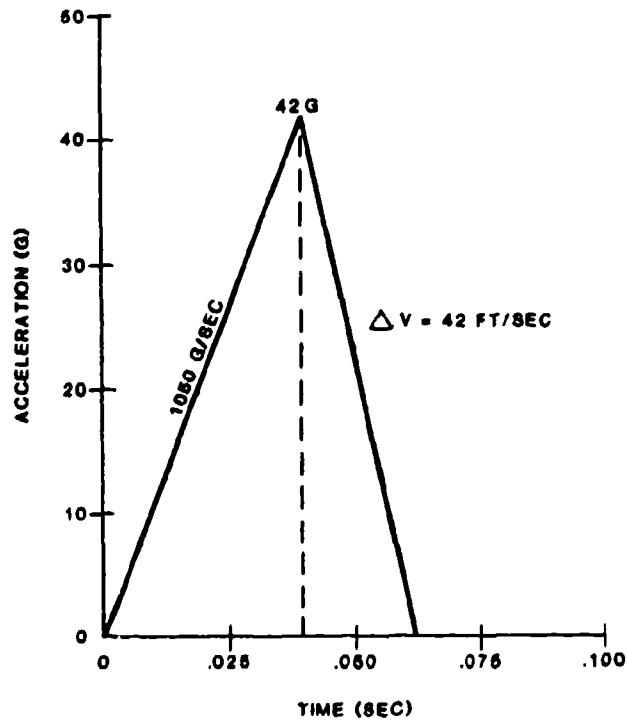   39

Figure 20. Triangular deceleration pulse describing
the nominal test condition.
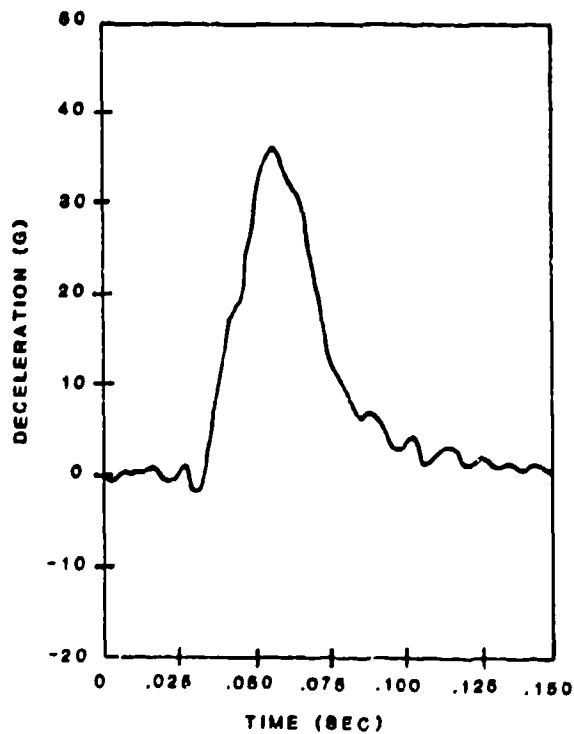
Figure 21. Typical baseline deceleration pulse for the
Wayne State University test facility.

41

LUMBAR
SPINE

LOAD
CELL

ACCELEROMETER
CAVITY
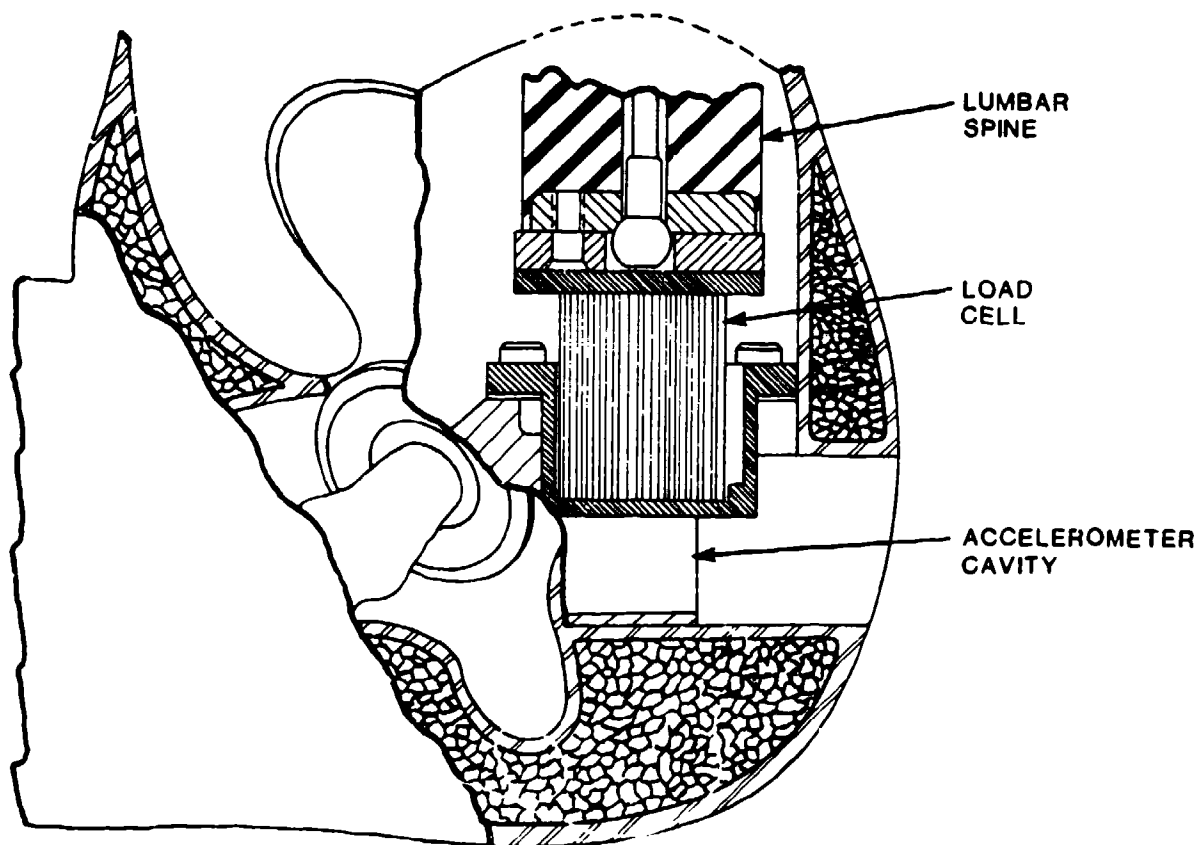
Figure 22. Part 572 pelvic segment with lumbar
spine and load cell assembly.
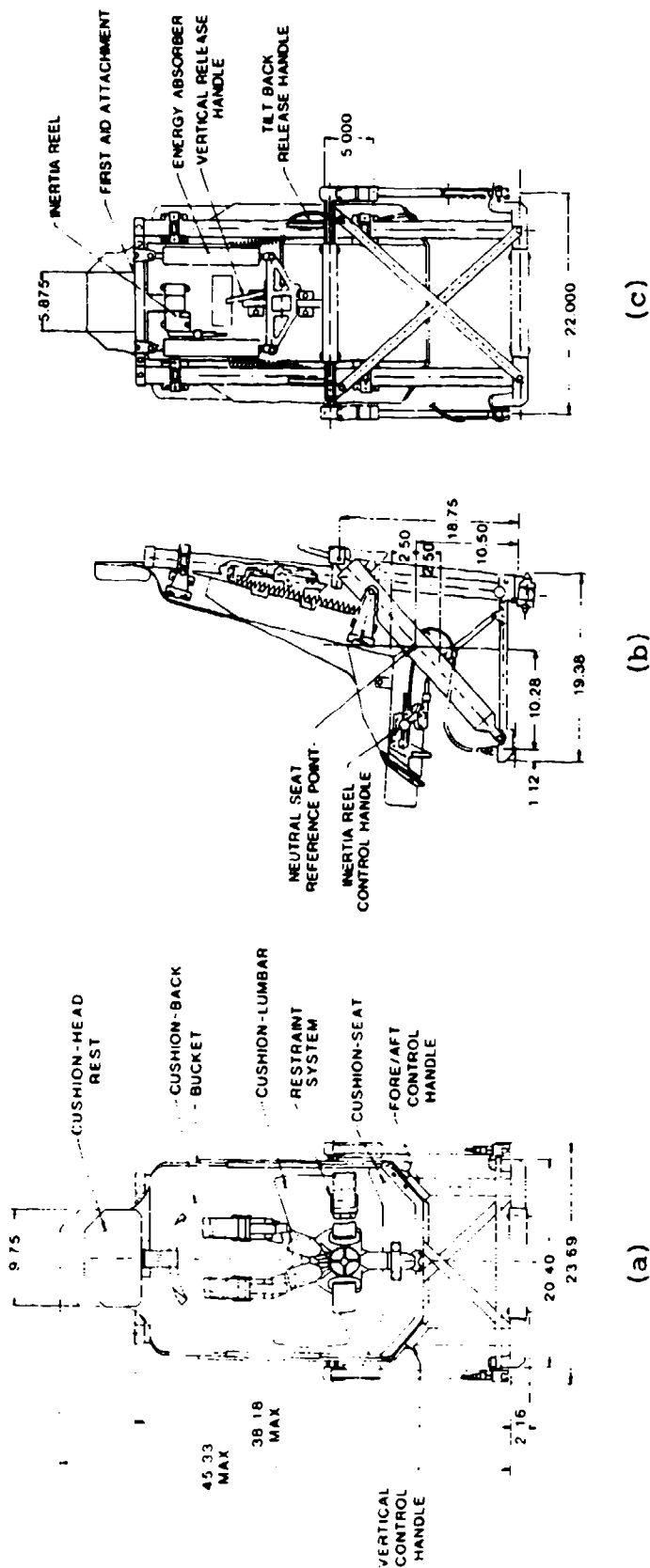
Figure 23. UH-60A Black Hawk crewseat assembly.

43

STROKED

PARTIALLY STROKED
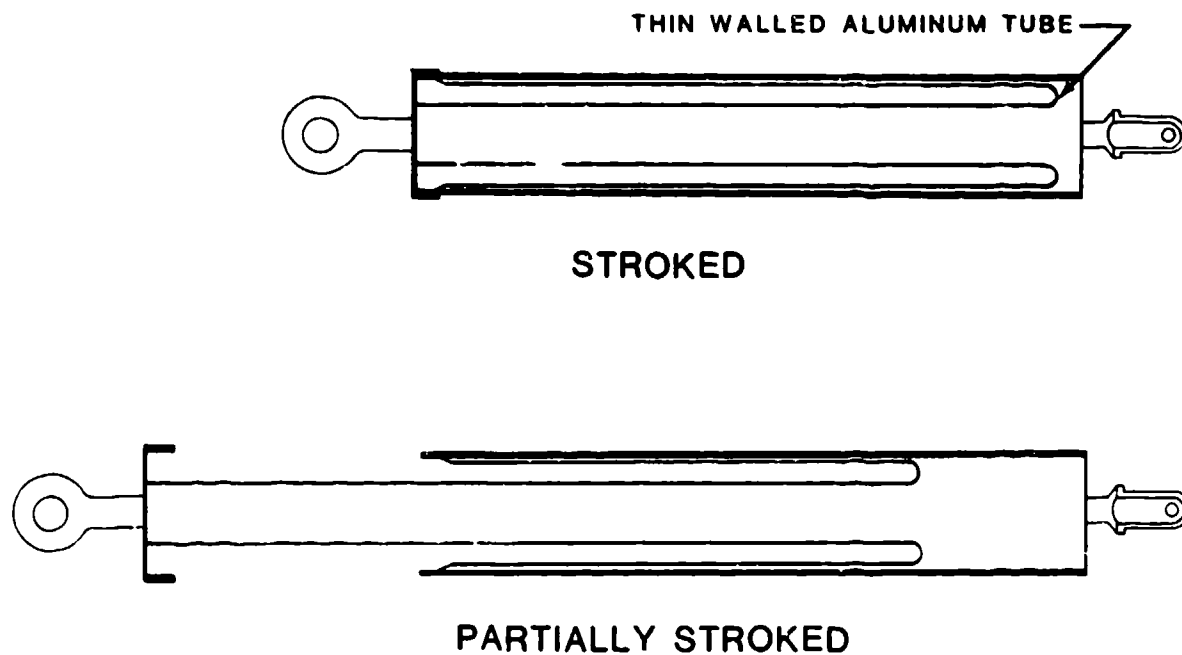
Figure 24.   Cross-sectional view of an inverted-tube energy absorber.

TIME (MS) X 10
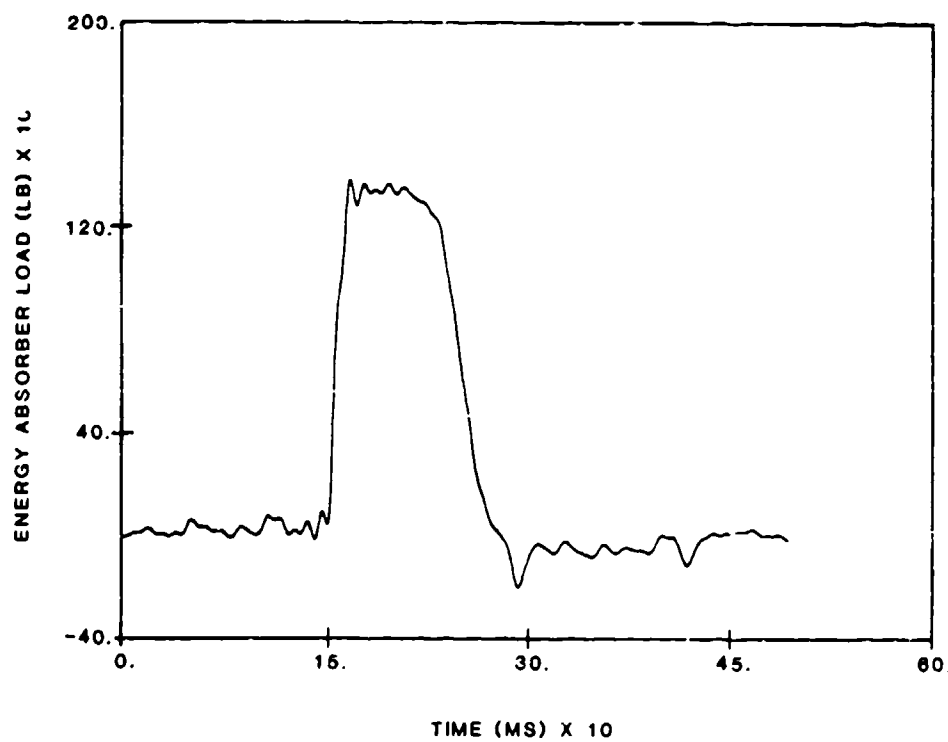
Figure 25.   Typical recorded time-history of an
inversion tube energy absorber load.

44

Inertia reel

Inertia reel strap

1.75-in.-wide
webbing

Shoulder
harness

Adjuster

2.00-in.-wide
webbing

Lower shoulder
strap

Pad

Rotary buckle

Plug-in fitting

Adjuster

Lap belt

2.25-in.-wide
webbing

Lap belt
anchor

Fixed fitting on
tiedown strap

Tiedown strap

1.75-in.-wide webbing

Tiedown anchor
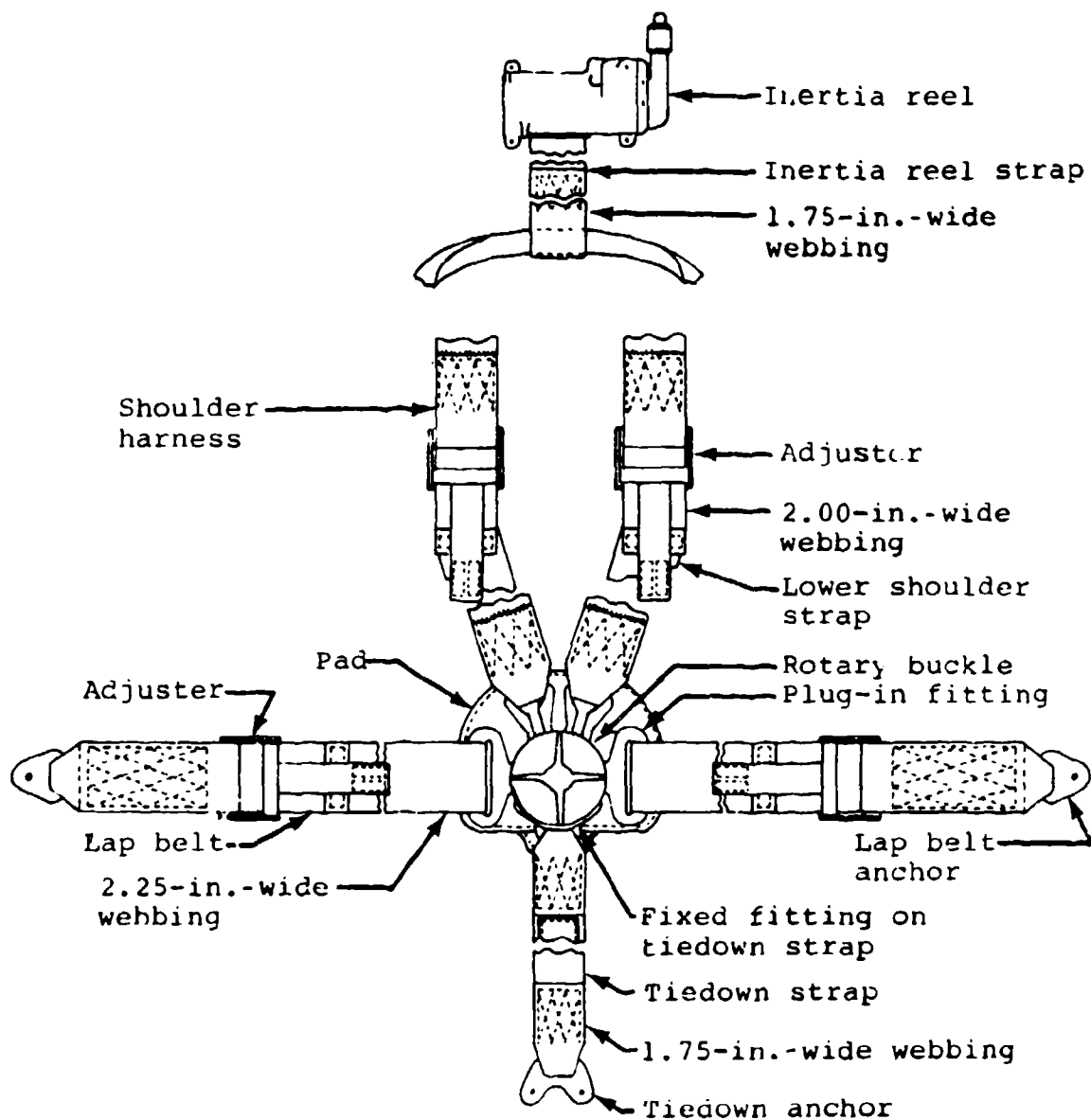
Figure 26. UH-60A restraint system.
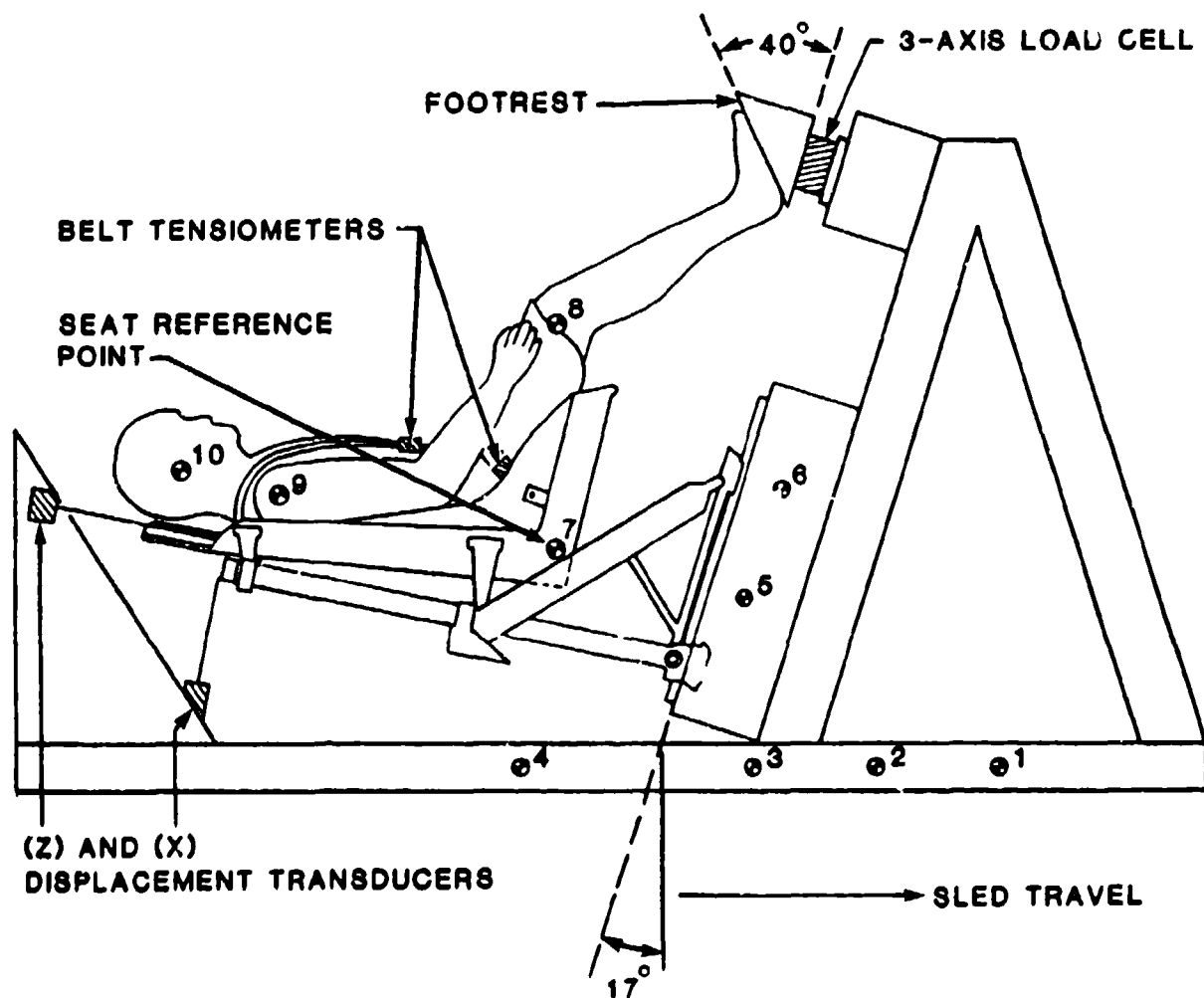
Figure 27. Vertical test, horizontal sled configuration (WSU).

Inertia reel

Inertia reel strap

1.75-in.-wide webbing

2.00-in. wide webbing

Shoulder harness

Adjuster

2.00-in.-wide webbing

Lower shoulder strap

Tensiometer in adapter

Tensiometer in adapter

Rotary buckle

Plug-in fitting

2-1/4-in. tensiometer

Pad

2-1/4-in. tensiometer

Adjuster

Lap belt

2.25-in.-wide webbing

Lap belt anchor

Fixed fitting on tiedown strap

Tensiometer

Tiedown strap

1.75-in.-wide webbing

Tiedown anchor

Figure 28.   Tensiometer placement on occupant restraint system.

47

4.0 BONE STRENGTH ANALYSIS

4.1 INTRODUCTION

In order to determine the quality of the spinal injury data obtained from the
dynamic test program, and in order to provide a method of normalizing that
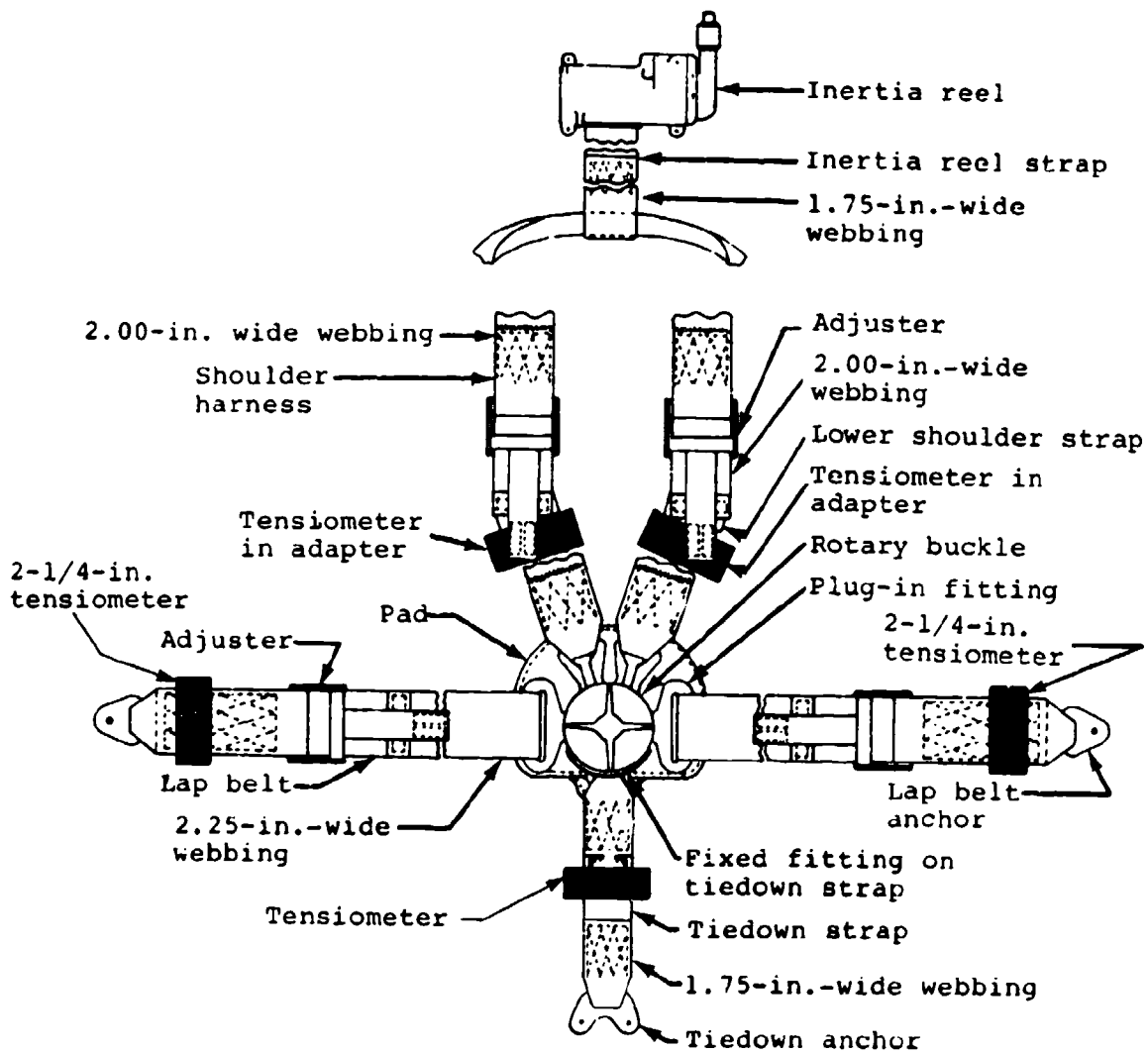data, a bone strength analysis was formulated. Vertebral compression tests
and a mineral analysis of each nonfractured vertebra were conducted by the
U.S. Air Force Aerospace Medical Research Laboratory (AFAMRL) and by Pollu-
tion Control Sciences, Inc. (PCS), Naimisburg, Ohio.

4.2 DESCRIPTION

The vertebral column sections, including damaged areas, were excised from the
cadavers used in the Black Hawk seat impact simulation tests conducted at
Wayne State University. AFAMRL radiographed and then stored these samples at
approximately -20°C to await both compression testing and mineral analysis.
The following description of the test procedures is based on reports provided
by Captain E. Paul France and Lt. Kristin N. Swenson, both of AFAMRL.

4.2.1 Compression Testing

In preparation for compression testing, the vertebral columns were thawed and
sectioned into separate vertebrae. Each vertebra was further prepared by elim-
inating all surrounding soft tissue including muscles, ligaments, and inter-
vertebral disc material, and by removing the posterior process at the base of
the pedicle. The posterior and anterior heights of the remaining prepared
centrum were measured with a micrometer to the nearest .01 cm. The superior
and inferior bony end plate surfaces were photographed at 3X magnification
using a Polaroid camera. From these photographs, the pretest average area
was measured for each specimen. The specimens were then stored in sterile
water at 4°C.

Polymethylmethacralate was used to make thin platens for the superior and in-
ferior surfaces of the centrum. These platens provided parallel load trans-
mission surfaces to uniformly distribute the compressive force across the en-
tire bony end plate surface. The specimens were refrozen for an additional
period of two weeks before testing.

The compression tests were performed with an MTS Universal Testing System.
The prepared vertebral centrums were compressed to 70 percent of the original
height (that being the average between posterior and anterior height measure-
ments) at a constant displacement rate of 210 in./min.* In all cases, these
constraints were sufficient to cause failure. Typically, the ultimate com-
pressive load was achieved at 3 to 10 percent reduction in vertebral segment
height, the bone structure then realigned itself and was able to sustain ad-
ditional, although lower, compressive load.

---

* AFAMRL selected the compressive loading rate of 210 in./min. as a standard
  for these tests based on results from previous test programs.

The raw data obtained from each test, combined with height and average load area, were reduced to provide load displacement curves and values for engineering strength parameters.

A sample of the output data can be found in Appendix C. The parameters include ultimate load (lb); displacement (in.); stress, which was calculated by dividing ultimate load by the pretest average area for each specimen (lb/in.^{2}); strain (in./in.); and strain energy (in.-lb). After testing, the specimens were refrozen in the sterile water in which they had been stored to await mineral analysis.

4.2.2 Bone Mineral Analysis

After compression testing, the vertebral centrums were sent to PCS where they were subjected to a destructive mineral analysis. The weight percent of calcium, the weight percent of phosphorus, and the calcium to phosphorus ratio were determined for each vertebra of each cadaver.

The samples were prepared for analysis using basic established drying, weighing, and nitric acid digestion techniques. Each centrum was placed in a desiccation chamber for dehydration and removed when a constant weight was achieved after three consecutive weekly measurements. The fat was not extracted from the bone prior to drying. The bone was then digested in nitric acid solution and used to determine the calcium and phosphorus content. Also, the distilled water in which the bone had been stored was filtered to extract the ions that went into solution.

Vertebral centrum phosphate content was determined colorimetrically. The basic chemical procedure was to form phosphomolybdic acid by adding ammonium molybdate and potassium antimonyl tartrate in an acid medium to the sample.

The addition of ascorbic acid to this solution reduced the phosphomolybdic acid to intensely colored molbydenum blue. The color change was determined with the Hitachi Model 102 Spectrophotometer. The sample phosphate content was determined from standard curves.

Vertebral centrum calcium content analyses were performed with flame atomic absorption spectrophotometry. Standard practices and procedures for sample preparation and analysis were followed. Serum calcium measurements were obtained by using an atomic absorption spectrophotometer. A nitrous oxide/acetylene flame was used in these analyses to eliminate the need for extensive sample pretreatment for the removal of serum matrix elements. Flame-induced calcium ionization problems were removed by the addition of potassium to the serum sample before analysis. Digested vertebral centrum calcium determinations were made with an Instrumentation Laboratory Model 951 Atomic Absorption Spectrophotometer. Standard curves were used to determine calcium concentration.

The mineral analysis data comprises Appendix D. Included in the tabulated data is the dry weight of each vertebral centrum, and the weight percentage of calcium and phosphorus which was measured against the dry weight for every specimen.

49

4.3 USE OF THE BONE STRENGTH ANALYSIS DATA

An analysis based on the ultimate compressive load, stress, and the calcium content properly describes the bone strength for each vertebra. A collective data analysis of all the vertebrae for each cadaver reveals an overall strength of the vertebral column. Specifically however, the vertebral ultimate compressive strength was used in conjunction with the dynamic test data to determine the quality of the spinal injury data. The ultimate compressive strength of the L5 vertebral body was used to normalize the dynamic test data. Section 5.0 describes the data analysis process.

50

5.0 ANALYSIS OF RESULTS

5.1 ANALYSIS METHODOLOGY

The goal of the analysis described in this section was to provide a baseline
for interpreting the spinal injury data developed in the dynamic testing pro-
gram. The question that needed to be answered was "How can a threshold
energy absorber limit-load setting be established based on tests conducted
with cadavers that do not represent the populations in question, i.e., U.S.
Army aviators and U.S. adult civil flying populations?" In the initial
planning stages of this study it was suggested that this might be accom-
plished by evaluating the vertebral compression strength of each cadaver and
using these data as a baseline to assess each injury received during the
dynamic test program. With this in mind the spinal column of each cadaver
was excised following the dynamic test, segmented into individual vertebral
bodies, and subjected to testing (as described in Section 4.0) to provide an
estimate of the actual strength. However, it was not until later in the
research effort that a method was devised to normalize the injury data. This
methodology is described below.

The premise for conducting this analysis was based on the following two
assumptions:

1. If a spinal fracture occurred it was caused by an applied load
   within the spine, and this applied load was proportional to the
   energy absorber limit-load setting.

2. The ability of the vertebral body to resist the applied load was
   directly related to its ultimate compressive strength.

The goal then was to use the ratio of applied load to available compressive
strength as a measure of susceptibility to fracture in each test for each in-
dividual cadaver. If a pattern could be established between this "spinal
load/strength ratio" and the actual injuries, then this ratio could be used
to determine the injury potential for any population using the vertebral com-
pressive strength for this group.

In the course of conducting this analysis it was found that a measure such as
the spinal load/strength ratio did have merit in assessing the relative poten-
tial for spinal injury. The following sections describe this analysis in de-
tail.

5.2 SPINAL LOAD/STRENGTH RATIO (SLSR)

The parameter used to assess the potential for spinal injury was the SLSR.
The SLSR was nominally defined as:

$$\text{SLSR} = \frac{\text{Applied Axial Spinal Load}}{\text{Ultimate Compressive Strength}}$$

51

5.2.1 Estimation of Applied Axial Spinal Load

Ideally, the applied axial spinal load would have been measured at the actual site of the fracture during the dynamic test. Obviously, an invasive measurement procedure such as this could in itself alter the test results. The procedure that was followed to establish a measure of the spinal load was to conduct additional dynamic tests using a modified Part 572 anthropomorphic dummy.* A six-axis load cell was incorporated at the base of the elastomeric spine in the modified dummy, analogous to the L5 vertebral position in a human. Tests were conducted at Wayne State University to duplicate specific test conditions from the cadaver test series.

The parameter of interest from these tests with the instrumented dummy was the axial (z-axis) spinal load. Figure 29 shows the trends in the spinal load as a function of the energy absorber limit-load factor for the two test orientations.

It was found that the combined orientation resulted in higher axial lumbar loads. The correlation shown in Figure 29 was used to assess the magnitude of the applied load for each cadaver test. It is not known if the forces measured in the instrumented dummy would closely approximate the magnitude of forces measured in a human spine. However, for the analysis conducted in this section, a relative comparison of the severity of each test was of primary importance. The use of the instrumented dummy as a "calibrated test device" providing a relative measure of spinal loading appeared to be justified as the most appropriate approach available.

The procedure for calculating the applied load for each cadaver test was as follows.

(1) Calculate the effective energy absorber limit-load factor:

$$\text{Effective Energy Absorber Limit-Load Factor} = \frac{\text{Energy Absorber Forces}}{\text{Moveable Seat Weight} + \text{Effective Occupant Weight**}}$$

$$= \frac{(\text{Measured Right Energy Absorber Force} + \text{Measured Left Energy Absorber Force})}{60.1 \text{ lb} + 0.8 \text{ (Cadaver weight)}}$$

(2) Using the effective energy absorber limit-load factor and the test orientation, Figure 29 was used to predict the lumbar spinal loads.

---

* Developed by Simula Inc. under U.S. Army Contract DAMD17-81-C-1175 (Reference 107).

** The effective occupant weight is a measure of the body weight supported by the seat. It has been experimentally measured as approximately 80 percent of the total body weight.

5.2.2 Vertebral Compressive Strength

The vertebral compressive strength used in the calculation of the spinal load/strength ratio was based on the vertebral compression tests described in Section 4.0. For each cadaver a number of individual vertebral segments were compressed to failure. Figure 30 shows the trends in the measured ultimate compressive loads as a function of vertebral level in the spine for each cadaver.

The spinal load/strength ratio was calculated using the L5 ultimate compressive load for each cadaver to normalize the test data since the L5 vertebral level corresponds to the approximate location of the load cell in the instrumented dummy.

A linear least-squares approximation was used to fit the experimentally measured compression test data shown in Figure 30 for each cadaver. The reasons for using the least-squares approximation were: 1) to try to remove some of the anomalies from individual compression tests, and 2) to extrapolate to the L5 vertebral level for cadavers in which the compression tests were not conducted at the L5 spinal level. Instead of using the experimentally measured L5 compressive strength values for those cadavers that had them, the least-squares approximation was still used for consistency. Table 4 shows the least-squares correlation parameters (slope, intercept, and correlation coefficient) and the resulting L5 ultimate load strength. Also tabulated is the experimentally measured L5 compressive strength for the respective cadavers. The predicted L5 ultimate compressive strength shown in Table 4 was used in the calculation of the spinal load/strength ratio for each cadaver test.

5.2.3 Calculation of the Spinal Load/Strength Ratio (SLSR)

Table 5 shows the calculation of the spinal load/strength ratio for each individual cadaver test condition. The actual formula used for calculating the SLSR was:

$$SLSR = \frac{\text{Predicted Lumbar Spinal Load (lb)}}{\text{Predicted L5 Ultimate Compressive Strength (lb)}}$$

Note in Table 5 that the magnitude of the SLSR is always below a value of 1.0. If the lumbar spinal load predicted from the instrumented dummy tests is approximately the correct value then this is an indication that actual segments fail under crash conditions at a fraction of the compressive strength of the vertebral body. This is expected due to the difference in load-bearing area between the compression test and actual vertebral loading conditions. Figure 31 illustrates this difference in effective load-bearing area for the two conditions. In the case of the compression test, the entire vertebral area is loaded in compression. For the loading condition that combines compression and forward bending of the vertebral bodies, the loads are distributed unevenly, concentrating on the anterior segment of the vertebral body.* Thus, it would be expected that the load required to cause fracture

---

*Even for pure vertical loading on the body, there will be a moment about the spinal column causing forward rotation since the c.g. of the body is forward of the spinal axis.

53

TABLE 4. LEAST-SQUARES APPROXIMATION OF VERTEBRAL COMPRESSIVE
STRENGTH VALUES FOR EACH CADAVER

Test No.	Cadaver	Slope	Intercept	Correlation Coefficient	Predicted L5 Ultimate Compressive Strength (lb)	Measured L5 Ultimate Compressive Strength (lb)
AFO20	4784	63	541	1.0	1612	1612
AFO21	4784	63	541	1.0	1612	1612
AFO25	4840	143	-681	0.91	1750	1973
AFO28	4850	145	-273	0.91	2192	N/M
AFO29	4850	145	-273	0.91	2192	N/M
AFO31	4875	91	55	0.91	1602	N/M
AFO33	4921	-	-	-	-	-
AFO35	4975	72	530	0.95	1754	1921
AFO37	4983	149	176	0.97	2709	2785
AFO39	5229	168	1025	0.92	3881	N/M
AFO40	5257	75	370	0.95	1645	N/M
AFO41	5343	91	802	0.67	2349	N/M
AFO42	99	141	-463	0.89	1934	N/M
AFO43	135	98	-73	0.67	1593	N/M
AFO44	140	28	678	0.26	1154	N/M

N/M = Not Measured.

TABLE 5. CALCULATION OF THE SPINAL LOAD/STRENGTH RATIO FOR EACH CADAVER TEST

Test No.	Cadaver No.	Energy-Absorber Limit Load Factor (g)	Effective Energy-Absorber Limit Load Factor (g)	Test Orientation*	Extrapolated Lumbar (L5) Spinal Load** (lb)	Predicted L5 Ultimate Compressive Strength*** (lb)	Spinal Load/Strength Ratio SLSR	Vertebral Fracture Pattern
AF020	4784	14.5	14.26	V	805	1612	.4994	NO FX
AF021	4784	14.5	13.77	C	1067	1612	.6619	T12-L1
AF025	4840	14.5	13.80	V	760	1750	.4343	L3
AF028	4850	14.5	14.99	V	873	2192	.3983	NO FX
AF029	4850	14.5	14.37	C	1124	2192	.5128	T12
AF031	4875	14.5	14.23	V	803	1602	.5012	T9
AF033	4921	11.5	8.75	C	598	N/M	N/M	L1
AF035	4975	11.5	12.28	C	929	1754	.5296	L3
AF037	4983	11.5	10.94	C	804	2709	.2968	L1
AF039	5229	8.5	6.57	C	396	3881	.1020	NO FX
AF040	5257	8.5	7.74	C	507	1645	.3082	L2
AF041	5343	8.5	7.53	C	486	2349	.2069	NO FX
AF042	99	8.5	8.00	C	529	1934	.2735	T9,L4
AF043	135	8.5	8.41	C	568	1593	.3566	T5-T9
AF044	140	8.5	7.59	C	491	1154	.4255	T12

*V = Vertical Mode, C = Combined Mode.

**Based on spinal load correlation shown in Figure 29.

***Based on linear regression analysis.

N/M = Not measured.

would be much smaller in the latter case compared to compression test data. Ewing, King, and Prasad have shown that the ability of the spine to withstand vertical loading (in ejection seats) can be greatly increased by providing proper alignment and support of the spine to maintain a large load-bearing area (Reference 109).

Table 6 shows a listing of tests arranged according to numerical value of the spinal load/strength ratio. The data have been divided into three groupings, and the rate of spinal injury occurring in each grouping has been calculated. There appears to be a definite trend that increasing the ratio of applied load to available compression strength increases the chances of spinal injury. This trend is plotted in Figure 32, which indicates that to maintain a 10-percent injury rate the spinal load/strength ratio should be kept at or below 0.26 by appropriately selecting the energy absorber limit-load factor.

5.3 PREDICTED SPINAL INJURY RATE

The spinal injury rate for various populations can be predicted based on the correlation shown in Figure 32, which was derived from the individual cadaver tests. The two populations in question in this study were the U.S. Army aviators and the U.S. adult civil flying population.

Figure 33 shows a comparison of the age distribution for these two populations. The mean age of the U.S. Army aviators and the U.S. adult civil flying population is 26 and 44 years, respectively.

The vertebral compression strengths for these populations, based on data for the mean age, are shown in Figure 34. The U.S. Army Aviator population is represented by the compression test data reported by Kazarian and Graves for four young male cadavers with a mean age of 31 years (Reference 18). The second population, the U.S. adult civil flying population, is based on the compressive strength data for the cadavers used in this study, which ranged in age from 44 to 63. Their mean age was 56 years, which is older than the adult civil mean of 44 years and therefore inserts some conservatism in conclusions for this group being based on the cadaveric sampling.

Using the data contained in Figure 34 for the compressive strengths, the spinal injury rate shown in Figure 32, and the correlation between peak spinal load and energy absorber limit-load factor from Figure 29, the most important correlation can be achieved. This correlation, shown in Figure 35, presents the estimated spinal injury rate as a function of the energy absorber limit-load factor for both populations. This curve is based on the assumption that the vertical mode test condition represents the most probable impact scenario for helicopter accidents. Table 7 lists the data used to calculate the correlation shown in Figure 35.

The graph shown in Figure 35 for the U.S. Army aviator population predicts that a 14.5-G energy absorber limit-load setting would result in a spinal injury rate of approximately 20 percent. Although these curves are based on a limited number of cadaver tests, actual field experience with the UH-60A Black Hawk crewseat (with a 14.5-G energy absorber limit-load setting) appears to fall within or below this correlation. Out of 14 accident victims, three received spinal injuries. Out of these three injuries, one injury was not believed to be related to the seat functioning and two injuries occurred

TABLE 6. SPINAL INJURY RATE BASED ON GROUPING
OF TEST DATA ACCORDING TO THE SPINAL
LOAD/STRENGTH RATIO

Test No.	Cadaver No.	Spinal Load/Strength Ratio	Fracture Pattern	Ratio Grouping	Spinal Injury Rate (%)
AF039	5229	0.1020	No Fx	0.0000-	
AF041	5343	0.2069	No Fx	0.2499	0
AF042	99	0.2735	T9,L4		
AF037	4983	0.2968	L1		
AF040	5257	0.3082	L2		
AF043	135	0.3566	T5,T9	0.2500-	75
AF028	4850	0.3983	No Fx	0.4999	
AF044	140	0.4255	T12		
AF025	4840	0.4343	L3		
AF020	4784	0.4994	No Fx		
AF031	4875	0.5012	T9		
AF029	4850	0.5128	T12	0.5000-	
AF035	4975	0.5296	L3	0.7499	100
AF021	4784	0.6619	T12-L1		

TABLE 7. DATA USED TO CALCULATE THE SPINAL INJURY RATE - ENERGY ABSORBER LIMIT-LOAD CURVE

	I Spinal Injury Rate Percent	II Spinal Load/Strength Ratio*	III L5 Ultimate Compressive Strength (lb)**	IV Spinal Load (lb)***	V Effective E/A Limit Load Factor Combined Mode (G)+	VI Effective E/A Limit Load Factor Vertical Mode (G)+
U.S. Army Aviator	10	0.26	2,669	693.9	9.7	13.0
	15	0.28	2,669	747.3	10.4	13.7
	50	0.46	2,669	1227.7	15.4	18.7
U.S. Adult Civil Flying Population	10	0.26	1,914	497.6	7.8	11.0
	15	0.28	1,914	535.9	8.1	11.4
	50	0.46	1,914	880.4	11.8	15.1

* From Figure 32.
** From Figure 34.
*** Column IV shows the product of Columns II and III.
+ From Figure 29.

with extenuating circumstances.* Thus, an injury rate between zero percent (0 out of 13 injuries) to 15 percent (2 out of 13 injuries) has been established under actual crash conditions.

5.4 ACCEPTABLE SPINAL INJURY RATE

The goal of this study was to minimize the potential for spinal injury due to vertical crash forces. The word minimize is used because it does not appear possible to eliminate all spinal injuries. There will always be extenuating circumstances in a certain percentage of the accidents that contribute to spinal injury. These circumstances could include: preexisting spinal trauma or disease, initial position of the occupant, secondary impact hazards, etc. Also, there is a trade-off to be made between reducing the energy absorber limit load to decrease the potential for spinal injury which permits greater seat stroke. This has the effect of increasing the possibility of "bottoming-out," resulting in a high probability of spinal injury.

In the UH-60A Black Hawk aircraft there have been 14 pilots and copilots involved in accidents to date in which their energy-absorbing crewseat functioned to limit spinal loads. Out of these 14 occurrences there is believed to be a spinal injury rate of between zero and 15 percent with one probable occurrence of bottoming out. If the energy absorber limit-load factor had been set at 11.5 G (versus 14.5 G) as recommended in USARTL TR-79-22, then it is estimated that in at least one-third of these cases the pilots and copilots could have bottomed out. Thus, the potential for spinal injury could

*As reported by the U.S. Army Safety Center.

58

have been much higher at the lower energy-absorber limit-load setting. Without further statistical analysis of accident conditions it is impossible to specify an energy absorber limit-load setting that will further reduce injury. However, it is concluded that the energy absorber limit-load setting should be set as high as possible, even to the extent of allowing a small injury rate of the less severe type, to avoid the bottoming-out hazard.

As a point of reference, the U.S. Air Force strives to achieve a 4- to 5-percent injury rate by using a Dynamic Response Index (DRI) value of 18.0. The Air Force has calibrated the DRI using cadaver tests and actual ejection data and found that a value of 18.0 corresponds to the desired injury rate. The DRI could be used in a similar manner to evaluate energy-absorbing seats. However, in extensive testing conducted with anthropomorphic dummies, under U.S. Army Contract DAAK51-79-C-0026, it was found that the DRI did not have a strong correlation to test severity for energy-absorbing seats (based on seat pan or pelvic acceleration).

However, if the U.S. Air Force approach was followed (i.e., attempting to achieve a 4- to 5-percent spinal injury), then the model developed in this study predicts that an energy absorber limit-load setting of approximately 12.3 G would be required for U.S. Navy aviators. However, from a practical standpoint, the goal of incorporating the necessary 12.3 G limit-load setting to achieve this minimal level of spinal injury does not appear possible. The primary reason for not being able to attain this is the stroke distance required to safely decelerate the occupant without bottoming out. For example, with a 14.5-G limit-load setting a minimum of 12 in. of available stroke distance is required. However, if the limit load factor was reduced to 12.3 G, a minimum stroke distance of approximately 13.7 in. would be required. Based on crashworthy aircraft designed to date this does not appear to be possible. The UH-60A Black Hawk and the AH-64A Apache were designed with 12.0 and 7.3 in. of minimum stroke distance, respectively.

Thus, in future U.S. Army aircraft the 14.5-G limit-load setting will probably represent a reasonable compromise between crashworthy performance of the crewseat and other flightworthiness constraints that demand minimization of cockpit height.

The U.S. adult civil flying population has a wide variation in age, physical condition, and hence bone strength. Design of an energy-absorbing seat to prevent spinal injuries carries with it a higher uncertainty due to the resulting variation in tolerance to spinal loading. The method developed in this study suggests that a 4- to 5-percent spinal injury rate would result from using an energy absorber limit-load setting of approximately 10.5 G for this population. A case could be made for selecting a higher energy absorber limit-load setting (e.g., between 11.0 and 13.0 G) if it were known that a specific segment of the population could be expected to utilize the seat. This might be the case for certain business aircraft (and helicopters), and may especially be true for pilot and copilot seats.

TEST	ORIENTATION	LIMIT LOAD (X) (G)	SPINAL LOAD (Y) (LB)
1	COMBINED	14.5	1136
2	COMBINED	11.5	856
3*	VERTICAL	14.5	795 ⎫
4	VERTICAL	14.5	860 ⎬ AVE = 827.5
5**	VERTICAL	11.5	

* NO TEST.

** DUMMY LEADS BROKE.
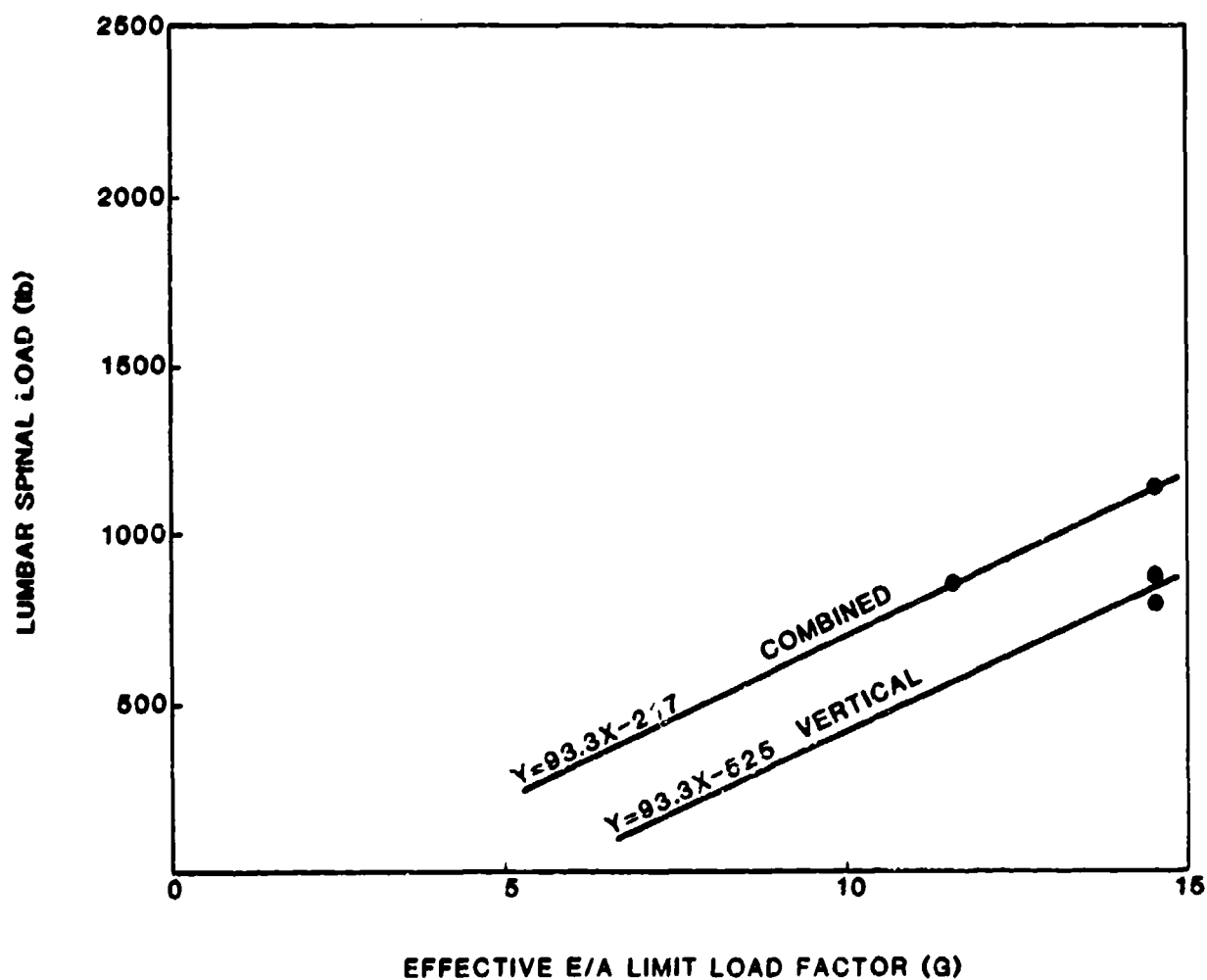
Figure 29. Correlation between peak lumbar spinal load measured in the instrumented anthropomorphic dummy and energy absorber limit-load factor.
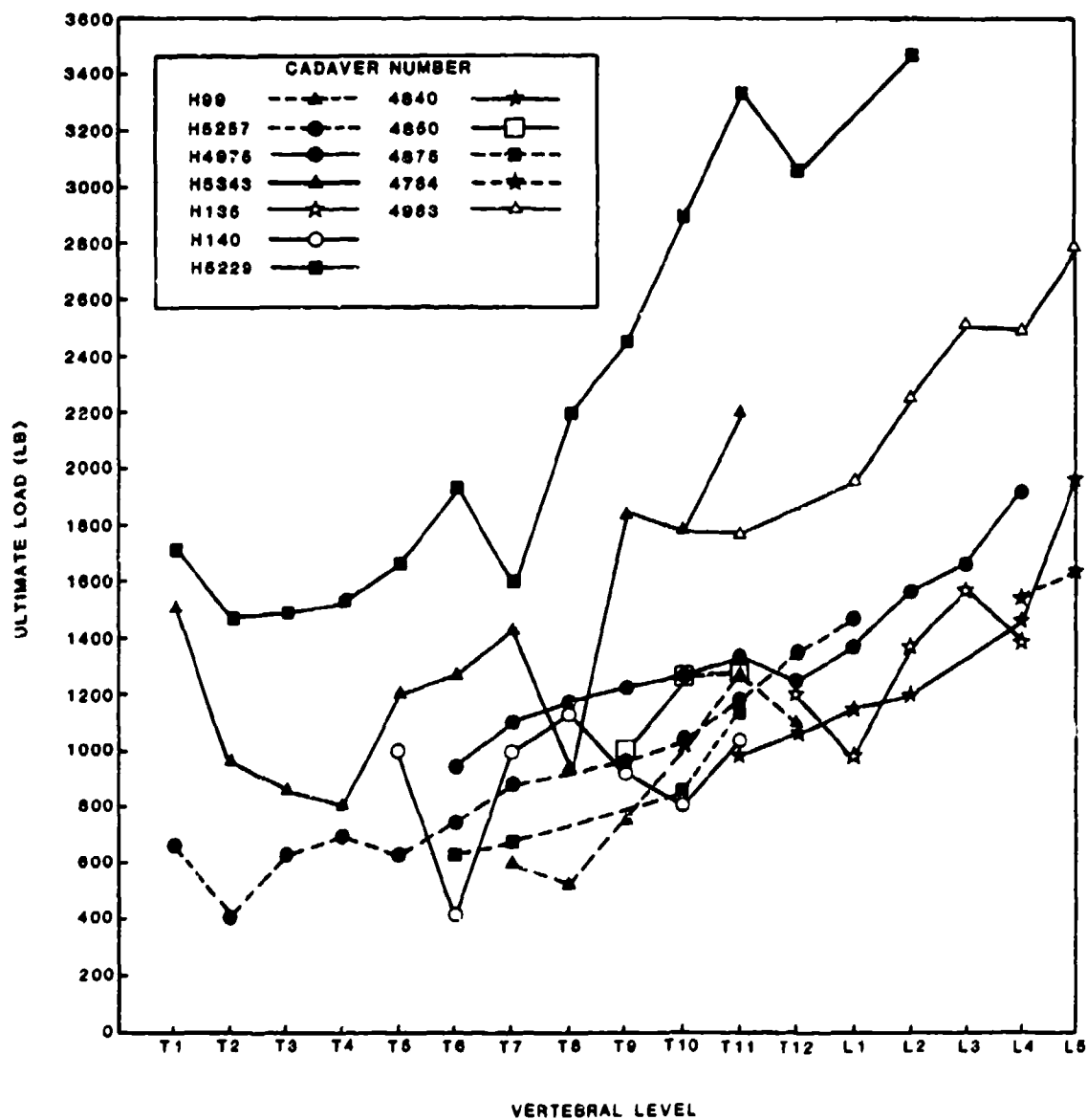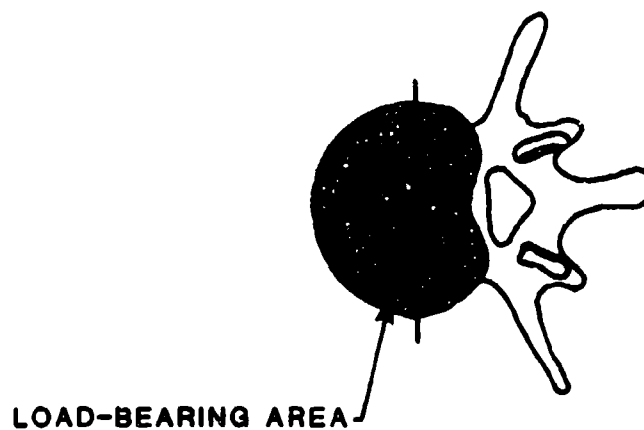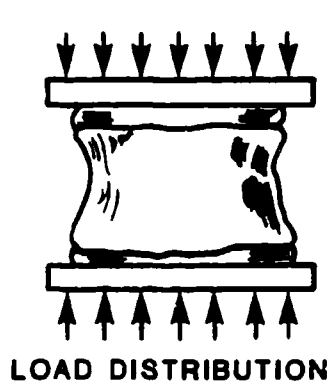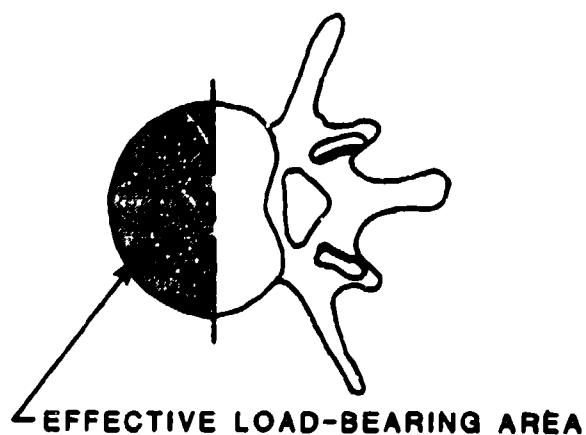
60

Figure 30. Experimentally measured ultimate load values for
individual cadavers as a function of vertebral
level in the spinal column.

61

a. COMPRESSION TEST LOAD DISTRIBUTION
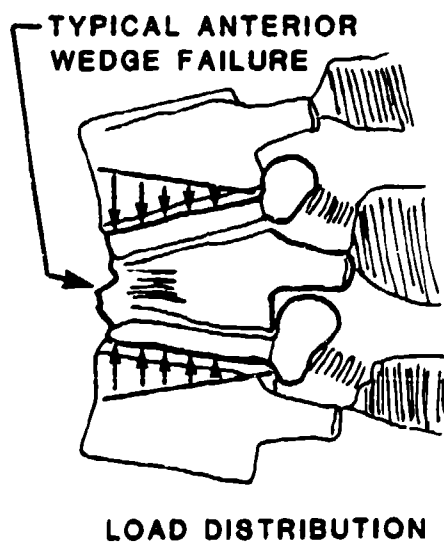
b. COMBINATION OF AXIAL COMPRESSION AND
FORWARD BENDING DUE TO CRASH LOADING

Figure 31. Force distribution and effective load-bearing
area for various loading conditions.

62
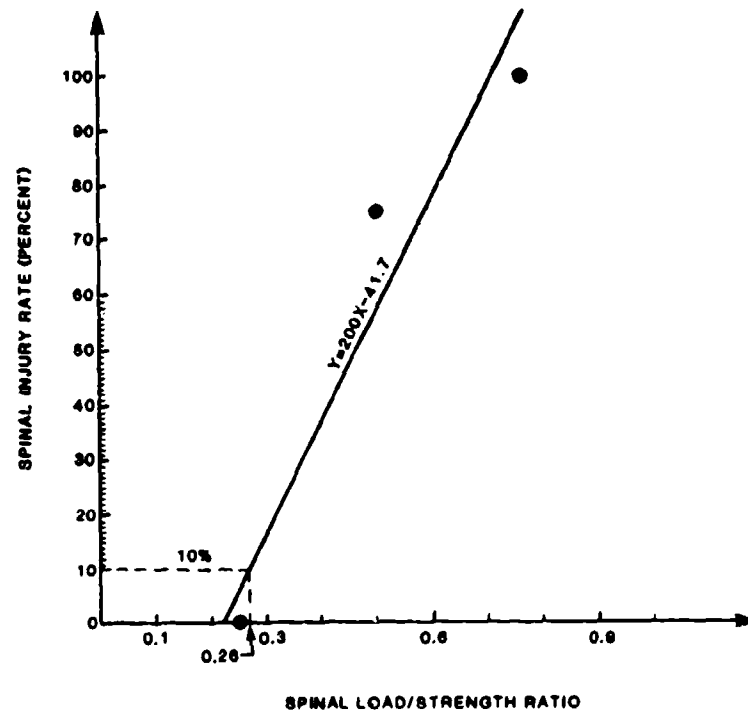
Figure 32. Spinal injury rate as a function of spinal load/strength ratio (SLSR).
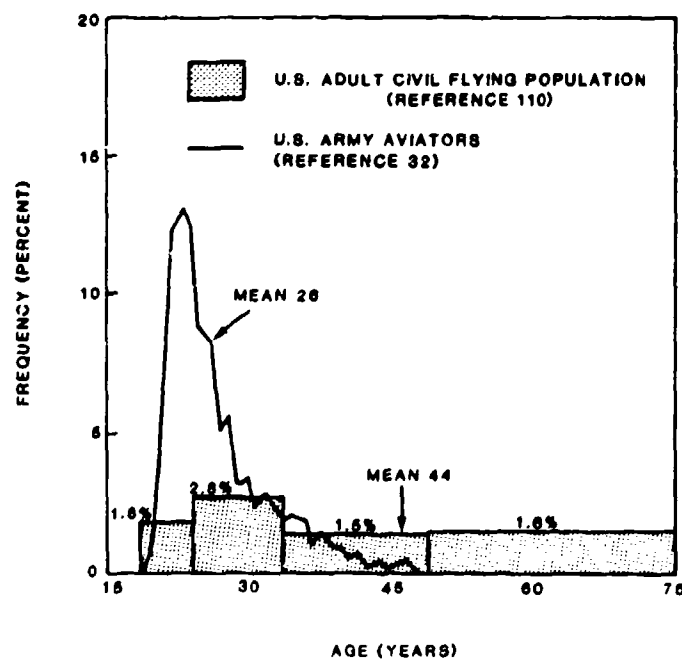
Figure 33. Comparison of age distributions for U.S. Army aviators and the U.S. adult civil flying populations.

63
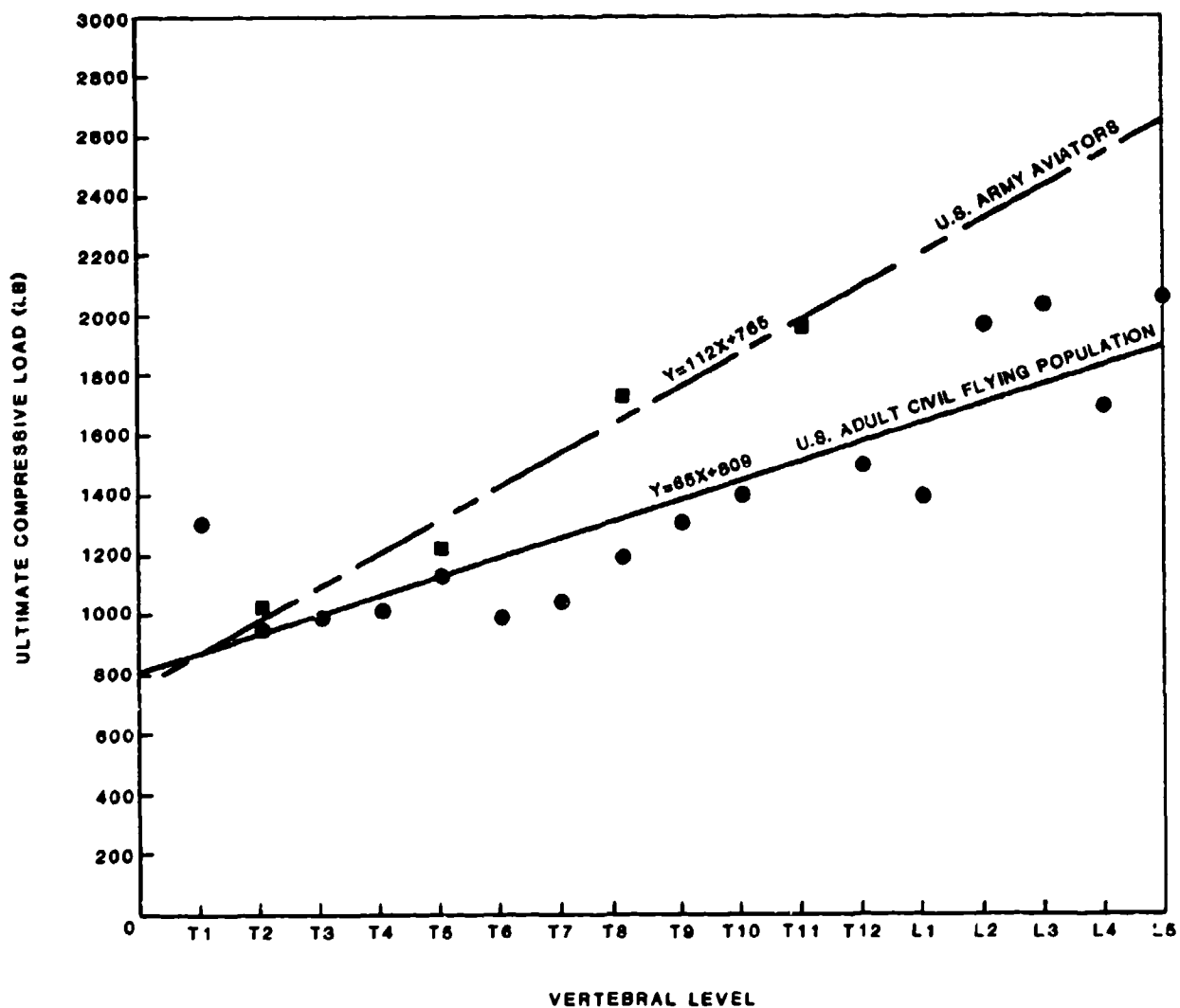
Figure 34. Vertebral ultimate compressive strength for various populations.
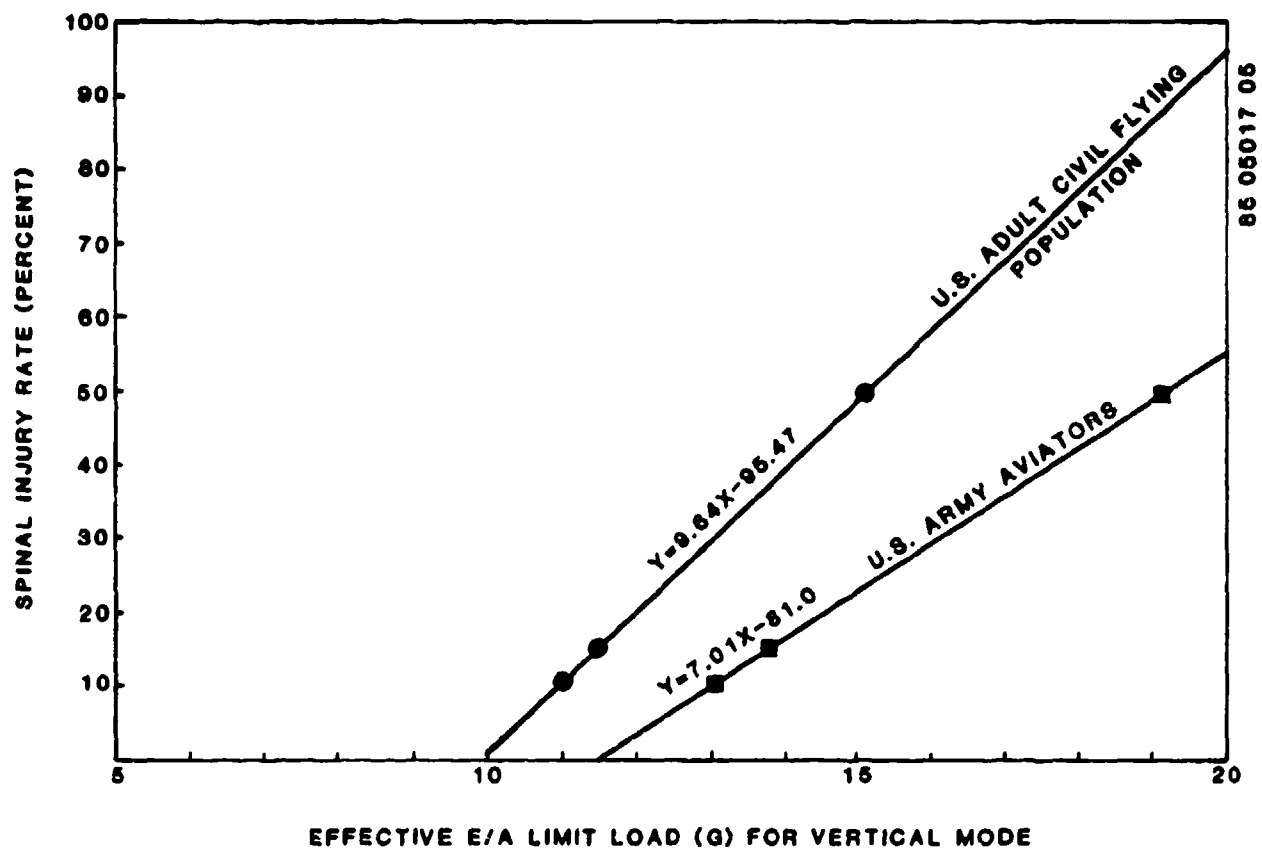
Figure 35. Correlation between the energy-absorber
limit-load factor and spinal injury rate.

6.0 CONCLUSIONS

Based on the results of this study it was concluded that:

1. The cadaver specimens available for testing in this program were not representative of the U.S. Army aviator population, either in anthropometry, age, or physical condition.

2. The cadaver specimens used may, arguably, represent an older segment (in poorer health) of the U.S. adult civil population, although it is certainly a conservative approach to use their properties to represent the adult civil flying population.

3. As would be expected, some of the older female cadavers exhibited signs of osteoporosis which manifested lower bone strength. Use of female cadavers was therefore discontinued since this was felt to impose an undue bias on the spinal injury study.

4. Use of cadavers for multiple impact tests in which the goal was to evaluate potential traumatic injury was not desirable since the skeletal injuries could not be reliably diagnosed between tests, and since the cumulative effects of repeated impacts could not be adequately assessed.

5. The type and location of spinal injuries which occurred in the dynamic test program were found to be representative of those that occurred to live subjects under actual crash conditions. The predominant spinal injury was an anterior wedge compression fracture in the T8 to L3 region with the highest incidence in the T12 and L1 vertebral segments.

6. From the literature review presented in Section 2.0, age, sex, and illness can have a significant influence on bone strength in general and spinal strength in particular. There is a definite trend toward a reduction in strength with increasing age. The primary influence due to sex is from the effects of osteoporosis in postmenopausal females. Illness and accompanying medications can have a very serious effect on bone strength, which was a great concern in the selection of cadavers for use in this study.

7. Compression testing of vertebral segments was a reasonably reliable indicator of spinal strength; the primary parameter of interest was the ultimate failure load.

8. Using an instrumented dummy (with spinal load cell) to evaluate the relative magnitude of spinal loads and moments under dynamic test conditions similar to those used for the cadavers, the measured spinal loads showed a strong relationship to the energy absorber limit-load factor and the seat orientation at impact.

9. A parameter called the spinal load/strength ratio (SLSR), which was developed in this study, appears to have merit in determining the potential for spinal injury. The parameter was based on the numerical ratio between the experimentally determined compressive load in

66

a dummy's spine and the ultimate compressive strength of the cada-veric vertebral body. In this study, the SLSR was calculated for each cadaver test and used as the method to "normalize" the data scatter. A relationship was found between the magnitude of the SLSR and the spinal injury rate.

10. Using the relationship between the spinal load/strength ratio and the spinal injury rate, a method was developed to predict the cor-relation between spinal injury rate and energy absorber limit-load. This correlation was established for both the U.S. Army aviator population and the U.S. adult civil flying population. The correlation was dependent upon use of an average vertebral compres-sion strength for each of the populations which was derived from existing studies.

11. The spinal injury rate versus energy absorber limit-load method was used to determine the expected spinal injury rate for various design conditions. For example, the energy absorber limit-load setting used in the current generation of the U.S. Army aircraft is 14.5 G. The method predicts that this would coincide with a 20 percent injury rate. Analysis of actual Army accident data indicates that the current spinal injury rate in the UH-60A Black Hawk with the Norton/Simula crewseat has a possible range of zero to 15 percent. This tends to lend some support that the method developed in this study represents a conservative approach. For comparison, the method predicts that to achieve a 20 percent spinal injury rate for the U.S. adult civil flying population an energy absorber limit-load setting of 12.0 G would be required. The lower limit-load setting for the civil population can be attributed primarily to the reduction in spinal strength with age.

12. The U.S. Army Aircraft Crash Survival Design Guide (USARTL-TR-79-22) recommends an energy absorber limit-load factor of 11.5 G. However, the method developed using the results of the cadaver test program supports the current value of 14.5 G specified in MIL-S-58095(AV) by verifying that a reasonably low injury rate should occur at this setting. Actual accident data indicates that the rate is even lower than predicted by the method developed in this study.

13. Total elimination of spinal injuries is not achievable and a small percentage of spinal injuries will always occur. This conclusion is based on the following two factors:

● Extenuating circumstances such as preexisting spinal condi-tions, posture, impingement of the functioning seat on or by external objects, etc., will always be present in actual ac-cidents.

● Reduction of the energy absorber limit load to a low value to prevent decelerative spinal injuries may actually increase the spinal injury rate since in a greater number of accidents the seat will "bottom out," increasing the likelihood of spinal injury.

The selection process for the optional energy absorber limit-load setting should be based on minimization of the number and severity of spinal injuries considering the effect of limit-load setting on spinal load, available stroke length, probability of bottoming out, and the statistical distribution of crash severity.

68

7.0 RECOMMENDATIONS

The recommendations presented in this section are divided into those for the U.S. Army aviators and those for the U.S. adult civil flying population due to the inherent differences in population characteristics.

1. **U.S. ARMY**

   ● Retain the 14.5-G energy absorber limit-load factor currently used on energy-absorbing seats for U.S. Army aircraft for the near future. This recommendation is based on the results of this study which indicates that, at most, a 20-percent spinal injury rate could occur and limited accident data which indicates that the rate is actually lower.

   ● Monitor accident statistics closely to determine the actual spinal injury rate. If, based on additional accident data, the actual spinal injury rate exceeds 15 percent, it is recommended that the energy absorber limit load be reduced to not lower than 13.5 G.

   ● Utilize variable-load energy absorbers wherever possible to prevent excessive spinal loading for light occupants and bottoming out of heavier occupants.

   ● Conduct a statistical analysis of field accidents to help determine an optimum energy absorber limit-load setting consistent with the type of aircraft.

   ● Develop measurement techniques for spinal loads and moments as a performance parameter for evaluating the adequacy of energy-absorbing seats.

2. **U.S. ADULT CIVIL FLYING POPULATION**

   ● It is recommended that an 11.0-G limiting load factor be used as a starting point for the design of energy-absorbing seats for those commercial and light aircraft needing energy-absorbing stroke to protect the spine. This is believed to be a conservative approach.

   ● Consideration should be given to selecting a higher limit-load setting (11 to 13 G) if a specific segment of the population is expected to use the seat.

   ● For certification testing of energy-absorbing crewseats, the modified dummy used in this program, or its equivalent, should be used to evaluate performance.

8.0 REFERENCES

1. Hicks, J. E., and Adams, B. H., "A Systematic Technique for the Identification of Crash Hazards in U.S. Army Aircraft," Aviation, Space, and Environmental Medicine 51 (9), 1043, 1980.

2. Reed, W. H., Proposed Military Standard for Improved Crew/Passenger Survival Seat and Body Retention Systems, AVSER Technical Report 65-14, Aviation Safety Engineering and Research, Phoenix, Arizona, September 1965.

3. Desjardins, S. P., and Harrison, H., The Design, Fabrication, and Testing of an Integrally Armored Crashworthy Crewseat, Dynamic Science, Division of Marshall Industries; USAAMRDL Technical Report 71-54, U.S. Army Air Mobility Research and Development Laboratory, Fort Eustis, Virginia, January 1972, AD 7421733.

4. Eiband, A. M., Human Tolerance to Rapidly Applied Accelerations: A Summary of the Literature, NASA Memorandum 5-19-59E, National Aeronautics and Space Administration, Washington, D.C., June 1959.

5. Crash Survival Design Guide, Dynamic Science, A Division of Marshall Industries, USAAMRDL Technical Report 71-22, Eustis Directorate, U.S. Army Air Mobility Research and Development Laboratory, Fort Eustis, Virginia, 1971, AD 733358.

6. Military Specification, MIL-S-58095(AV), Seat System: Crashworthy, Non-Ejection, Aircrew, General Specification For, Department of Defense, Washington, D.C., 27, August 1971.

7. Singley, G. T., III, and Desjardins, S. P., "Crashworthy, Helicopter Seats and Occupant Restraint Systems," in Operational Helicopter Aviation Medicine, AGARD Conference Proceedings No. 255, North Atlantic Treaty Organization, Advisory Group for Aerospace Research and Development, Neuilly sur Seine, France, May 1978.

8. Desjardins, S. P., Laananen, D. H., et al., Aircraft Crash Survival Design Guide, Volumes I-V, USARTL Technical Report 79-22 A through E, Simula Inc.; Applied Technology Laboratory, U.S. Army Research and Technology Laboratories (AVRADCOM), Fort Eustis, Virginia, 1980, AD A093784, AD A082512, AD A089104, AD A088441, AD A082513.

9. Coltman, J. W., Design and Test Criteria for Increased Energy-Absorbing Seat Effectiveness, Simula Inc; USAAVRADCOM-TR-82-D-42, Applied Technology Laboratory U.S. Army Research and Technology Laboratories, Fort Eustis, Virginia, March 1983, AD A128015.

10. White, A. A. and M. M. Panjabi, Clinical Biomechanics of the Spine, J. B. Lippincott Co., Philadelphia, Pennsylvania, 1978.

11. Lockhart, R. D., G. F. Hamilton, and F. W. Fyfe, Anatomy of the Human Body, Lippincott, Philadelphia, Pennsylvannia, 1960.

12. Eycleshymer, A. C. and D. M. Shoemaker, A Cross-Section Anatomy, Appleton-Century-Crofts, New York, 1970.

70

13.   Sances, A. Jr., et al., "Bioengineering Analysis of Head and Spine Injuries," CRC Critical Reviews in Bioengineering 5 (2): 79-122, 1981.

14.   Kazarian, L., "Dynamic Response Characteristics of the Human Vertebral Column," Act. Orth. Scand., Supplement 146, 1972.

15.   Kazarian, L., "Injuries to the Human Spinal Column: Biomechanics and Injury Classification," Exercise Sports Science Review 9: 297-352, 1982.

16.   Scances, A. Jr., et al., "The Biomechanics of Spinal Injuries," CRC Critical Reviews In Biomedical Engineering, 11 (1): 1-76, 1984.

17.   Rockoff, S. D., E. Sweet, and J. Bleustein, "The Relative Contribution of Trabecular and Cortical Bone to the Strength of Human Lumbar Vertebrae," Calc. Tis. Res. 3: 163-175, 1969.

18.   Kazarian, L. and G. A. Graves, "Compressive Strength Characteristics of the Human Vertebral Centrum," Spine 2 (1): 1-14, 1977.

19.   Lange, C., "Untersuchangen Uber Elasticitatsver Haltnisse in den Menschlichen Puckenwirbelin mit Bemerkungen Uber die Pathogenese der Deformitaten," Ztschi. f. Orthop. Chir., 10:47, 1902.

20.   Gocke, C., "Das Verhalten Spongiosen Knochens im Druck und Schlogversuch," Verh. Dtsh. Orhop. Ges., 20:114, 1926.

21.   Gocke, C., "Traumatische Wirbelum Formung im Versuch," Hefte Unfallheilk. H. 8:136, 1931.

22.   Ruff, S., Brief Acceleration: Less Than One Second, German Aviation Medicine, World War II, I, U.S. Government Printing Office, Washington D.C., 584, 1950.

23.   Perey, O. U., "Fracture of the Vertebral End Plate in the Lumbar Spine: An Experimental Biomechanical Investigation," Acta. Orthop. Scand. Suppl., 25, 1957.

24.   Brown, R. T., R. Hanson, and A. Yorra, "Some Mechanical Tests on the Lumbo-Sacral Spine with Particular Reference to the Intervertebral Discs," Journal of Bone and Joint Surgery, 39A: 1135-1163, 1957.

25.   Rockoff, D., E. Sweet, and J. Bluestein, "The Relative Contribution of Trabecular and Cortical Bone to the Strength of Human Lumbar Vertebrae," Calc. Tiss. Res. 3:163, 1969.

26.   Yamada, H., "Strength of Biological Materials," Ed. F. G. Evans, Williams & Williams Co., Baltimore, Maryland, 1970.

27.   Lin, H. S., Y. K. Liu, and K. H. Adams, "Mechanical Response of the Lumbar Intervertebral Joint Under Physiological (Complex) Loading," Journal of Bone and Joint Surgery, 60-A (1): 41-55, 1978.

28. Hansson, T., B. Roos and A. Nachemson, "The Bore Mineral Content and Ultimate Compressive Strength of Lumbar Vertebrae," Spine 5 (1): 46-55, 1980.

29. Roaf, R., "A Study of the Mechanics of Spinal Injuries," Journal of Bone and Joint Surgery, 42B, 810, 1960.

30. Brinckmann, P., et al., "Deformation of the Vertebral End Plate Under Axial Loading of the Spine," Spine 8 (8): 851-856, 1983.

31. Tencer, A. F., and A. M. Ahmed, "The Role of Secondary Variables in the Measurement of the Mechanical Properties of the Lumbar Intervertebral Joint," Journal of Biomechanical Engineering 103: 129-137, 1981.

32. Hutton, W. C., B. M. Cyron and J. R. R. Stott, "The Compressive Strength of Lumbar Vertebrae," Journal of Anatomy 129(4): 753-758, 1979.

33. Nachemson, A. L., A. B. Schultz, and M. H. Berkson, "Mechanical Proper-ties of Human Lumbar Spine Motion Segments. Influences of Age, Sex, Disc Level, and Degeneration," Spine 4(1): 1-8, 1979.

34. White, A. A. III, "Analysis of the Mechanics of the Thoracic Spine in Man" Acta Orthopaedica Scandanavia, Suppl. 127, 1969, 1-1051.

35. Farfan, H. F., et al., "The Effects of Torsion on the Lumber Inter-vertebral Joints: The Role of Torsion in the Production of Disc Degeneration," Journal of Bone and Joint Surgery 52-A (3): 468-497, 1970.

36. Tencer, A. F., A. M. Ahmed, and D. L. Burke, "Some Static Mechanical Properties of the Lumbar Intervertebral Joint, Intact and Injured," Journal of Biomechanical Engineering, 104: 193-201, 1982.

37. Miller, J. A. A., K. A. Haderspeck, and A. B. Schultz, "Posterior Element Loads in Lumbar Motion Segments," Spine 8 (8): 331-337, 1983.

38. Adams, M. A., and W. C. Hutton, "The Mechanical Function of the Lumbar Apophyseal Joints," Spine 8 (3): 327-329, 1983.

39. Nachemson, A., "Lumbar Intradiscal Pressure," Acta Orthopaedica Scandinavia, Suppl. 43, 1960.

40. Shah, J. S., W. G. J. Hampson, and M. I. V. Jayson, "The Distribution of Surface Strain in the Cadaver Lumbar Spine," Journal of Bone and Joint Surgery 60-B (2): 246-251, 1978.

41. Lin, H. S., et al., "Systems Identification for Material Properties of the Intervertebral Joint," Journal of Biomechanics 11: 1-14, 1978.

42. Lorenz, M., A. Patwardhan, and R. Vanderby, "Load Bearing Character-istics of Lumbar Facets in Normal and Surgically Altered Spinal Segments," Spine 8 (2): 122-130, 1983.

43. Hakim, N. S. and A. I. King, "A Three-Dimensinal Finite Element Dynamic Response Analysis of a Vertebra with Experimental Verification," Journal of Biomechanics 12: 222-292, 1979.

44. Galante, J., "Tensile Properties of the Human Lumbar Annulus Fibrosus," Acta Orthopaedica Scandinavia, Suppl. 100: 1-91, 1967.

45. Nachemson, A. L., "The Lumbar Spine: An Orthopedic Challenge," Spine 1 (1): 59, 1976.

46. Jenson, G. M., "Biomechanics of the Lumbar Intervertebral Disc: A Review," Physical Therapy 60 (6): 765-773, 1980.

47. Jayson, M., and J. S. Barks, "Structural Changes in Intervertebral Discs," Ann. Rhemm. Dis, 32: 10-15, 1973.

48. Coventry, M. B., R. K. Ghormley, and J. W. Kernohan, "The Inter-vertebral Disc: Its Microscopic Anatomy and Pathology," Journal of Bone and Joint Surgery 27 (2): 233-247, 1945.

49. Markolf, K. L., and J. M. Morris, "The Stuctural Components of the Intervertebral Disc," Journal of Bone and Joint Surgery, 56-A (4): 675-686, 1974.

50. Hickey, D. S., and D. W. L. Hukins, "Relation Between the Structure of the Annulus Fibrosis and the Function and Failure of the Intervertebral disc," Spine 5 (2): 106-116, 1980.

51. Nachemson, A. L., and J. M. Morris, "In Vivo Measurement of Intradiscal Pressure," Journal of Bone and Joint Surgery 46-A (5) 1077-1092, 1964.

52. Nachemson, A. L., "Disc Pressure Measurements," Spine 6 (1): 93-97, 1981.

53. Shirazi, S. A., S. C. Shirvastava, and A. M. Ahmed, "Stress Analysis of the Lumbar Discbody Unit in Compression: A Three-Dimensional Nonlinear Finite Element Study," Spine 9 (2): 120-134.

54. Quinnell, R. C., H. R. Stockdale, and D. S. Willis, "Observations of Pressures Within Normal Discs in the Lumbar Spine," Spine 8 (2): 166-169, 1983.

55. Bortulossi, C., J. C. Dosdat, and H. Roberts, " Approache Biomechanique du Disque Intervertebral Lombaire Sous Differents Types de Charges par Mesure De Pression Intranudecire," Journal of French Bisphys. Et Med. Nud. 3: 1·3-167, 1979.

56. Horst M., and P. Brinkmann, "Measurement of the Distribution of Axial Stress on the End Plate of the Vertebral Body," Spine 6 (3): 217-232, 1981.

57. Hansson, T., and B. Roos, "The Relation Between Bone Mineral Content, Experimental Compression Fractuies, and Disc Degeneration in Lumbar Vertebrae," Spine 6 (2): 147-153, 1981.

58. Kulak, R. F., et al., "Nonlinear Behavior of the Human Intervertebral Disc Under Axial Load," Journal of Biomechanics 9,377, 1976.

59. Burns, M. L. and I. Kaleps, "Analysis of Load-Deflection Behavior of Intervertebral Discs Under Axial Compression Using Exact Parametric Solutions of Kelvin-solid Models," Journal of Biomechanics 13: 959-964, 1980.

60. Spiller, R. L., D. M. Daugirda, and A. B. Schultz, "Mechanical Response of a Simple Finite Element Model of the Intervertebral Disc Under Complex Loading," Journal of Biomechanics 17 (2): 103-112, 1984.

61. Broberg, K. B., "On the Mechanical Behavior of Intervertebral Discs," Spine 8 (2): 151-165.

62. Nachemson, A., "The Load o _ ubar Discs in Different Positions of the Body," Oin. Orthop. 45, 1C, 366.

63. Morris, J. M., D. B. Lucas, and B. Bresler, "Role of the Trunk in Stability of the Spine," Journal of Bone and Joint Surgery 43-A (3): 327-351, 1961.

64. Davis, P. R., "The Use of Intra-Abdominal Pressure in Evaluating Stresses on the Lumbar Spine," Spine 6 (1): 90-92, 1981.

65. Schultz, A., et al., "Loads on the Lumbar Spine," Journal of Bone and Joint Surgery 64-A (5): 713-720, 1981.

66. Andriacchi, T., et al., "A Model for Studies of Mechanical Interactions Between the Human Spine and Rib Cage," Journal of Biomechanics 7: 497-507, 1974.

67. Belytschko, T., L. Schmer, and A. Schultz, A Model for Analytic Investigation of Three-Dimension Spine-Head Dynamics, AMRL-TR-76-10, Aerospace Medical Research Laboratory, Wright-Patterson AFB, Ohio, 1976.

68. Vulcan, A. P., A. I. King, and G. S. Nakamura, "Effects of Bending on the Vertebral Column During +G_z Acceleration," Aerospace Medicine 41 (3): 294-300, 1970.

69. Orne D., and Y. K. Liu, "A Mathematical Model of Spinal Response to Impact," Journal of Biomechanics 4: 49-71, 1971.

70. Payne, P. R., and E. G. U. Band, A Four Degree of Freedom Lumped Parameter Model of the Seated Human Body, Wyle Lab Payne Division Working Paper No. 59101-6, 1969.

71. Hess, J. L., and C. F. Lombard, "Theoretical Investigations of Dynamic Response," Journal of Aviation Medicine 29: 66-75, 1958.

72. Terry, C. 1., and V. L. Roberts, "A Viscoelastic Model of the Human Spine Sub-_ t_1 to +G_z Accelerations," Journal of Biomechanics 1:161, 1968.

73. Liu, Y. K., Pontius, U., Hosey, R., The Effects of Initial Configuration on Pilot Ejection, Final Report, Contract Number DABC-01-73-C-1068, U.S. Army Aeromedical Research Laboratory, Fort Rucker, Alabama, 1973.

74. Prasad, P., and A. I. King, "An Experimentally Validated Dynamic Model of the Spine," Journal of App. Mech., 546-550, 1974.

75. Cramer, H. J., Y. K. Liu and D. U. Von Rosenberg, "A Distributed Parameter Model of the Inertially Loaded Spine," Journal of Biomechanics 9: 115-130, 1976.

76. Liu, Y. K., H. Cramer, and D. U. Von Rosenberg, A Distributed Parameter Model of the Inertially Loaded Human Spine: A Finite Difference Solution, Dept. No. AMRL-TR-73-65. Aerospace Medical Research Laboratory, Wright-Patterson AFB, Ohio, 1973.

77. Belytschko, T., L. Schmer, and E. Privitzer, "Theory and Application of a Three-Dimensional Model of the Human Spine," Aviation, Space, and Environmental Medicine 49 (1): 158-165, 1978.

78. Belytschko, T., and E. Privitzer, Refinement and Validation of a Three-Dimensional Head-Spine Model, Report AMRL-TR-78-7, Aerospace Medical Research Laboratory, Wright-Patterson AFB, Ohio, 1978.

79. Soechting, J. F. and P. R. Pasley, "A Model for the Human Spine During Impact Including Musculature Influence," Journal of Biomechanics 6: 195-203, 1973.

80. Nicoll, E., "Fractures of the Dorso-Lumbar Spine," Journal of Bone and Joint Surgery, 31,-B (3), 1949.

81. Holdsworth, F. W., "Fractures, Dislocations and Fracture-Dislocations of the Spine," Journal of Bone and Joint Surgery 45-B (1): 6-20, 1963.

82. McAffe, P. C., H. A. Yuan, and N. A. Lasda, "ne Unstable Burst Fracture," Spine 7(4): 365-373, 1982.

83. Denis, F., "Spinal Instability as Defined by the Three Column Spine Concept in Acute Spinal Trauma," Clinical Orthopaedics and Related Research 189: 65-76, 1974.

84. De La Torre, J. C., "Spinal Cord Injury Review of Basic and Applied Research," Spine 6 (4): 315-335, 1981.

85. King, A. I., "The Vertebral Column: Experimental Aspects" in The Biomechanics of Trauma, A. M. Nahum and J. Melvin ed., Appleton-Century-Crofts, Norwalk, Connecticut, 1985.

86. Kazarian, L., K. Beers, and J. Hernandez, "Spinal Injuries in the F/FB-111 Crew Escape System," Aviation, Space, and Environmental Medicine, 50 (9): 948-957, 1979.

87. Rotondo, G., Spinal Injury After Ejection in Jet Pilots: Mechanism Diagnosis, Follow-up, and Prevention, 1975.

88. Smith, G. R., C. H. Northrop and J. Loop, "Jumpers Fractures: Patterns of Thoracolumbar Spine Injuries Associated with Vertical Plunges," Radiology 122: 657-667, 1977.

89. Holdsworth, F. W., "Fractures, Dislocations, and Fracture-Dislocations of the Spine," Journal of Bone and Joint Surgery, 52-A (8): 1534-1551, 1970.

90. Smith, W. S., and H. Kaufer, "Patterns and Mechanisms of Lumbar Injuries Associated with Lap Seat Belts." Journal of Bone and Joint Surgery 51-A (2): 239-254, 1969.

91. Burke, D. C., "Hyperextension Injuries of the Spine," Journal of Bone and Joint Surgery 53-B (1): 3-12, 1971.

92. Payne, P. R., and E. L. Stech, Human Body Dynamics Under Short-Term Acceleration, Frost Engineering and Development Corporation, Denver, Colorado N64 14779, AD #429027, Technical Report No. 115, 1963.

93. Kazarian, L. E., J. W. Hahn, H. E. Von Gierke, Biomechanics of the Vertebral Column and Internal Organ Response to Seated Spinal Impact in the Rhesus Monkey (Macaca Mulatta), Report AMRL-TR-70-85, Aerospace Medical Research Laboratory, Wright-Patterson AFB, Ohio.

94. Jones, W. L., W. F. Madden, and G. W. Luedman, "Ejection Seat Accelerations and Injuries," Aerospace Medicine, 559-561, 1964.

95. Chubb, R. M., W. R. Detrick, and R. H. Shannon, "Compression Fractures of the Spine During USAF Ejections," Aerospace Medicine 36: 968-972, 1965.

96. Synder, R. G., Human Impact Tolerance, Int. Automobile Safety Configuration Compensation Paper 700398, Society of Automotive Engineers, New York, 1970.

97. Kaplan, B. H., "Method of Determining Spinal Alignment and Level of Probable Fracture During Static Evaluation of Ejection Seats," Aerospace Medical, 45 (8): 942-944, 1974.

98. Crooks, L. M., "Long-Term Effects of Ejecting From Aircraft," Aerospace Medical, 41 (7): 803-804, 1976.

99. Ewing, C. L., "Non-Fatal Ejection Vertebral Fracture and Its Prevention," AGARD Configuration Procedure No. 110 on Current Status in Aerospace Medicine, 1972.

100. Levy, P. M., "Ejection Seat Design and Vertebral Fractures," Aerospace Medical, 545-549, 1964.

101. Beck, A., "Proposal for Improving Ejection Seats with Respect to Seating Comfort and Ejection Posture," Aviation, Space, and Environmental Medical, 46 (5): 736-739, 1975.

102. Personal Communication with Dr. Dennis Shanahan, Major MC, U.S. Army Safety Center, May 28, 1985.

103. Hearon, B. F., J. W. Brinkley, and J. H. Raddin, "Vertical Impact Evaluation of the F/FB-111 Crew Restraint Configuration, Headrest Position, and Upper Extremity Bracing Technique," Aviation, Space, and Environmental Medicine, 54 (11): 977-987, 1983.

104. Ewing, C. L., "Vertebral Fractures in Jet Aircraft Accidents: A Statistical Analysis for the Period 1959 Through 1963, U.S. Navy," Aerospace Med. 505-508, 1966.

105. Hirsch, C., and A. Nachemson, "Clinical Observations on the Spine in Ejected Pilots," 10 Acta Ortho. 31 (2): 135-145.

106. Hearon, B. F., J. H. Raddin, and J. W. Brinkley, "Guidance for the Utilization of Dynamic Preload in Impact Injury Prevention," in Impact Injury; Mechanisms, Prevention and Cost, North Atlantic Treaty Organization, Advisory Group of Aerospace Research and Development, Neuilly sur Seine, France, April 1982.

107. Laananen, D. H., and J. W. Coltman, Measurement of Spinal Loads in Two Modified Anthropomorphic Dummies, Simula Inc. TR-82405, Final Report, Contract DAMD17-81-C-1175, U.S. Army Aeromedical Research Laboratory, Fort Rucker, Alabama, May 1982.

108. Desjardins, S. P., et al., Crashworthy Armored Crewseat For the UH-60A Black Hawk, paper presented at 35th Annual National Forum of the American Helicopter Society, Washington, D.C., May 1979.

109. Ewing, C. L., A. I. King, and P. Prasad, "Structural Considerations of Human Vertebral Column Under $+G_z$ Impact Acceleration," Journal of Aircraft, Vol. 9, No. 1, pp. 84-90, 1972.

110. The Gallup Organization, Inc. The Frequency of Flying Among the General Aviation Public, 1981, conducted for Air Transport Association of America, September 1981.

DYNAMIC TEST DATA FOR AF020
VERTICAL MODE
CADAVER NO. 4784
(FILTERED AT 100 HZ)

HEAD ACCELERATION

83

TIE DOWN

AF. 20.3 04/03/80

FORCES (LBS)

TIME (MS) X10

LT. FOOT

RF: 20. 3 04/03/80

Z-FORCES (LBS) X10

75.

25.

-25.

15.   30.   45.

TIME (MS)   X10

60.

RT. FOOT

RF: 20. 3 04/03/80

Z-FORCES (LBS) X10

90.

30.

-30.

15.   30.   45.

TIME (MS)   X10

60.

LT. FOOT

RF: 20. 3 04/03/80

X-FORCES (LBS) X10

45.

15.

-15.

15.   30.   45.

TIME (MS)   X10

60.

RT. FOOT

RF: 20. 3 04/03/80

X-FORCES (LBS) X10

45.

15.

-15.

15.   30.   45.

TIME (MS)   X10

60.
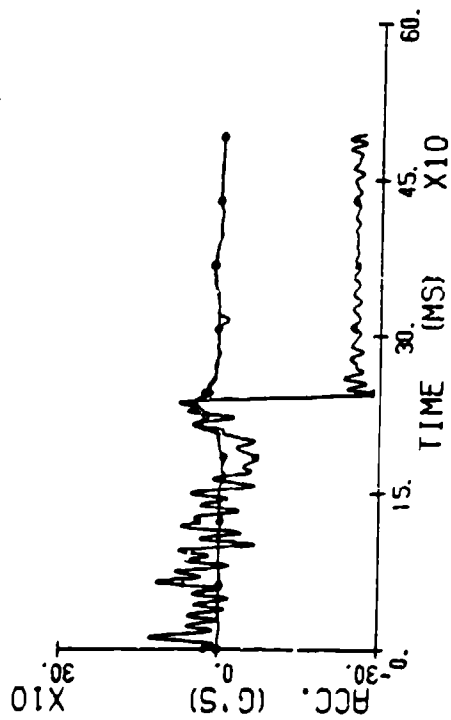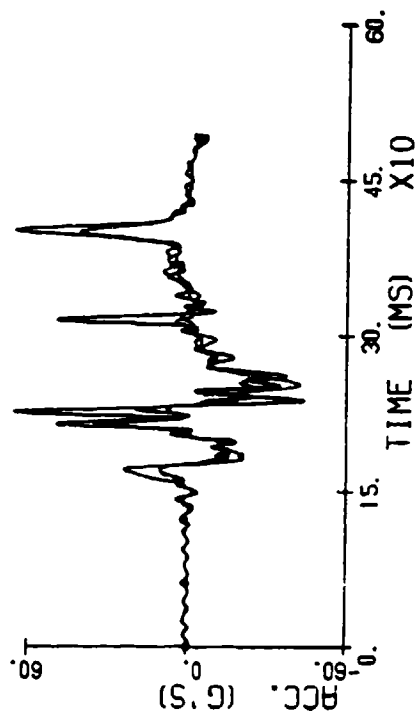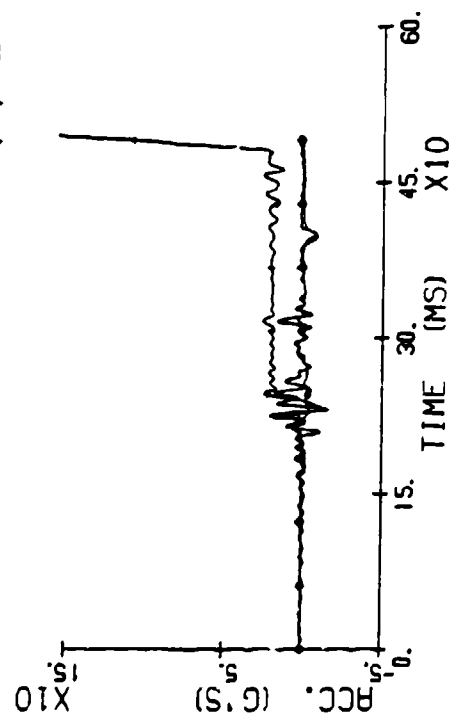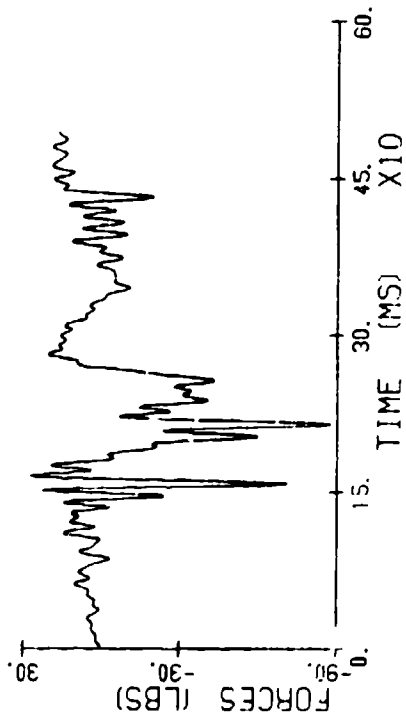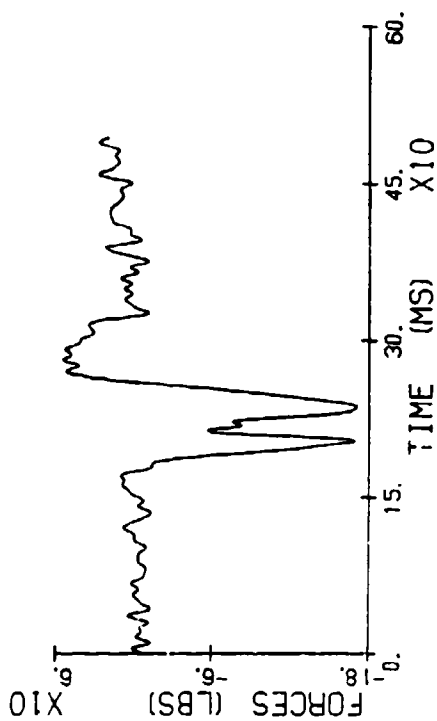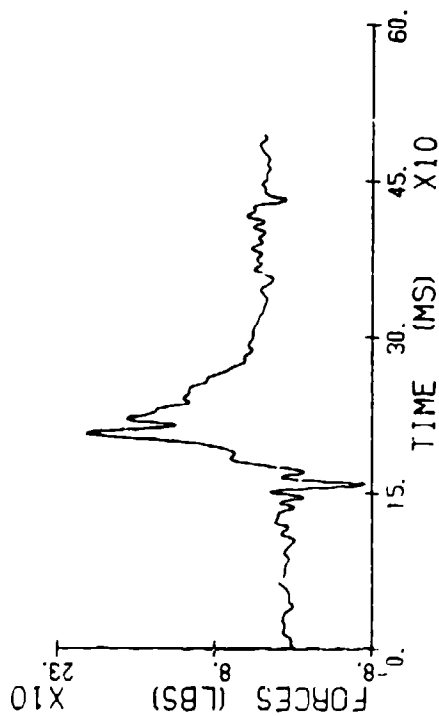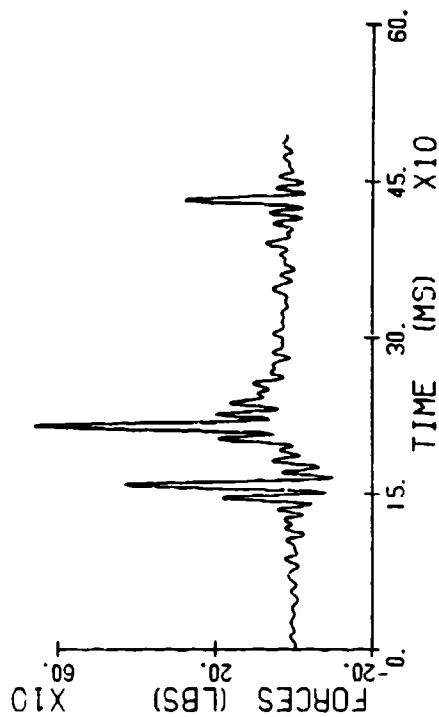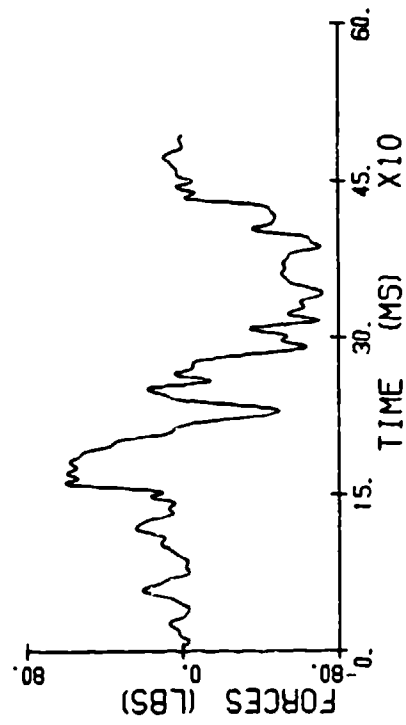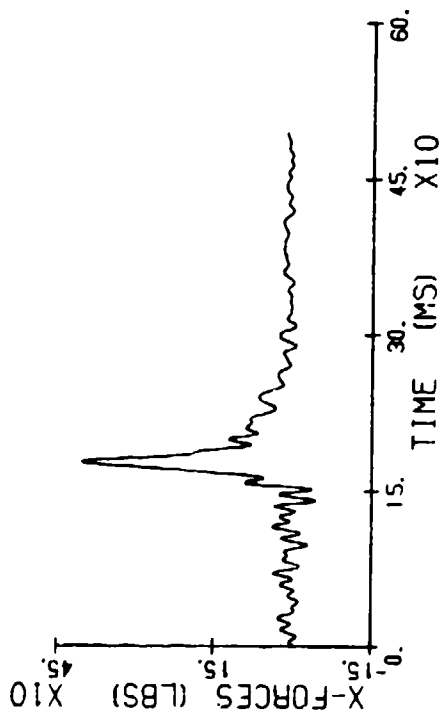
DYNAMIC TEST DATA FOR AF021
COMBINED MODE
CADAVER NO. 4784
(FILTERED AT 100 HZ)

PELVIS

RF:21.1 04/04/80

PELVIS

RF:21.1 04/04/80

PELVIS

RF:21.1 04/04/80

91

HEAD ACCELERATION

93

TIE DOWN

RF.21.3 04/04/80

FORCES (LBS) X10

TIME (MS) X10

95

96
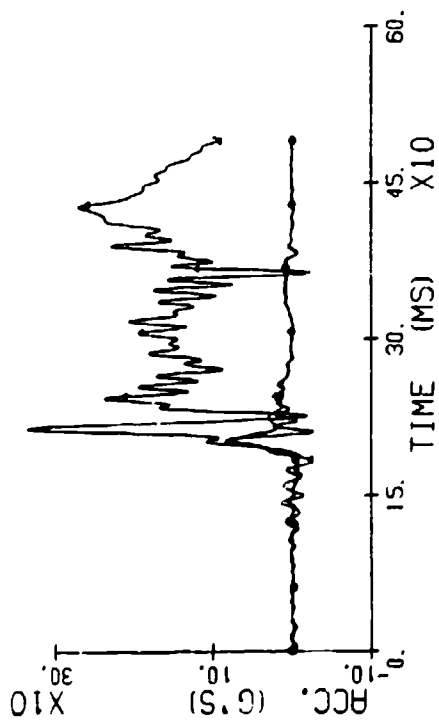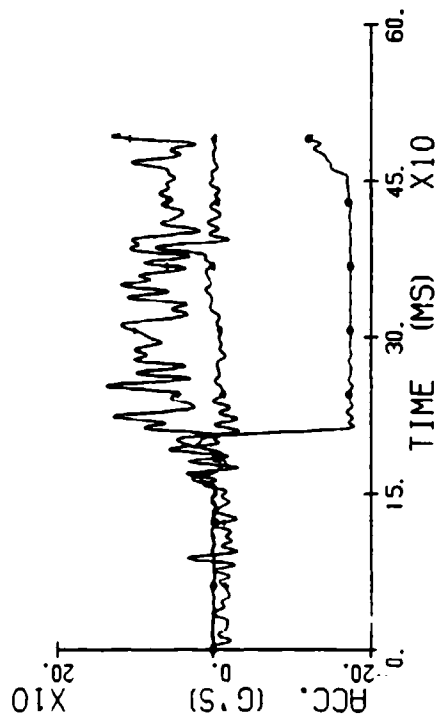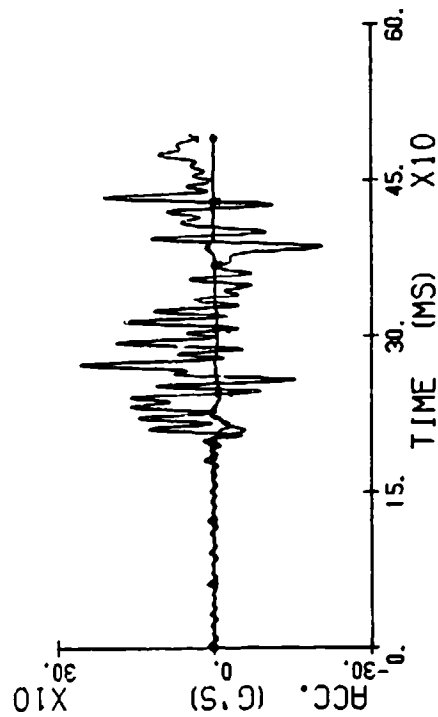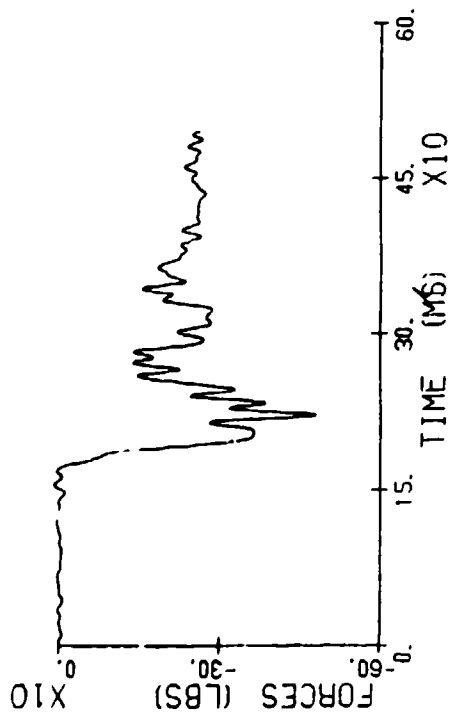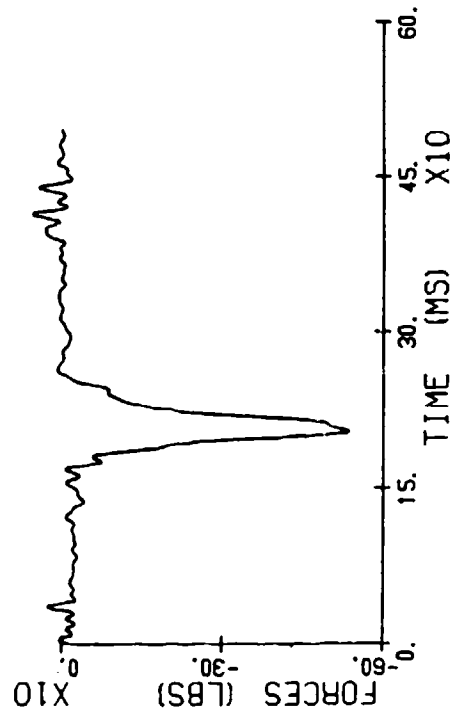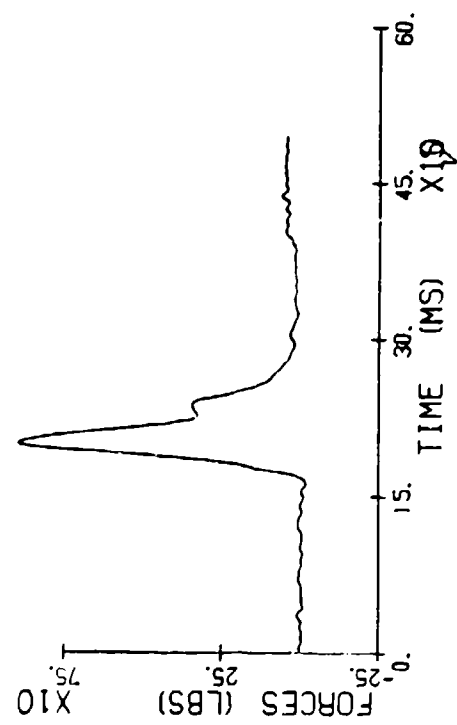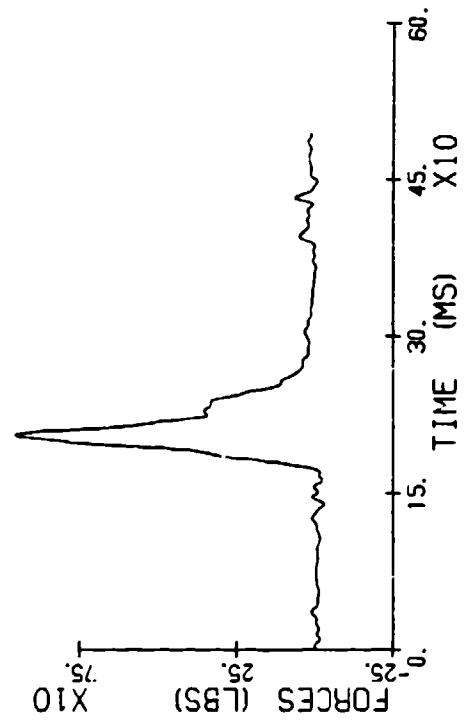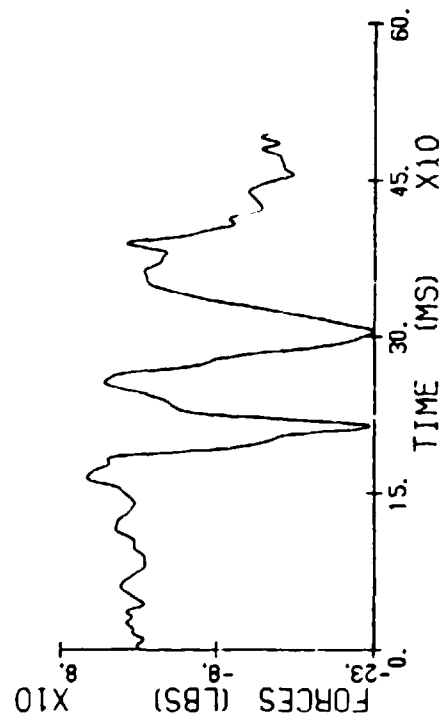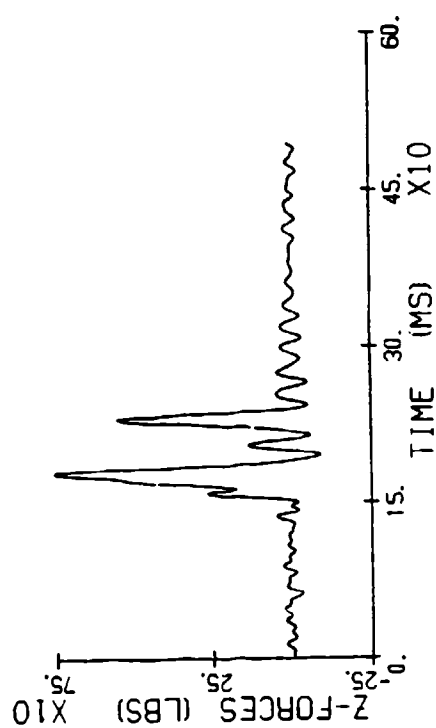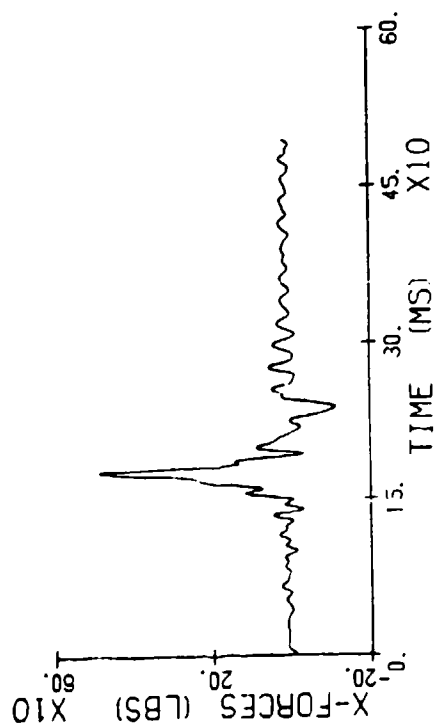
SAMPLE OF COMPRESSION TEST DATA
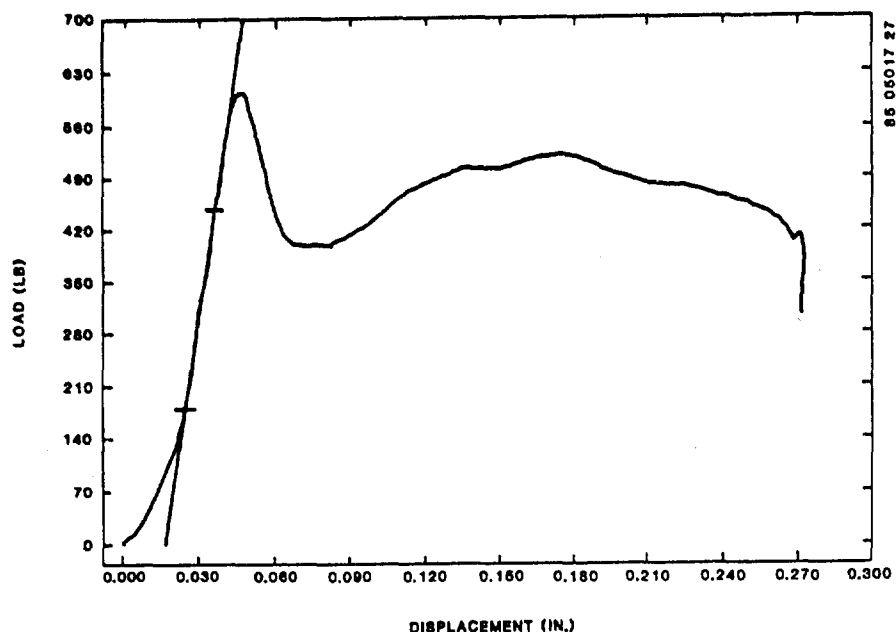
DISPLACEMENT (IN.)

Input Data

ID test number	= 1	
Subject id	= H99	
Column position	= 7	
OB level	= 17	
Desired displacement rate	= 210.00	in./min.
Computed displacement rate	= 194.59	in./min.
Maximum strain	= 0.30000	in./in.
Specimen pretest length	= 0.90000	in.
Specimen pretest average area	= 1.7636	sq/in.
Preload	= 0.00000	lb
Load cal	= -2500.0	lb
Displacement cal	= -0.50000	in.
Operator specified strain	= 0.00000	in./in.

Data Reduction Results

Stiffness	= 23427.	lb/in.
Modules	= 11955.	lb/sq. in.

Task	Load (lb.)	Displacement (in.)	Stress (lb./sq.in.)	Strain (in./in.)	Energy (in.-lb)
Field load	0.00	0.000	0.00	0.00000	
Ultimate load (disc)	0.00	0.000	0.00	0.00000	0.000
Ultimate load (body)	608.22	0.045	344.87	0.05036	10.358
Maximum displacement	0.00	0.000	0.00	0.00000	0.000
Residual displacement		0.000		0.00000	0.000

PRECEDING PAGE BLANK

APPENDIX D

MINERAL ANALYSIS DATA

TABLE D-1. COMPRESSION TEST AND MINERAL ANALYSIS DATA FOR BLACK HAWK TEST CADAVERS

Cadaver #	Spinal Level	Total Dry Weight (lb)	Ca wt. %	P wt. %	Ca/P Ratio
4840	T11	-	12.98	6.17	2.10
	T12	-	12.88	6.10	2.11
	L1	-	12.44	6.21	2.00
	L2	-	9.06	4.83	1.87
	L4	-	8.28	1.38	6.00
	L5	-	9.60	3.60	2.67
4850	T9	-	15.95	7.20	2.21
	T10	-	16.14	6.99	2.31
	T11	-	14.93	6.37	2.34
4875	T10	-	13.07	5.97	2.19
	T11	-	11.77	5.52	2.13
	T6	-	12.30	5.78	2.13
	T7	-	10.42	5.05	2.06
4784	L4	-	11.86	5.31	2.04
	L5	-	13.15	6.13	2.14
4983	T10	-	19.21	8.33	2.31
	T11	-	12.43	6.62	1.88
	L1	-	16.77	7.52	2.23
	L2	-	17.73	8.32	2.13
	L3	-	14.58	7.30	2.00
	L4	-	16.23	7.42	2.19
	L5	-	8.66	3.31	2.62
99	T7	0.0203	11.75	5.12	2.29
	T8	0.0216	11.54	4.59	2.51
	T9	0.0225	11.94	5.19	2.30
	T10	0.0265	12.70	5.38	2.36
	T11	0.0301	12.38	5.24	2.36
	T12	0.0338	11.72	5.23	2.24
5257	T1	0.0082	17.25	6.90	2.50
	T2	0.0082	16.16	6.60	2.45
	T3	0.0085	15.23	6.50	2.34
	T4	0.0100	15.39	6.18	2.49
	T5	0.0105	9.43	6.09	1.55
	T6	0.0123	8.69	5.98	1.45
	T8	0.0162	9.02	6.27	1.44
	T9	0.0189	4.89	5.87	0.83
	T10	0.0224	8.10	5.53	1.47
	T11	0.0269	8.95	4.90	1.83
	T12	0.0322	8.27	5.66	1.46
	L1	0.0351	14.69	5.80	2.53

PRECEDING PAGE BLANK

TABLE D-1 (CONTD.) COMPRESSION TEST AND MINERAL ANALYSIS DATA FOR BLACK HAWK TEST CADAVERS

Cadaver #	Spinal Level	Total Dry Weight (1b)	Ca wt. %	P wt. %	Ca/P Ratio
4975	T6	0.0139	16.64	6.79	2.45
	T7	0.0157	16.17	6.71	2.41
	T8	0.0179	16.93	6.75	2.51
	T9	0.0190	11.68	6.80	1.72
	T10	0.0234	15.40	6.41	2.40
	T11	0.0305	13.46	4.58	2.41
	T12	0.0343	13.45	5.55	2.42
	L1	-	11.38	5.70	2.00
	L2	-	10.29	4.54	2.27
	L4	-	7.21	2.61	2.73
	L5	-	7.42	3.14	2.36
5343	T1	0.0135	18.18	7.51	2.29
	T2	0.0135	17.22	8.69	1.98
	T3	0.0125	17.12	7.14	2.40
	T4	0.0129	17.42	6.90	2.52
	T5	0.0157	14.41	6.57	2.91
	T6	0.0170	14.72	5.71	2.58
	T7	0.0193	16.34	6.33	2.58
	T8	0.0232	16.52	6.52	2.53
	T9	0.0276	10.06	6.16	1.63
	T10	0.0299	16.05	6.17	2.60
	T11	0.0332	12.45	6.31	1.97
135	T12	0.0398	13.18	5.59	2.86
	L1	0.0413	12.39	5.58	2.22
	L2	0.0441	13.22	5.54	2.39
	L3	0.0528	10.18	5.45	1.87
	L4	0.0602	12.12	5.34	2.27
140	T5	0.0131	15.59	6.29	2.48
	T6	0.0134	13.67	6.31	2.17
	T7	0.0157	13.04	6.21	2.10
	T8	0.0194	15.51	6.33	2.45
	T9	0.0200	15.40	5.88	2.66
	T10	0.0197	13.50	5.81	2.32
	T11	0.0262	12.39	5.45	2.27
5229	T1	0.0147	18.77	8.24	2.28
	T2	0.0143	18.42	8.02	2.30
	T3	0.0120	18.04	8.29	2.18
	T4	0.0127	18.07	8.25	2.19
	T5	0.0144	18.46	8.31	2.22
	T6	0.0169	17.68	7.99	2.21

TABLE D-1 (CONTD.)	COMPRESSION TEST AND MINERAL ANALYSIS DATA FOR BLACK HAWK TEST CADAVERS				

Cadaver #	Spinal Level	Total Dry Weight (lb)	Ca wt. %	P wt. %	Ca/P Ratio
5229	T7	0.0197	18.81	7.76	2.42
	T8	0.0224	15.86	8.17	1.94
	T9	0.0256	18.94	7.98	2.37
	T10	0.0327	17.87	7.87	2.27
	T11	0.0404	15.93	7.49	2.13
	T12	0.0471	17.55	7.39	2.37
	L1	0.0538	16.59	7.37	2.25
	L2	0.0560	15.86	6.93	2.29

145-86